

UC Berkeley

UC Berkeley Electronic Theses and Dissertations

Title

Context-Dependent Regulation of Epithelial Growth by Echinoid

Permalink

<https://escholarship.org/uc/item/2819h6zw>

Author

Spitzer, Danielle C

Publication Date

2023

Peer reviewed|Thesis/dissertation

Context-Dependent Regulation of Epithelial Growth by Echinoid

By

Danielle C Spitzer

A dissertation submitted in partial satisfaction of the

requirements for the degree of

Doctor of Philosophy

in

Molecular and Cell Biology

in the

Graduate Division

of the

University of California, Berkeley

Committee in charge:

Professor Iswar Hariharan, Chair

Professor David Bilder

Professor Richard Harland

Professor Gian Garriga

Summer 2023

Abstract

Context-Dependent Regulation of Epithelial Growth by Echinoid

by

Danielle C Spitzer

Doctor of Philosophy in Molecular and Cell Biology

University of California, Berkeley

Professor Iswar Hariharan, Chair

The size of an animal is determined by the growth, proliferation, and survival of every cell in its body. Individual cells must respond to local cues and properly adjust their growth behavior to collectively generate tissues and organs of the proper size. How cells regulate their growth, and how they coordinate to regulate the size of the organs, are two fundamental questions which have long captivated developmental biologists, and which remain incompletely understood.

Much of what is already known about growth regulation has been learned from the study of mutants. Mutations affecting multiple signaling pathways can lead to overgrowth or undergrowth. However, the study of genetic mosaics has shown that outcome of growth-disrupting mutations depends not only on the properties of affected cells, but also on the interactions those cells have with their neighbors. For example, cells heterozygous for a class of mutations called *Minute* are slow growing but viable when all cells carry the mutation, but are eliminated in the presence of wild type neighbors. This phenomenon, termed cell competition, highlights how cells can non-autonomously influence growth and survival within a mosaic tissue.

I conducted a genetic screen in *Drosophila* to identify new genes which regulate growth in mosaics, focusing specifically on cell adhesion genes. The screen identified 9 genes which, when knocked down in clones in the wing imaginal disc, alter the size, shape, or number of clones which are recovered later in development. Of particular interest was the gene *echinoid* (*ed*): clones of cells lacking *ed* are small, round, and underrepresented, but *ed* mutations affecting large populations of cells can cause tissue overgrowth. My dissertation work is aimed at understanding the mechanistic basis of these seemingly contradictory phenotypes and to clarify the role of *ed* in regulating cellular and tissue growth. I demonstrate that cells lacking *ed* die by apoptosis at increased rates, at least in part because they express lower levels of the anti-apoptotic protein Diap1. This contributes to the elimination of *ed*-deficient clones in mosaic tissues. I also confirm that organs which are mostly or entirely deficient of *ed* overgrow because of a failure to terminate growth when the organ has reached its appropriate final size.

Ed has been previously shown to have a function in restricting growth via its interactions with the Hippo pathway, which regulates the expression of pro-growth and anti-apoptotic genes downstream of the transcription factor Yorkie (Yki). I show that this prevailing model cannot account for many of the phenotypes observed in *ed*-depleted tissues. Contrary to other reports, I found that many—but not all—Yki target genes are expressed at lower levels in *ed*-depleted cells. In mosaics, many of these same Yki targets are expressed at higher levels in the wild-type neighbors of *ed* clones. These observations are consistent with clonal elimination but inconsistent *ed* having a simple, growth-inhibitory effect via the Hippo pathway.

To understand why *ed* mutant organs overgrow, I screened for dominant modifiers of the overgrowth phenotype caused by Gal4-driven knockdown of *ed* in the wing. The top hit in this screen was *upd2A*, which suppressed overgrowth and enhanced cell death. While characterizing these modification phenotypes, I determined that they were *ed*-independent artifacts of a *UAS* construct present in the *upd2A* allele which interacts with Gal4. Although ultimately uninformative to the overgrowth phenotype associated with *ed*, this line of inquiry uncovered important information about the properties of the *upd2A* allele which may be of interest to researchers who use this allele, or other alleles generated in a similar manner.

Overall, this work advances our understanding of how growth is regulated by *echinoid*, highlights the context-dependence of *ed*'s effects on growth, and paints a more complicated picture of how *ed* interacts with the Hippo pathway than previously appreciated.

Table of contents

Abstract	1
Table of contents	i
List of figures	iii
List of tables	iv
Author contributions	v
Acknowledgments	vi
1 Introduction	1
1.1 <i>Growth is a genetically regulated developmental process</i>	1
1.2 <i>Drosophila as a model for studying organ size regulation</i>	3
1.3 <i>Echinoid is a cell adhesion molecule involved in development</i>	5
1.4 <i>Goals and overview of dissertation research</i>	8
2 <i>ed</i> loss leads to apoptotic clonal elimination	1
2.1 <i>Introduction</i>	1
2.2 <i>Results</i>	1
2.3 <i>Discussion</i>	4
2.4 <i>Figures and tables</i>	6
3 <i>ed</i> loss in broad domains leads to organ overgrowth	29
3.1 <i>Introduction</i>	29
3.2 <i>Results</i>	29
3.3 <i>Discussion</i>	30
3.4 <i>Figures</i>	32
4 Downstream effects of <i>ed</i> perturbations	35
4.1 <i>Introduction</i>	35
4.2 <i>Results</i>	35
4.3 <i>Discussion</i>	37
4.4 <i>Figures</i>	39
5 Genetic modifiers of <i>ed</i>-mediated overgrowth	45

5.1	<i>Introduction</i>	45
5.2	<i>Results</i>	45
5.3	<i>Discussion</i>	48
5.4	<i>Figures and tables</i>	51
	Conclusion	70
	Materials and Methods	72
	References	75

List of figures

Figure 2.1: A genetic screen to identify CAMs which regulate growth in mosaics.	6
Figure 2.2: MARCM <i>ed</i> clones are underrepresented, small, and round in the wing disc epithelium.	8
Figure 2.3: <i>ed</i> ^{-/-} clones are eliminated from the wing disc epithelium.	9
Figure 2.4: <i>ed</i> ^{-/-} clones are eliminated from the eye.	10
Figure 2.5: Elevated levels of apoptosis are seen in <i>ed-RNAi</i> tissue.	11
Figure 2.6: Blocking apoptosis rescues elimination of <i>ed-RNAi</i> clones.	12
Figure 2.7 Diap1 is reduced in <i>ed-RNAi</i> clones.	13
Figure 2.8 Hippo pathway-dependent transcription of <i>diap1</i> is reduced in <i>ed-RNAi</i> cells, but overall <i>diap1</i> transcript levels are similar to wild-type.	14
Figure 3.1: Loss of <i>ed</i> in large domains causes overgrowth.	32
Figure 3.2: <i>hh-Gal4, UAS-ed-RNAi</i> wing discs grow slowly, but eventually exceed appropriate final size.	33
Figure 3.3: The C-terminal intracellular domain of Ed is not required to regulate wing size but is required for elongation of the wing.	34
Figure 4.1: <i>ed-RNAi</i> non-autonomously increases the expression of Yorkie target genes outside of clones.	39
Figure 4.2 Localization of Yki:GFP is not obviously changed in or around <i>ed-RNAi</i> clones.	40
Figure 4.3: <i>ed-RNAi</i> in the posterior compartment has different effects on different Yorkie target genes.	41
Figure 4.4: <i>ed</i> overexpression has diverse effects on Yorkie target genes.	42
Figure 4.5: <i>ed-RNAi</i> clones have high levels of Fat.	43
Figure 4.6: <i>ed-RNAi</i> clones have lowered levels of Cic.	44
Figure 5.1: Genetic scheme used for the dominant modifier screen.	51
Figure 5.2: <i>ed</i> genetically interacts with the Hippo pathway.	52
Figure 5.3: <i>ed</i> genetically interacts with the Notch pathway.	53
Figure 5.4: Co-depletion of <i>ed</i> and <i>cno</i> has a synergistic negative effect on growth.	54
Figure 5.5: The <i>upd2Δ</i> allele dominantly modifies the <i>nub-Gal4, UAS-ed-RNAi</i> wing phenotype.	55
Figure 5.6: High levels of apoptosis in <i>upd2Δ/+; nub-Gal4, UAS-ed-RNAi</i> wing imaginal discs.	56
Figure 5.7: Various members of the Jak-STAT pathway do not modify the <i>nub-Gal4, UAS-ed-RNAi</i> phenotype in the same manner as <i>upd2Δ</i>	57
Figure 5.8: Depletion of <i>upd2</i> using reagents other than the <i>upd2Δ</i> allele does not modify the <i>nub-Gal4, UAS-ed-RNAi</i> phenotype.	58
Figure 5.9: Genetic scheme used for recombination mapping.	59
Figure 5.10: <i>upd2Δ</i> does not strongly genetically interact with the null <i>ed^{IF20}</i> allele.	60
Figure 5.11: <i>upd2Δ</i> , which contains a <i>UAS</i> misexpression site, genetically interacts with <i>nub-Gal4</i>	61

List of tables

Table 2.1: Initial candidate list.....	15
Table 2.2: Genes excluded from screen.	22
Table 2.3: Results from lines which were screened.....	25
Table 5.1: Results from dominant modifier screen.....	62

Author contributions

Study conception and design, data collection, analysis and interpretation of results, and dissertation preparation was done by Danielle Spitzer with input and oversight from Iswar Hariharan.

The contributions of additional researchers to this work are described below:

Anthony Rodríguez-Vargas also worked on the genetic screen described in Chapter 2 and produced some of the data presented in Figure 2.1.

William Sun conducted the experiments presented in Figures 2.5C-D, 4.2, and 4.6, and assisted with the experiments presented in Figures 5.5, 5.8, 5.10, and 5.11.

Luigi Viggiano provided substantial experimental and intellectual contributions to all the work presented in Chapter 5, including conducting experiments and collecting and analyzing data.

Chapters 2-4 are a partial reproduction of the following preprint:

The cell adhesion molecule Echinoid promotes tissue survival and separately restricts tissue overgrowth in *Drosophila* imaginal discs

Danielle C Spitzer, William Y Sun, Anthony Rodríguez-Vargas, Iswar K Hariharan
bioRxiv 2023.08.04.552072; doi: <https://doi.org/10.1101/2023.08.04.552072>

Acknowledgments

First and foremost, I want to thank my advisor and mentor, Iswar Hariharan. When I started grad school, everyone told me that picking a thesis advisor is the most important choice a grad student needs to make. They were right, and I picked well. Iswar is, of course, brilliant. He thinks about science with remarkable clarity and creativity, and he has a seemingly encyclopedic memory for every experiment that has ever been done. He is also kind, caring, generous, and brimming with integrity. When the pandemic threw the world upside down, he was steady and kind. I admire how he is far more concerned with actually fixing problems than with taking credit for fixing them—an uncommon quality which I watched him put into practice often as MCB co-Chair. He always reminds me to slow down, think carefully, and not worry too much about the minute hand on a clock. I'm proud to be one of his trainees.

I'm also deeply thankful to the other members of the Hariharan lab who I had the great fortune to work with (and work out with). I cannot overstate how much of a difference it made to go to work every day knowing I'd be spending my time with people who I really care about and enjoy being around, and who uplift one another. They were sources of scientific and emotional support, laughter, encouragement, mentorship, and friendship.

First, I need to thank my fellow graduate students:

- When I was just starting in the lab, an all-star cast of senior grad students—Jo Bairzin, Linda Setiawan, and Taryn Sumabat—were finishing. I'm thankful for the time we overlapped and for all the lessons they taught me in the fly room, ranging from fly genetics to feminism to personal finance.
- Maya Emmons-Bell and Nick Everetts were both only one year ahead of me in grad school, but their scientific maturity and independence felt years beyond that. This would have been extremely intimidating if they weren't such kind, silly, wonderful people.
- Sophia Friesen and I were co-tons and joined the lab together—I cannot imagine a better person to go through grad school with. They were my rock throughout it all and I truly cannot imagine doing this without them. More on Sophia later.
- And of course, the best bay mate a scientist could ask for—Joyner Cruz. Joyner brightens up our lab with his deep laugh and clever wit. He's a great person to celebrate with, commiserate with, or just vibe with. Something I really admire about Joyner is the way he interacts with his undergraduate mentees. He has a talent for mentorship that comes from his drive to help and uplift the people around him.

Next, the postdocs:

- Jamie Lahvic is kind of person who I look up to not just scientifically, but also personally and ethically. She's someone with conviction who looks at the world, sees all the ways that it is broken, and then gets to work fixing it. She also is an incredible dancer and even taught me a few moves, which I have already forgotten how to do but nonetheless think of fondly.

- I often feel like I hit the secret jackpot and got a second incredible dissertation advisor: Melanie Worley. I don't think I've ever met anyone who loves an experiment more than Melanie or who is better suited to this line of work. I could not count the number of times she helped me troubleshoot an experiment, make sense of confusing data, or think more deeply about my project. Melanie always shared her love of nature (especially birds) and adventure with the lab and was a grounding force for the rest of us. The future members of the Worley lab are extremely lucky.

The people who worked with me on this project:

- Anthony Rodríguez-Vargas worked on the clonal screen during his rotation. Although he joined a different lab, I've still had pleasure to have him as a friend and colleague since.
- William Sun joined the lab as I was wrapping up, and quickly picked up the torch to keep this project going. In a short time, he has already made big contributions to this work.
- I must give a special thanks to Luigi Viggiano, who worked with me on Team Echinoid in my final year of grad school. Luigi dove head-first into the world of *Drosophila* genetics and embraced every opportunity he encountered. His wonder and enthusiasm for science is refreshing, and his penchant for making memes about our project brought me a lot of laughter and delight. I am very excited to see where his drive and talent take him next.

I am thankful to the other wonderful people who have been a part of this of the lab, especially Riku Yasutomi, Dennis Sun, and Rebecca Chang. I owe a great deal of gratitude to Lupita Hernandez, whose invaluable contributions to the lab have made my work possible.

Next, I need to thank the many people who set me on the path to grad school in the first place, starting with my high school biology teacher, Jason Goldberg. Jay taught me that it's good to be a nerd. He knows that when you give students the support they need, they can take on difficult tasks and excel at them—that's why a bunch of kids like me were cloning plasmids and solving Michaelis-Menton equations in the basement of our otherwise unremarkable public high school. He saw my passion for biology and nurtured it in countless ways—when I ran out of his classes to take, he enrolled me in independent study and gave me the freedom and bench space to experiment. He is the reason I started on this path, and he made sure I had all the tools I needed to travel it with ease.

When I went to college, I immediately found my scientific home in Scott Williams' lab. From the moment I joined I was treated like a valued colleague whose contributions to the lab were taken seriously. The lab has a culture of respect, collaboration, scientific rigor, and fun, and I attribute much of this to Scott. He is a stand-up guy and generous mentor never hesitates to go up to bat for his mentees. He opened countless doors for me, and he continues to be someone I turn to for guidance and support.

Because Scott is a magnet who attracts all the best people to his lab, I had the great pleasure to work with awesome labmates including Kendall Lough, Kevin Byrd, Carlos Patiño-Descovich, Bethany Wagner Brown, Michelle Mac, Jeet Patel, Abby Bergman, and Jina Yom. Kendall was the grad student who I worked with directly, and I am so enormously grateful for that. He is a creative, careful, innovative scientist who really served as the role model for the kind of researcher I aspired to be. He is also lighthearted and exuberant, and he reminds me that doing science is joyful and fun, even when it is hard. I am so thankful that Kendall continues to be a close mentor and friend.

Two of my best friends to this day are my fellow Williams lab wondergrads, Jeet and Abby. Jeet and I met during the first week of college, then awkwardly discovered we were competing for the same job. Fortunately, Scott decided to hire us both, and the rest is history. We've been two peas in a pod ever since. It's a rare and special thing when you meet someone whose brain just seems to run on the same frequency as yours, and that's what it is like with me and Jeet. Whether we are talking about science or just having out as friends, we are totally in sync. Abby didn't join the lab until my senior year, but we've also grown very close, especially after graduating. She made the unfortunate decision to go to grad school at Stanford, which worked out well for me because it means she was close by. Jeet, Abby, and I all went different schools, but it still feels like we have gone to grad school together. I cherish our reunions and zoom chats and am so thankful that we have stayed close.

I am indebted to my professors at UNC who nurtured my love and understanding of biology in the classroom, especially Brian Hogan, Kelly Hogan, Mark Peifer, Gidi Shemer, and Blaire Steinwand. It's not hard to see how I ended up on path toward a career in university teaching, because I had no shortage of excellent role models to learn from and emulate. In particular, I am endlessly grateful to Blaire and Kelly, who are the people who taught me how to teach—it was a privilege to be their apprentice and to learn from the best. I have benefitted from their mentorship and support in a million ways already and they continue to be big influences in my life. If I become half the educator that either one of them is, I will be so proud.

I've also had numerous other mentors and colleagues who have been a part of my scientific journey. I'm thankful to Kara Gulak, who mentored me during my summer at UAlbany, and Thibaut Brunet, who mentored me during my rotation in the King lab. I'm thankful to my Amgen cohorts at Columbia and NIH, and especially to Mark Aronson and Katie Strelau who I've stayed good friends with since. I met many lifelong colleagues and friends in Woods Hole at the Marine Biological Laboratory as an Embryology student (#Embryo19) and TA (#Embryo21); it is a privilege and an honor to be a part of this course and to be in such impressive company.

The MCB faculty and staff have supported my growth as a scientist in countless ways. The staff of the Graduate Affairs Office worked tirelessly to facilitate the success of grad students like me—they do so much for the department and I appreciate it greatly. I am extremely grateful to David Bilder, Richard Harland, Gian Garriga, and David Weisblat for their support as members of my qualifying exam and/or thesis committees. I'm also

especially thankful to Diana Bautista, Ellen Lumpkin, and Robin Ball, who have supported me in many ways, particularly related to teaching.

I'm extremely lucky to be a part of many communities in Berkeley which have shaped my life these past six years. I went through grad school with my MCB2017 cohort, and it has been humbling to see how impressive my peers are, as scientists and as people. I am thankful to David Bilder, Nicole King, and the members of their labs for making me feel welcome during my rotations—they didn't make Awkward Week easy, and I am lucky to have had such a tough decision to make. Through MCB more broadly, I've been involved in the communities of iMCB and SACNAS, and I am glad to have worked with the fantastic people in these groups to make UC Berkeley a better place. I'm also a proud member of UAW-2865/SRU-UAW, which organizes and fights for better working conditions at the UC. I never expected or hoped to spend six weeks of graduate school on the picket line rather than at the bench, but it was an honor to do so alongside, and in solidarity with, thousands of my fellow academic workers.

Many teaching groups I've participated in have been very important to me during my time in graduate school. I'm thankful to everyone who is a part of the Science Education Journal Club for becoming my teaching community here at Berkeley, and especially to Madeline Arnold, who is both a good friend and someone who I worked with closely on multiple projects related to teaching. I also want to thank my SABER Buddies—Joshua Caulkins, Skye Comstra, Rob Furrow, Petra Kranzfelder, and Laurel Lorenz. Our monthly meetings always brightened my day and I hold our network of support dear.

Outside of science and school, my cycling communities have been a tremendous source of fun, friendship, stress relief, and adventure. I spent countless hours riding around the east Bay with my Mario Kart Peloton crew—Julia Bleier, Vinson Fan, Sonali Mali, Chloe McCollum, Carlos Ng, Lisa Strong, Vivien Tran, and Justin Zhong. I've made so many friends through the Berkeley Bike Club and always looked forward the Friday morning WTFN ride, even if it meant waking up way too early. I think every person on that ride has had to listen to me describe this research while we were climbed Tunnel Road at least once, and they were all very good sports about it.

My friends have been the people who have been by my side through it all during this process. I am especially thankful to Jessica Hitt and Ericka Crankshaw, who have been my friends since high school and who I have stayed close with all these years. I'm also grateful to my college friends, especially Jeet and Abby who I have written about already, and my good friend and former roommate Sarah Sturdivant. I've continued to be extremely lucky in the roommate department, and I want to give special thanks to my Squid Friends—Molly Brothers, Natalie Dall, Sophia Friesen, and Daisy—who have really been my Berkeley family.

- Molly has taught me to appreciate the little things in life, especially mushrooms. She's one of the most talented scientists and hard workers I've ever met and she's a devoted cat mom. She is one of the most poised, put together, mature people I've ever met, and at the same time she is one of goofiest and raunchiest people I know. Whether I need a laugh, a hug, or advice, I know I can turn to Molly.

- Natalie is the kind of friend who makes friendship easy. It doesn't really matter what we are doing—we can stay at home in pajamas watching trash TV, solve a whole puzzle in one sitting, go out on an adventure, or check out some fun event together, whatever. If I'm doing something with her, that's what matters. She's also my number one source of Pittsburgh knowledge, which has really come in handy.
- Sophie and I lived together, worked together, and often that still wasn't enough, so we'd hang out more on top of that. They are just an incredible person, the kind you can set your moral compass to. And they're not only a great scientist and friend, but also a talented writer, artist, and bread baker. I really admire their wit, humor, and commitment to eating any edible leaf and berry they stumble upon while walking about Berkeley, regardless of whether it tastes good or not, but just for the joy of foraging. After doing basically everything together out mind meld is nearly completely, and I wouldn't have it any other way.
- Daisy may be Molly's cat, but she is still the sunshine of my life, and a source of endless love and delight and fur. There is nothing more soothing than giving her pats or having her curl up on my lap. Her antics are a constant source of laughter and content for the group chat. She's the best kitty in the world and I love her so much.

Lastly, I need to thank my family. Nothing I have done would be possible if I hadn't grown up with their love and support. My parents have worked so hard to give me the best shot at pursuing my dreams, which is an enormous privilege that I never take for granted. I am also thankful for the values they raised me with. My dad has a mantra which he always emphasized to me and my sister: Attitude and Effort. There are a lot of things in life we cannot control, but we can always control the attitude we take toward the cards we are dealt, and the effort we give to the work that we do, whether it's playing little league softball or completing a PhD. And of course, I am thankful for my sister, Missy. She is my best friend, role model, and closest confidant. I love her so much and I am so glad to have her as such a big part of my life.

1 Introduction

1.1 Growth is a genetically regulated developmental process

One of the most conspicuous features of the diversity of animal life is enormous range in body size. Just within extant mammals, the range of adult body weight spans eight orders of magnitude (Blackburn & Gaston, 1994). Despite this massive range, most animals begin life as a single cell, the zygote, which develops into a larger multicellular animal with a predictable shape and size for its species. The adult body size depends on the sizes of the constituent organs, which ultimately depends on the number and size of the cells making up those organs. Thus, an understanding of growth regulation at the cellular levels is essential to understanding the growth and size regulation at multiple scales.

That growth fundamentally occurs at the level of individual cells presents a conundrum: how do cells align their growth behavior to the needs of the organs they collectively make up? There is not a single answer, but it is clear that growth is a highly regulated process, with cells responding to both systemic (*e.g.*, hormones, nutrition) and organ-intrinsic (*e.g.*, paracrine signaling, mechanical forces) cues via multiple signaling pathways including Hippo, Tor, Insulin, RTK/Ras, Myc, and JAK/STAT (Hafen & Stocker, 2003; Hariharan, 2015). Differences in the activities of these pathways underlie variations in growth and size across and within species. For example, body size in dogs is determined in large part by the Insulin pathway, with circulating IGF-1 levels and *IGF1* haplotype strongly correlated with body size (Eigenmann et al., 1984; Sutter et al., 2007). Mutations disrupting *ras* or *myc* can play a role in the pathology of diseases of growth like hypertrophic cardiomyopathy (Kai et al., 1998). Cancer is perhaps the most well-known disease type associated with dysregulated growth, and mutations in many growth regulatory pathways can cause or contribute to malignancy (Yang & Xu, 2011).

Somatic mutations affecting growth can arise at any time throughout development, generating clones of cells with different growth properties than their neighbors. This can happen during the natural life of an animal, such as when a spontaneous or mutagen-induced change occurs during DNA replication. Although not all somatic mutations affect growth or are pathogenic, the generation of mutant somatic clones with dysregulated growth is a defining feature of cancer (Martincorena & Campbell, 2015). Somatic clones can also be generated experimentally, enabling researchers to study how particular cell populations are related to and interact with their neighbors. Clonal analysis has a long history in the field of developmental biology, beginning with lineage tracing experiments that allowed researchers to study which cells in an organism descend from a particular precursor cell injected with a dye (Conklin, 1905). Now, a variety of clonal generation systems enable researchers to induce clones with different properties from their neighbors, especially in genetically-tractable models like the fruit fly *Drosophila melanogaster* (Blair, 2003; del Valle Rodríguez et al., 2012).

Studying the growth of clones in genetic mosaics has revealed an array of heterotypic interactions that influence cell growth and/or survival non-autonomously. One example of growth regulation unique to mosaics is cell competition, the process by which slow-growing “loser” cells are eliminated from mosaic tissues, despite their viability in non-mosaic tissues. Cell competition was discovered in flies by studying *Minute* (*M*) alleles, which are loss-of-function alleles of genes encoding ribosomal proteins. Heterozygous *M/+* cells grow slowly but are viable and generate adult animals of a relatively normal size. However, when clones of cells containing two functional copies of a *M* allele (+/+) are made in a heterozygous (*M/+*) background, the (+/+) clones occupy disproportionately large territories within compartments (Morata & Ripoll, 1975). Importantly, the overrepresentation of the (+/+) “winner” cells is greater than would be expected from a difference in cell division rate alone. This is because slower growing “loser” cells at the clonal interface die by apoptosis (Moreno et al., 2002). The increased representation of “winner” cells at the expense of “loser” cells is a defining feature of cell competition.

Cell competition is now recognized as a more general phenomenon that can be triggered by myriad mutations—such as, famously, mutations in *myc*—not just those affecting ribosomal genes. Not all mutations affecting growth rate induce competition, as demonstrated by experiments showing that *Dp110* or *CycD+Cdk4* overexpression clones have an increased growth rate, but do not impact the growth rate or survival of unaffected neighbors (de la Cova et al., 2004). However, mutations causing cell competition almost always affect growth rates (Amoyel & Bach, 2014; Baker, 2011; Levayer & Moreno, 2013; Simpson, 1979; Simpson & Morata, 1981). Although much of the work on cell competition has been done in flies, there is now strong evidence that competition also occurs in other taxa. Mutations that behave like *Minutes* have been found in mice (Oliver et al., 2004), multiple forms cell competition have been shown to occur in vertebrate cells in culture (Hogan et al., 2009; Kajita et al., 2010; Leung & Brugge, 2012; Mamada et al., 2015; Norman et al., 2012; Penzo-Méndez et al., 2015; Tamori et al., 2010), and a growing number of studies show that competition occurs in vertebrate embryos (Akieda et al., 2019; Clavería et al., 2013; Hashimoto & Sasaki, 2019; Sancho et al., 2013) and numerous adult tissues (J. Ding et al., 2011; Ellis et al., 2019; Liu et al., 2019; Martins et al., 2014; Oertel et al., 2006).

It is unclear whether cell competition plays a role in organ size control during typical development. Blocking competition in *Minute* mosaic flies does not lead to organs of abnormal size, despite the persistence of cells with differing growth rates within the organ (Martín et al., 2009). However, cell competition can lead to the elimination of mutant cells that would otherwise overgrow (Kanda & Igaki, 2020), and in this way may contribute to organ size control by preventing instances of tumorous overgrowth (Lahvic & Hariharan, 2019). For example, loss-of-function mutations in neoplastic tumor suppressor genes like *scribble*, *discs-large*, and *lethal giant larvae* in both flies and vertebrates leads to malignant transformation and overgrowth of affected tissues (Bilder et al., 2000; Zhan et al., 2008). However, clones of cells with these mutations do not overgrow but instead experience increased cell death at the clonal interface, which can

lead to partial or complete clonal elimination (Brumby & Richardson, 2003; Norman et al., 2012; Tamori et al., 2010).

Cell competition is one of many ways heterotypic interactions between genetically dissimilar cells can regulate growth. A phenomenon sometimes accompanying cell competition is the generation of “oncogenic niche cells.” These mutant cells are not themselves hyperplastic—many, in fact, are cell competition “losers”—but stimulate growth in neighboring cells via the release of growth factors and other short-range signaling molecules (Enomoto et al., 2015). Another example is the physical expulsion of differently fated clones of cells from tissues, which occurs in cases such as the clonal misexpression of selector genes or an activated form of Ras, Ras^{V12}, in flies (Bielmeier et al., 2016). This process involves and requires increased actomyosin contractility at the clonal interface, and unlike classical cell competition, the “loser” and “winner” statuses in these competitive contexts are determined by relative arrangements of different cell types (e.g. a Ras^{V12} clone is extruded when surrounded by wild-type cells, but when wild-type cells are surrounded by Ras^{V12} cells, the wild-type cells will be extruded). A similar physical expulsion response to clonal transformation with Ras^{V12} also occurs in mammalian cell culture (Hogan et al., 2009).

1.2 *Drosophila* as a model for studying organ size regulation

All growth occurs at the level of individual cells responding to local cues, yet collectively these cells generate organs with characteristic sizes, patterns, and proportions. How cells within an organ coordinate their growth to achieve this feat has long-fascinated scientists and remains an area of active investigation (G. Vogel, 2013). Studies of the fruit fly *Drosophila melanogaster* have generated a wealth of knowledge concerning the genetic basis of organ size control (Hariharan, 2015). Much of this research focuses on sac-like larval organs termed imaginal discs, which give rise to adult structures following metamorphosis.

In particular, many studies have focused on the wing imaginal disc, which gives rise to the adult wing blade, hinge, and portions of the thorax. The wing disc begins as a cluster of ~30 cells which grow into a highly patterned organ containing approximately 30,000-50,000 cells (A. García-Bellido & Merriam, 1971; Madhavan & Schneiderman, 1977; Martín et al., 2009; Worley et al., 2013). The wing disc is divided into subdivisions called compartments, which are lineage-restricted territories—cells in one compartment do not freely intermix with cells in another, and instead respect divisions termed “compartment boundaries” (A. García-Bellido et al., 1973). There are two major compartment boundaries in the wing imaginal disc: the anterior-posterior (A-P) and dorsal-ventral (D-V) boundaries. The A-P and D-V boundaries also function as the sites of signaling centers which produce Decapentaplegic (Dpp) and Wingless (Wg), respectively.

In *Drosophila*, compartments are thought to be the level at which organ size regulation occurs. The A and P compartments of wing discs will each stop growing once the appropriate final size is reached, even when growing at different rates (Martín & Morata, 2006). Even so, the growth of one compartment may indirectly influence the growth of another. For example, a manipulation which reduces the size of the posterior

compartment may lead to a less robust induction of the Dpp signaling center (which is formed in response to Hedgehog secreted from P cells), which in turn reduces the growth of the anterior compartment. More generally, the phenomenon of “accommodation” describes the how compartments sometimes adjust their size in response to perturbed growth in a connected compartment (Díaz-Benjumea et al., 1989; Milán et al., 1997). Accommodation may arise in part from the physical constraints imposed by tissues of considerably different sizes on their shared interface.

How exactly imaginal discs sense their size and accordingly adjust the growth behavior of individual cells remains uncertain. Classical transplantation experiments demonstrate a disc-intrinsic mechanism for organ size control. *Drosophila* imaginal discs transplanted into the abdomens of adult females grow until they reach an appropriate final size, at which point growth terminates (A. García-Bellido, 1965). This is true even when the disc is injured and must regenerate (Bryant & Levinson, 1985). Thus, cells within the disc can somehow sense when this disc has reached a particular size, even in the absence of systemic cues that would be present in the native larval environment.

One essential, disc-intrinsic component of wing disc size regulation is the Dpp morphogen gradient. Dpp promotes growth in the disc—loss of Dpp signaling prevents growth and proliferation (Burke & Basler, 1996), whereas increased Dpp signaling causes discs to grow excessively, especially in the lateral regions of the wing pouch (Nellen et al., 1996; Worley et al., 2013). Dpp is produced in the signaling center along the A-P compartment boundary and disperses laterally. A gradient forms with Dpp levels highest medially and progressively lower laterally (Teleman & Cohen, 2000). Although it is clear that Dpp is an important piece of organ size control in the disc, questions remain about how cells interpret and respond to the Dpp gradient. Briefly, some hypotheses which have been presented include that cells may compute the slope of the Dpp gradient (Day & Lawrence, 2000) or changes to the level of Dpp over time (Wartlick et al., 2011), or that Dpp is not required for growth *per se*, but instead functions to equalize otherwise non-uniform growth rates across the disc (Restrepo et al., 2014).

Additional or alternative disc-intrinsic mechanisms may contribute to organ size in wing discs. Several hypotheses have been proposed that involve cells adopting graded positional values—which may or may not reflect the Dpp gradient—which the cells compare with their neighbors, perhaps by expressing cell surface proteins such as adhesion molecules in proportional amounts to the positional value. Cells that sense sufficient difference between their value and that of their neighbor divide and generate daughter cells with an intermediate value. This increases the total number of cells and reduces the magnitude of difference between adjacent cells. The process continues until cells are sufficiently similar to their neighbors that comparison does not trigger cell division, at which point growth terminates (Day & Lawrence, 2000; A. C. García-Bellido & García-Bellido, 1998; Wolpert, 1989). Other models of disc-autonomous size control invoke mechanical forces like stretch and compression as instructive inputs to growth of cells within the disc. The possibility of a mechanical component to organ size control is especially attractive in the light of the discoveries showing that a major growth control

pathway, the Hippo pathway, is capable of sensing and responding to physical cues (Dupont et al., 2011; Wada et al., 2021; Zhao et al., 2007).

It is important to note that no one hypothesis presented above fully explains or fits the available experimental data, and that the hypothesized mechanisms are not mutually exclusive (see also: Hariharan, 2015; Restrepo et al., 2014). The mystery of how organs terminate growth at the appropriate size remains unsolved and will likely require a synthesis of new research with the decades of experimental and theoretical work that scientists have already dedicated to this problem.

1.3 Echinoid is a cell adhesion molecule involved in development

Echinoid (Ed) is a cell adhesion molecule (CAM) that contains extracellular Ig and fibronectin type III domains, a transmembrane domain, and an intracellular domain with a PDZ-binding motif (Bai et al., 2001; Wei et al., 2005). Ed localizes to the adherens junctions *in vivo* (Escudero et al., 2003; Wei et al., 2005) and can promote aggregation of S2 cells *in vitro* through homophilic or heterophilic (with Neuroglian) interactions (Islam et al., 2003; Rawlins, Lovegrove, et al., 2003). The extracellular domain is required for Ed self-association and therefore cell-cell adhesion (Spencer & Cagan, 2003), and the intracellular domain is required for binding to intracellular partners such as Bazooka (Baz) and Canoe (Cno) (Wei et al., 2005).

The Ig-superfamily is the largest protein family in vertebrates and invertebrates, with over 100 identified member proteins in *Drosophila* alone (Shimono et al., 2012; C. Vogel et al., 2003). Proteins in this family share a common domain, the Ig-loop, and often participate in cellular recognition (via processes including adhesion, signaling, and guidance) in neurons and epithelia. Ed belongs to this superfamily and has been described as a nectin and an L1-type molecule. Vertebrate nectins—and their obligate intracellular binding partner Afadin (Cno in *Drosophila*)—localize to adherens junctions in epithelia cells and have roles in cell adhesion, migration, polarization, proliferation, and pattern formation (Takahashi et al., 1999; Takai et al., 2003, 2008; Togashi, 2016). L1 cell adhesion molecules have well-defined roles in neural processes like axon guidance and fasciculation (Hortsch, 1996; Rathjen & Schachner, 1984). Although Ed, nectins, and L1 CAMs are all calcium-independent members of the Ig-superfamily, Ed has neither sufficient sequence or structure similarity nor evidence of direct homology to warrant classification as an L1-type molecule (Hortsch, 2003) or nectin (Duraivelan & Samanta, 2020; Mandai et al., 2013; Tepass & Harris, 2007). Moreover, expression of some mammalian nectin isoforms in Ed-depleted cells failed to rescue phenotypes associated with Ed loss (Wei et al., 2005). Ed is still often considered a “functional analog” of nectins¹ on the basis of similar domains (extracellular Ig loops), localization to adherens junctions in epithelia, intracellular binding to Afadin/Cno, and developmental roles in adhesion and cell sorting (Finegan & Bergstralh, 2020). Ed has one paralogue in *Drosophila*, Friend of Echinoid (Fred) (Chandra et al., 2003).

¹Although some groups describe Ed as “nectin-like,” I advise against this terminology since it can mistakenly imply homology to the mammalian nectin-like (Necl) family of molecules, which, unlike Ed, *are* directly homologous to nectins.

Differences in cell adhesion can lead to cell sorting, where cells with different adhesiveness physically segregate from one another (Brodland, 2002; Steinberg, 1963). Such is the case with *ed*-expressing and -non-expressing cells: experimentally induced *ed* clones are much rounder than control clones and form a smooth boundary at the apical interface with wild-type neighbors. The borders of *ed* clones are deficient for adherens junction components including Ed and E-cadherin, and an actomyosin cable forms in the Ed-expressing cells at this interface (Wei et al., 2005). These features are also seen at endogenous interfaces between *ed*-expressing and -non-expressing cells, where they appear to serve important developmental functions. For example, follicular roof cells lack Ed but *ed* expression in neighboring cells is required for proper morphogenesis of the eggshell dorsal appendages. The actomyosin cable formed in *ed*-expressing leading edge epithelial cells at the interface with Ed-deficient amnioserosa cells is required for coordinated dorsal closure (Laplante & Nilson, 2006).

In addition to mediating cell-cell adhesion and cytoskeletal organization, Ed can interact with and modify multiple signal transduction pathways, including EGFR, Notch, and Hippo.

EGFR

A mutagenesis screen conducted by Bai et al., (2001) identified *ed* mutations as dominant enhancers of a hypermorphic allele of the EGF receptor, *Ellipse (Elp)*. This suggested that Ed may negatively regulate the EGFR pathway. It was shown that loss of *ed* in *Drosophila* eyes increases EGFR signaling in the areas where it normally occurs, leading to an excess of photoreceptors, cone cells, and pigment cells and aberrant photoreceptor specification (Bai et al., 2001; Rawlins, White, et al., 2003; Spencer & Cagan, 2003). Conversely, overexpression of *ed* reduces the number of cells with EGFR-dependent recruitment and/or specification in the eye (Islam et al., 2003), although EGFR signaling is not abolished (Spencer & Cagan, 2003). The antagonism of EGFR signaling by Ed requires the intracellular domain of Ed, whereas the extracellular domain is dispensable (Bai et al., 2001; Islam et al., 2003).

The interaction between *ed* and the EGFR pathway may be tissue-specific, since perturbations to *ed* do not affect EGFR signaling in the ovarian follicle during oogenesis (Bai et al., 2001; Laplante & Nilson, 2006). Furthermore, although Ed and EGFR also have opposing effect on sensory bristle specification in the thorax, genetic evidence suggests that this phenotype is driven primarily by synergistic interactions between *ed* and *Notch*, rather than a direct antagonism of EGFR (Escudero et al., 2003; Rawlins, Lovegrove, et al., 2003).

Genetic analyses of *ed*/EGFR pathway double-mutants initially suggested that *ed* regulates the EGFR pathway downstream of (or in parallel to) *ras/raf*, but upstream of *ttk88*, in a *sina*-independent fashion. However, additional experiments showed that Ed and EGFR can interact directly and that EGFR is capable of phosphorylating Ed (Spencer & Cagan, 2003) and that *ed* can interact with multiple branches of the EGFR pathway (Fetting et al., 2009), suggesting an upstream interaction with the pathway. It is possible

that *ed* regulates EGFR through modulation of endocytic trafficking. EGFR signaling is extensively regulated by receptor endocytosis (Brankatschk et al., 2012; Tomas et al., 2014; Vieira et al., 1996), Ed and EGFR colocalize in endocytic vesicles, and loss of *ed* reduces EGFR endocytosis in some cells of the eye (Ho et al., 2010). *ed* could antagonize EGFR signaling by promoting the endocytosis of activated EGFR receptors, which would attenuate their signaling. Additional experiments are needed to confirm this model, and it does not preclude additional layers of regulation through other mechanisms.

Notch

Lateral inhibition, enabled by the Notch pathway, is used both to limit the number of neuroectodermal cells adopting a neural fate during embryonic neurogenesis and to limit larval sensory organ precursor specification. A group of studies (Ahmed et al., 2003; Escudero et al., 2003; Rawlins, Lovegrove, et al., 2003) demonstrated that *ed* mutant embryos have neuronal hyperplasia and *ed* loss-of-function leads to sensory bristle duplications in adults, indicative of lateral inhibition failure. These phenotypes can be suppressed by Notch pathway activation and enhanced by Notch pathway inhibition. Additionally, loss of *ed* also resulted in other phenotypes characteristic of reduced Notch signaling, such as wing notching, thickening of wing veins, and reduced expression of Notch target genes. These characteristic phenotypes and genetic interactions suggested that *ed* cooperates with the Notch pathway to restrict neurogenesis.

While the exact mechanism of *ed*'s interaction with the Notch pathway is still unclear, epistasis experiments place Ed upstream of the Notch^{ICD} release (Escudero et al., 2003). Ed does not coimmunoprecipitate with Notch, which suggests it does not bind Notch directly (Escudero et al., 2003). Ed does colocalize with N and D1 at the cell surface and in early endosomes, and overexpression of *ed* reduces D1 levels (Rawlins, Lovegrove, et al., 2003). *Cis*-endocytosis of D1 is required for activation of Notch in the signal-receiving cell (Parks et al., 2000), so it is possible that *ed* promotes Notch signaling by promoting the trafficking and/or degradation of D1.

Hippo

A link between *ed* and the Hippo pathway was first established by Yue et al. (2012), who reported that Ed functions as a tumor suppressor that positively regulates Hippo signaling, thereby reducing the expression of pro-growth and pro-survival Yorkie target genes. *ed* mutant flies have overgrown wings (see also: Bai et al., 2001) and depletion of *ed* in the eye leads to eye overgrowth (Yue et al., 2012). Various readouts of Hippo pathway activity (e.g., levels of *Diap1*, *expanded*, and *bantam* expression; phosphorylation and subcellular localization of Yorkie) indicated decreased activity of the Hippo kinase cascade in cells lacking Ed. Biochemical analyses indicated that Ed interacts with Salvador, Expanded, Merlin, Yorkie, and Kibra through its intracellular domain. These observations, combined with examination of Salvador levels and localization in WT and *ed*-depleted cells and tissues, led the authors to propose a model where Ed promotes signaling through the Hippo pathway through the stabilization and apical localization of Sav.

Another study, by Ding et al. (2016), examines Hippo pathway signaling in the context of neural stem cell activation. The authors manipulate two cell surface proteins, Ed and Crumbs (Crb), which both allegedly behave as tumor suppressors that restrict growth through the Hippo pathway. The evidence supporting this assumption is strong in the case of Crb (Chen et al., 2010; Grzeschik et al., 2010; Ling et al., 2010; Robinson et al., 2010) but in the case of Ed rests solely on the conclusions of Yue et al. (2012). Loss of either Ed or Crb leads to precocious reactivation of quiescent neural stem cells (NSCs), a phenotype which can result from activation of Yorkie target genes via the Hippo pathway (R. Ding et al., 2016; Poon et al., 2016). NSC reactivation is known to be triggered by nutrition (Chell & Brand, 2010; Sousa-Nunes et al., 2011), and expression of both Ed and Crb decreases at the onset of feeding. Although the authors claim that loss of Ed and Crb leads to reactivation because of their roles in the Hippo pathway, they do not present any evidence corroborating the claim that loss of Ed alone leads to decreased expression of Yorkie target genes. All experiments demonstrating a change to Hippo pathway read-outs are done with simultaneous depletion of Crb and Ed. The possibility remains that Crb is the primary driver of reactivation via the Hippo pathway, and that Ed loss promotes neural stem cell reactivation through a different mechanism. *ed* loss-of-function decreases Notch signaling and increases EGFR signaling; low levels of Notch are required for NSC reactivation in *Drosophila* (Sood et al., 2022), and increased EGFR signaling promotes the activation of other stem cell populations in *Drosophila*, including renal (Li et al., 2015) and intestinal stem cells (Buchon et al., 2010; Jiang et al., 2011; N. Xu et al., 2011).

1.4 Goals and overview of dissertation research

The growth and survival of a cell depends not just on its own intrinsic properties, but also on the interactions it has with its neighbors. With this in mind, I conducted a genetic screen by generating mosaic wing imaginal discs which contain RNAi clones surrounded by wild-type tissue. I screened RNAi lines targeting putative or known cell adhesion genes and identified nine which impacted the shape, size, or abundance of clones. I focused on characterizing one hit, *echinoid* (*ed*), because knockdown of *ed* in clones reduced clone size and number, but homogenous knockdown of *ed* leads to tissue overgrowth. The fact that *ed* reduction can result in seemingly different phenotypes in different contexts—clonal undergrowth in mosaics and tissue overgrowth in non-mosaics—suggests that the influence of neighboring cells may determine the outcome.

In **Chapter 2**, I describe the genetic screen and characterize the phenotypes associated with *ed* reduction in clones. I show that *ed* tissues expresses lower levels of the anti-apoptotic protein Diap1 and consequently have increased rates of apoptosis. This increase in cell death contributes significantly to the elimination of *ed* clones in mosaic tissues.

In **Chapter 3**, I focus on characterizing the phenotypes associated with *ed* loss in broader domains. I confirm that *ed*-depleted tissues can overgrow and show that these tissues fail to arrest growth at the appropriate final size, even when growing slower than wild-type tissue.

The phenotypes caused by *ed* loss in clones and in homogenous tissues are seemingly contradictory not just to each other, but also to what has been previously reported about *ed* (namely, that Ed restricts growth via interactions with the members of Hippo pathway). If Ed indeed restricts growth via Hippo pathway activation, then clones of cells lacking *ed* would be expected to have increased levels of Diap1 and behave as supercompetitors, which is not what I observed in Chapter 2. I investigate this contradiction in **Chapter 4** by examining the response of various Hippo pathway target genes to *ed* manipulations. I find that many, but not all, Hippo pathway target genes are reduced in *ed*-depleted tissues, and that the nuclear localization of Yki is not obviously impacted by *ed* loss. These results are inconsistent with the prevailing model of how *ed* regulates the Hippo pathway. Furthermore, I show that some Hippo pathway targets are increased in the neighbors of *ed*-depleted cells. In this way the neighbors resemble cells that behave as supercompetitors, which might also contribute to the elimination of *ed* clones.

In **Chapter 5**, I turn to the question of why *ed*-depleted organs overgrow. I designed a screen to identify dominant modifiers of the overgrowth phenotype caused by *nub-Gal4* driving the expression of *UAS-ed-RNAi* in the wing pouch. Initially, it appeared that the *upd2* gene genetically interacts with *ed* to reduce overgrowth and enhance cell death. However, I ultimately determined that this conclusion is unfounded. The phenotypes observed reflect the activity of a *UAS* misexpression construct present in the *upd2 Δ* allele, which interacts with *nub-Gal4* independently of *ed*. Although the question of why *ed*-depleted tissues overgrow remains unresolved, this line of investigation revealed important information about reagents which may be of interest to other researchers.

2 *ed* loss leads to apoptotic clonal elimination

2.1 Introduction

Mutations can occur in all cells of an organism, such as when germline mutations are inherited, or mosaically, such as when somatic mutations arise during development or in adulthood. In the mosaic context, phenomena like cell competition can occur, where the growth or survival of one cell type depends on the influence of its neighbors. This kind of non-autonomous growth regulation requires that cells compare themselves to their neighbors and adjust their behavior accordingly. Interestingly, many forms of cell competition are triggered by differences in intracellular components like the dosage of ribosomal genes or transcription factors, and it is not obvious how this difference is communicated between neighboring cells.

We hypothesized that cell-cell adhesion molecules (CAMs) might mediate survival or growth of cells in mosaic contexts since these molecules physically connect cells to their neighbors and many also have intracellular signaling functions. CAMs are expressed at the cell surface, placing them in correct location to function in a comparison process. Many also function as signaling molecules, which could allow for that information to be transmitted to the other parts of the cell (Fagotto & Gumbiner, 1996; Ruoslahti & Öbrink, 1996). A few CAMs have already been shown to impact growth, such as the large protocadherins Fat (Ft) and Dachshous (Ds), which can regulate the activity of the growth-restricting Hippo pathway. *Drosophila* have over one hundred unique CAMs, and many have been extensively studied in the contexts of epithelial organization or axonal pathfinding (Finegan & Bergstralh, 2020). However, despite being well-suited candidates for mediating processes like competition the impact of CAMs on regulating growth in mosaics has not been systematically explored.

Here I describe a genetic screen where we perturb the expression of cell adhesion molecules in a mosaic context and assess the impact on clonal growth and survival. We identified several hits—some previously characterized, others novel—and characterize one hit, *echinoid* (*ed*), in depth. In this chapter I focus on the phenotypes associated with loss of *ed* in clones specifically. I demonstrate that *ed* clones are eliminated from mosaic tissues due to increased apoptosis resulting, at least in part, from an autonomous decrease in the anti-apoptotic protein Diap1.

2.2 Results

A genetic screen for cell adhesion molecules which regulate growth in mosaics

We designed an RNAi screen to identify adhesion genes whose knockdown in clones affects clone size, shape, or number in the *Drosophila* wing disc epithelium. We used a brief heat shock to induce FLP-out Gal4 clones that express *UAS-RNAi* and a *UAS*-driven fluorescent protein (most expressed *UAS-GFP*, but a subset of lines was screened using the TIE-DYE clone generation system [Worley et al., 2013] express *UAS-RFP*). These

discs were examined by fluorescence microscopy; any RNAi lines that caused dramatic changes to the size and/or number of the marked clones, as compared to a *UAS-w-RNAi* control generated in the same manner, were flagged for further investigation.

I generated an initial candidate list of 151 known or putative cell-cell adhesion genes in *Drosophila*, composed of molecules containing cadherin or immunoglobulin domains as identified by Hynes & Zhao (2000) or Vogel et al. (2003) or curated manually (Table 2.1). Since this screen was conducted in the wing disc, I removed 43 genes with no expression in the wing imaginal disc epithelium based on a scRNA-seq dataset of 96h and 120h wing discs (Everetts et al., 2021). I additionally removed 9 which encode molecules known to not have adhesive functions (e.g., sarcomere components) (Table 2.2), which reduced the candidate pool to 99 genes. We screened 90 RNAi lines that targeted 74 unique genes. Of the genes screened, 7 caused a clonal undergrowth phenotype and 4 influenced clone morphology (Figure 2.1) (Table 2.3).

Increasing throughput of the screen came at the expense of tight control of developmental timing and larval density. We balanced the tradeoffs by using approximately the same number of parental flies per cross and limited egg laying to a 1-day interval as rough age- and density-control measures. This methodology was prone to batch effects and led to a control range of clone size and number that was sufficiently broad to limit the sensitivity of our assay such that only very strong effects on growth could be confidently identified. Due to these limitations, we focused our efforts on characterizing a single hit rather than screening all genes in the initial candidate pool. We chose to focus on *ed* because *ed-RNAi* clones are underrepresented but *ed*-depleted organs are viable and reported to overgrow (Yue et al., 2012), suggesting that Ed's impact on growth may be context-dependent.

Clones of cells lacking Echinoid are eliminated from the wing and eye disc epithelia
RNAi clones made using multiple RNAi lines (V104279, V3087, V938) targeting *ed* yielded wing discs with sparse, small, round clones that form smooth borders with wild-type neighbors (Figure 2.1J-L). The underrepresentation phenotype was more pronounced using V104279 or V3087 than with V938, consistent with another report that V104279 and V3087 produce stronger knockdown phenotypes than V938 (Yue, 2011). Unless otherwise noted, additional RNAi experiments were done using V104279, which is hereafter referred to as *UAS-ed-RNAi*. The round, smooth shape of these clones has also been previously documented (Chang et al., 2011; Escudero et al., 2003; Wei et al., 2005) and other groups have previously reported difficulty in recovering *ed*-depleted clones (Escudero et al., 2003; Wei et al., 2005). No mechanism has been proposed to explain why these clones are difficult to recover.

Generation of *ed*^{-/-} clones using the Mosaic Analysis of a Repressible Cell Marker (MARCM) technique (Lee & Luo, 1999) also yielded a clonal underrepresentation phenotype: *ed*^{IF20} or *ed*^{lx5} null clones were almost never recovered in the wing disc epithelium (Figure 2.2B, C), although large clones in the disc-associated myoblasts, as determined by cell morphology and location (non-epithelial and basal to the notum region of the disc proper), were often observed (Figure 2.2B'). MARCM clones made using the

hypomorphic *ed^{sIH8}* missense allele were more readily recovered than those made using null alleles but were still rarer than control clones (Figure 2.3D). Unless otherwise noted, “*ed*” is hereafter used synonymously with *ed^{lF20}*.

In their original description of cell competition, Morata & Ripoll (1975) observed that *Minute* clones were eliminated when they were generated early in development but were still observable when they were generated much later. To determine if this was also the case with *ed* clones, we used mitotic recombination to generate marked *ed^{-/-}* and *ed^{+/+}* twin clones in wing discs (Figure 2.3A). When wing discs were examined only 24h after clone induction, both *ed^{-/-}* and their *ed^{+/+}* twin clones were observed and were of similar size (Figure 2.3B, C). However, when clones were induced by heat shock 72h prior to dissection, no associated *ed^{-/-}* clones were observed in the wing discs despite the presence of large *ed^{+/+}* twins (Figure 2.3D, E). These data confirm that *ed* clones are initially generated, but subsequently eliminated from the wing disc epithelium. We also used *eyFLP*-driven mitotic recombination to generate mosaic eyes with white and red twin clones. A control condition which generates red and white twin clones, but does not alter *ed* expression, yielded eyes with roughly equal proportions of red and white tissue. When mitotic recombination generated white *ed^{-/-}* and red *ed^{+/+}* tissue, the adult eyes contained little to no white *ed^{-/-}* tissue (Figure 2.4). Taken together, these results indicate that clones of cells lacking *ed* survive for a short period of time before being eliminated from mosaic imaginal epithelia.

Elimination of *ed*-depleted clones depends on apoptosis

We hypothesized that the loss of *ed*-depleted clones from mosaic tissues could be explained by two general mechanisms: 1) physical expulsion of the mutant cells, and/or 2) death of the mutant cells. An expulsion mechanism of mutant clones has precedent; patches of cells misexpressing selector genes or activated Ras form round clones that are subsequently extruded from tissues as cysts (Bielmeier et al., 2016). If this mechanism explained the elimination of *ed^{-/-}* clones, we would expect to observe extruded cysts located outside the plane of the disc epithelium. Although *ed^{-/-}* clones have some features also seen in early-stage extruding cysts (rounded shape, smooth interface with wild-type neighbors, apical constriction) (Chang et al., 2011; Wei et al., 2005), close examination of discs following the generation of MARCM clones never uncovered evidence of extruded *ed^{-/-}* cysts that are discontinuous with the disc epithelium (nor were extruded cysts ever observed in discs with clones generated by any method used in this study). Although we cannot rule out physical expulsion entirely—especially if expelled cells subsequently die, as is sometimes the case (Bielmeier et al., 2016)—we conclude that large-scale cystic extrusion does not account for the elimination of *ed*-depleted clones.

To assess whether apoptosis plays a role in the elimination of *ed* clones, we measured caspase activity using an antibody recognizing cleaved death caspase-1 (Dcp-1), the activated effector caspase in *Drosophila*, in mosaic discs. We observed increased apoptosis in *ed-RNAi* clones as compared to neighboring WT tissue or control (*w-RNAi*) clones. Dcp-1 staining was especially apparent at clone boundaries, which may indicate that competition at the clone interface plays a role (Figure 2.5A-B). We also examined apoptosis when knocking down *ed* in a broader region, the *nubbin* domain (Figure 2.5C-

D). In this case, we still observed an overall increased level of apoptotic cell death in the *ed-RNAi*-expressing discs even far from the boundary with wild-type cells under conditions of *ed* knockdown. These results indicate that loss of *ed* leads to increased apoptosis in clonal and non-clonal contexts.

If apoptosis is indeed a major driver of *ed*^{-/-} clonal elimination as we suspected, then preventing apoptosis should also prevent the elimination. To test this hypothesis, we generated *ed-RNAi* clones that also express the anti-apoptotic gene *p35*. We observed that *ed-RNAi*, *p35* clones were recovered at a much higher rate than clones expressing *ed-RNAi* alone, which further supports the conclusion that apoptosis is a driver of *ed*^{-/-} clonal elimination (Figure 2.6).

Diap1 is reduced in *ed* clones

To understand why *ed*-depleted cells undergo apoptosis, we examined Diap1, a protein upstream of caspase activation in the apoptotic regulatory module which inhibits apoptosis. Antibody staining of *ed-RNAi* clones showed decreased Diap1 protein levels as compared to neighboring wild-type cells (Figure 2.7), contrary to what has been reported elsewhere (Yue et al., 2012). We often observed increased Diap1 protein in the immediate neighbors of *ed*-depleted clones—we examine this phenomenon in greater detail later (see Chapter 4, Figure 4.1 and associated text).

To determine whether *diap1* transcription is altered in *ed*^{-/-} clones, we performed Hybridization Chain Reaction to label *diap1* transcripts. We did not observe noticeable differences in mRNA levels between *ed-RNAi* clones and wild-type neighbors (Figure 2.8A). We also examined a reporter line that expresses GFP under the control of an array of eight identical Hippo Response Elements isolated from the *diap1* locus (*diap1-GFP.HREx8*) (Wu et al., 2008). The repeated array can amplify small differences in transcription, making it a highly sensitive qualitative assay for relative levels of Yki-dependent *Diap1* transcriptional activity. We observed lower expression levels of the *diap1-GFP.HREx8* reporter inside of *ed-RNAi* clones (Figure 2.8B). These results indicate that *ed* loss in clones reduces Hippo pathway-dependent *diap1* transcription, although overall mRNA abundance is not dramatically affected.

2.3 Discussion

Our genetic screen uncovered cell adhesion molecules whose knockdown affects cell growth and adhesion. Some of these hits were expected: the low viability of *shg* and *ed* clones, and the round, un-elongated phenotype of *ft* and *ds* clones have been well-documented elsewhere (Baena-López et al., 2005; Hall et al., 2019; Mao et al., 2011). *ama*, *sidestep-VII*, and *beat-Vc* are all known to mediate axon guidance, and the low viability of clones knocking down these genes in the wing discs suggest they could have unexplored roles in epithelial growth or survival. Clones depleted of *Contactin*, which encodes a component of septate junctions, also had low viability. We observed that *otk2* RNAi clones had regional differences in viability and that hinge clones were expelled as cysts from the disc epithelia. Understanding the regional variation in the response to *Otk2* loss in the disc epithelium remains an interesting and unexplored avenue for future research.

Our genetic screen also identified Ed as a cell adhesion molecule whose depletion leads to a clonal growth disadvantage. We found that *ed*-depleted clones are initially created but subsequently eliminated from imaginal disc epithelia in an apoptosis-dependent fashion. The increase in apoptosis is associated with a decrease in the levels of the anti-apoptotic protein, Diap1.

The reduction of Diap1 can account for the increase in apoptosis observed in *ed* clones, but questions remain about how loss of *ed* leads to a reduction in Diap1. We showed that Hippo pathway-dependent transcription of *diap1* is reduced in *ed* clones, but overall levels of *diap1* transcripts are not noticeably affected. Very subtle changes to mRNA level could potentially account for the more dramatic difference in protein levels if it reduces the rate of translation because Diap1 has a short half-life (Holley et al., 2002) and short-lived proteins are sensitive to translational regulation. It is also possible that a post-translational mechanism like proteasomal degradation could account for the greater reduction in Diap1 protein than mRNA.

In this chapter we have primarily focused on characterizing the phenotypes associated with mosaic loss of Ed. In the next chapter, we explore the effect of Ed depletion in a homogenous context.

2.4 Figures and tables

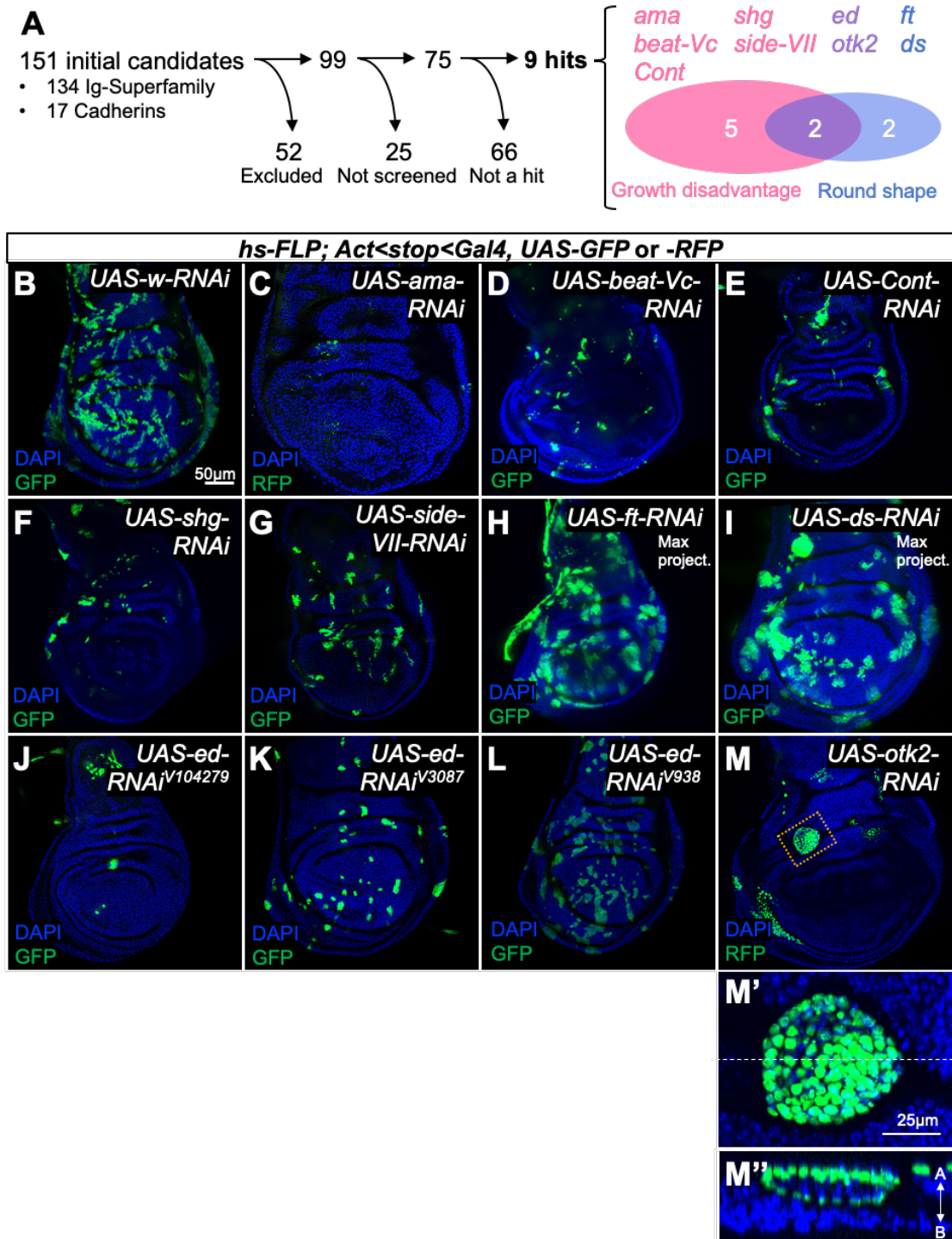


Figure 2.1: A genetic screen to identify CAMs which regulate growth in mosaics.

A) Overview of screen. B-M) Wing imaginal discs containing FLP-out Gal4 clones (green) expressing *RNAi* targeting a control gene, *white* (*w*) (B), or screen candidate genes (C-M). Control clones (B) are abundant and jagged in shape. Clones with *RNAi*

targeting *amalgam* (*ama*) (C), *beaten path Vc* (*beat-Vc*) (D), *Contactin* (*Cont*) (E), *shotgun* (*shg*) (F), or *sidestep VII* (*side-VII*) (G), have clones that are smaller and fewer in number than control clones. Clones with RNAi targeting *fat* (*ft*) (H) or *dachsous* (*ds*) (I) have a rounded morphology. Three RNAis targeting *echinoid* (*ed*) (J-L) led to clones which are small, round, smooth, and underrepresented in the disc epithelium. Clones with RNAi targeting *off-track2* (*otk2*) (M) were rarely recovered in the pouch and formed round cysts in the hinge. M' shows a magnified view of the yellow dashed box in M. M'' shows the X-Z plane through the dashed line in M'. A round, RFP+ cyst is visible in the apical space between the disc proper and peripodial epithelium. All clones were made using FLP-out Gal4, *UAS-GFP*, except the clones in C and M which were generated using the TIE-DYE technique. Control clones generated with TIE-DYE were similar in abundance and morphology to the FLP-out Gal4, *UAS-GFP* control in (A). Scale bars: 50 μ m (B-M), 25 μ m (M'-M'').

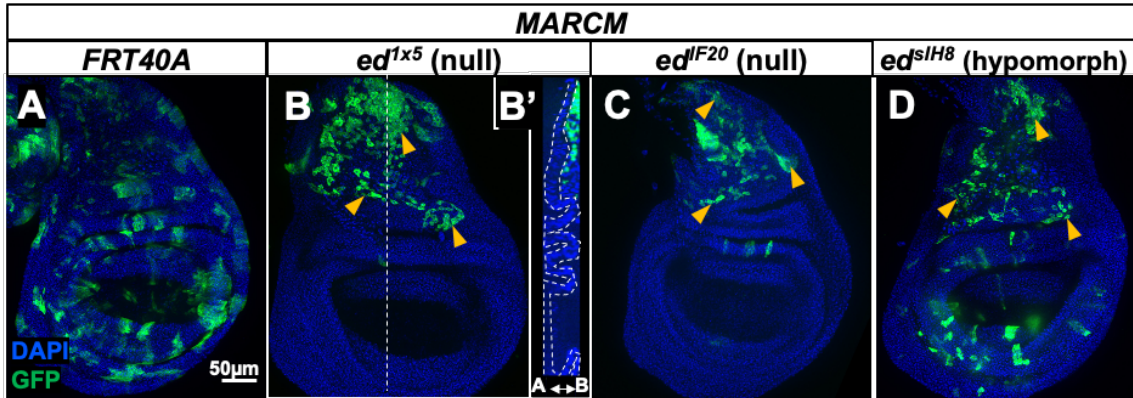


Figure 2.2: MARCM *ed* clones are underrepresented, small, and round in the wing disc epithelium.

Wing imaginal discs containing GFP-labeled MARCM clones (green) that are homozygous for WT *ed* (*FRT40A* control) (A), *ed*^{1x5} (null) (B), *ed*^{IF20} (null) (C), or *ed*^{siH8} (hypomorph) (D). *ed*^{-/-} clones are sparse or absent in the wing disc epithelium, although *ed*^{-/-} myoblast clones are readily recovered (B'). A-D are maximum intensity projections of Z-stacks. Scale bars: 50µm.

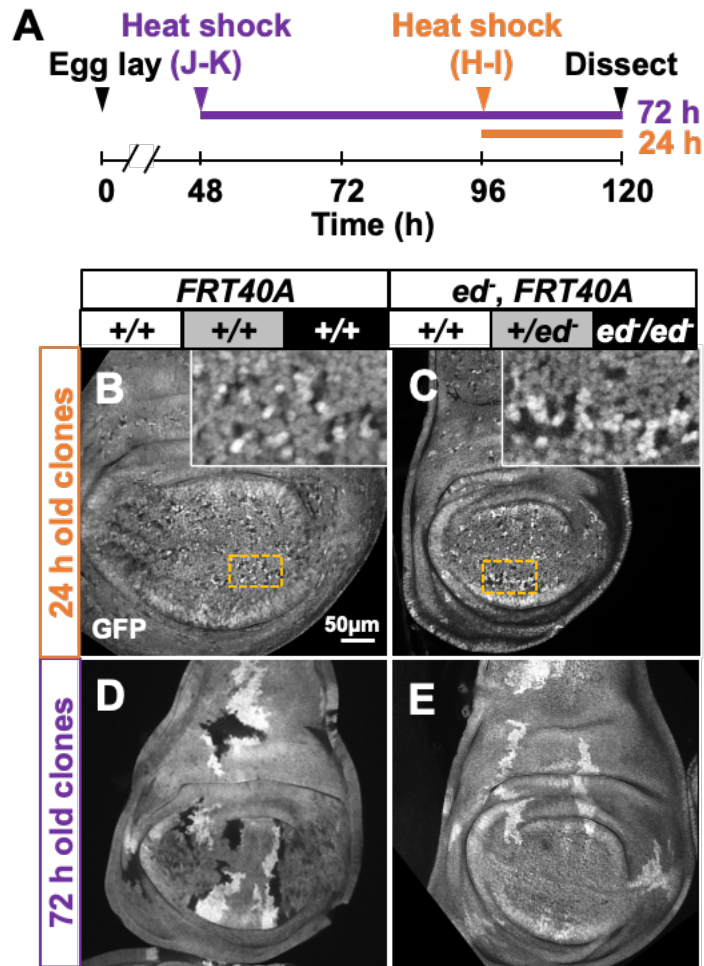


Figure 2.3: *ed*^{-/-} clones are eliminated from the wing disc epithelium.

A) Timeline of experiment. GFP-negative and GFP double-positive twin clones were induced by mitotic recombination in a heterozygous background 24h (B, C) or 72h (D, E) before dissection. When clones were induced 24h before dissection, GFP-positive and GFP-negative twin clones are recovered in both the *FRT40A* control condition (B, see inset) and when heterozygosity of *ed* is lost in twin clones (C, see inset). When clones were induced 72h before dissection, GFP-positive and GFP-negative twin clones are recovered in the *FRT40A* control condition (D). However, when heterozygosity of *ed* is lost in twin clones (E), the GFP-negative, *ed*^{-/-} twin clones are not recovered. Scale bars: 50µm.

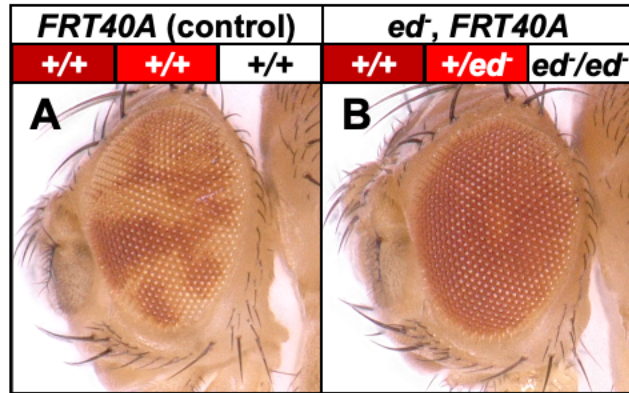


Figure 2.4: *ed*^{-/-} clones are eliminated from the eye.

Red and white twin clones were induced at initially equal proportions by mitotic recombination in a heterozygous background using *eyeless-FLP*. A) Red and white eye tissues are recovered in equal proportions in the *FRT40A* control condition. B) Little to no white tissue is recovered when the white tissue is *ed*^{-/-}.

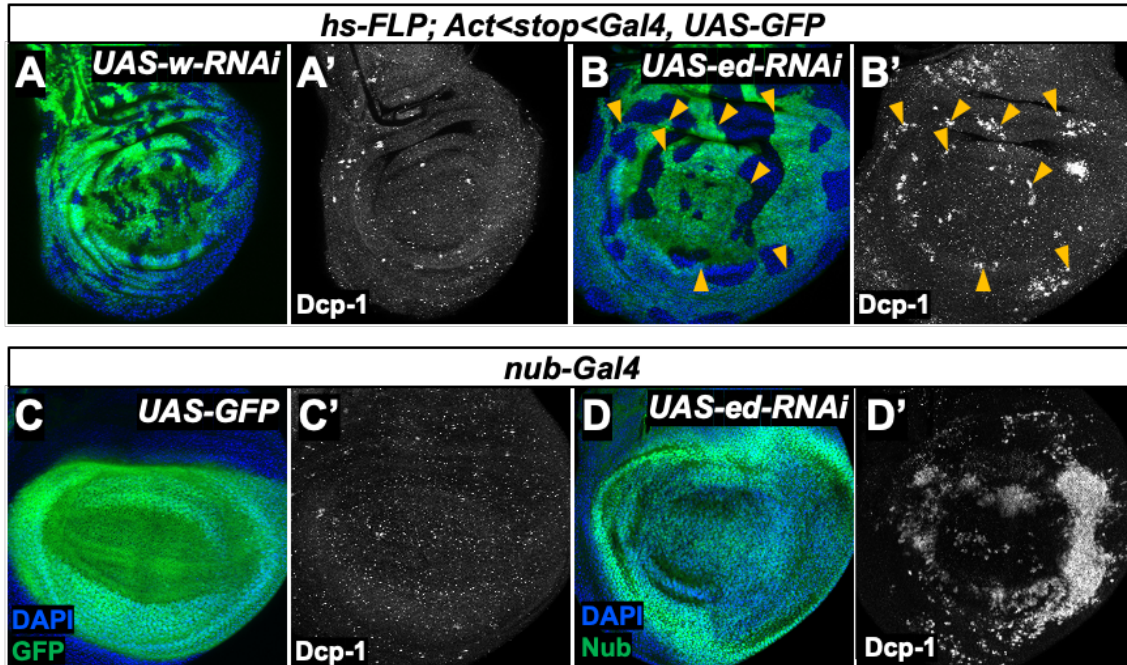


Figure 2.5: Elevated levels of apoptosis are seen in *ed-RNAi* tissue.

A) Very few Dcp-1+ cells are seen in discs with GFP-labeled *w-RNAi* clones. B) Dcp-1+ cells are abundant within GFP-labeled *ed-RNAi* clones, particularly at clone boundaries. Arrowheads in B and B'' indicate instances of cell death at clone boundaries. C) Very few Dcp-1+ cells are seen in discs with *nub-Gal4* driving expression of *UAS-GFP*. D) apoptosis levels are elevated in discs with *nub-Gal4* driving expression of *UAS-ed-RNAi*. Note: small white speckles seen in all Dcp-1 channels are background staining. Scale bars: 50µm.

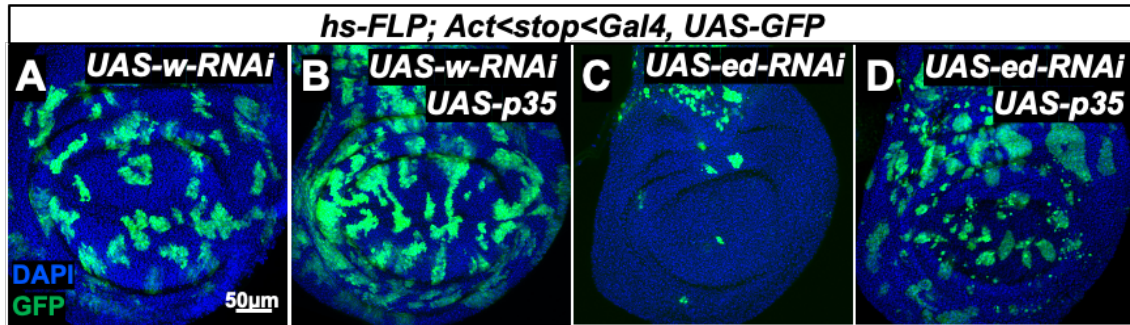


Figure 2.6: Blocking apoptosis rescues elimination of *ed-RNAi* clones.

Wing imaginal discs containing FLP-out Gal4 clones (green) that express *UAS-GFP* and *UAS-RNAi* targeting *w* alone (A), *w* with simultaneous expression of the anti-apoptotic protein p35 (B), *ed* alone (C), or *ed* with simultaneous expression of the anti-apoptotic protein p35 (D). All clones were generated 3 days after egg lay using a 12-minute heat shock to induce *hs-FLP*. Scale bars: 50µm.

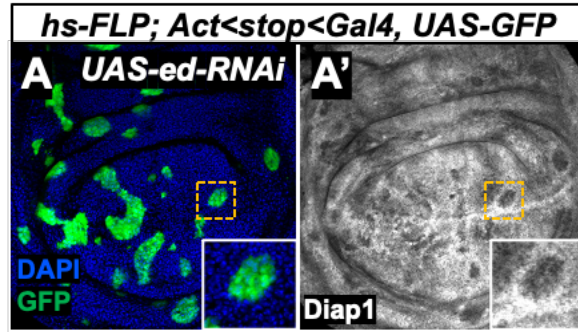


Figure 2.7 Diap1 is reduced in *ed-RNAi* clones.

ed-RNAi in wing disc clones leads to an autonomous decrease of Diap1 protein level. Insets show a clone at higher magnification. Scale bars: 25µm.

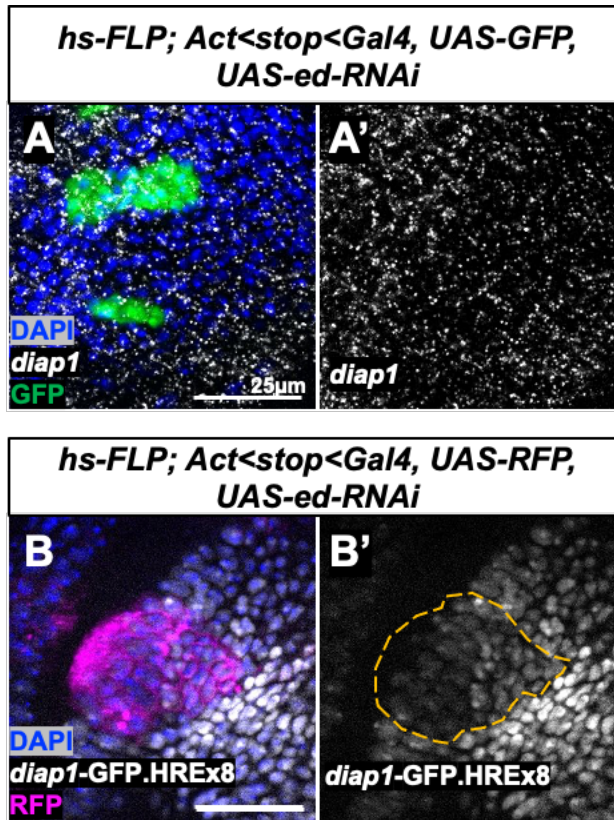


Figure 2.8 Hippo pathway-dependent transcription of *diap1* is reduced in *ed-RNAi* cells, but overall *diap1* transcript levels are similar to wild-type.

A) GFP+ cells express *ed-RNAi*. A') *diap1* transcripts are similarly abundant within and outside of GFP+ clones. B) RFP+ cells express *ed-RNAi*. B') the *diap1-GFP.HREx8* reporter is lower within the RFP+ clone (dashed yellow outline). Scale bars: 25µm.

Table 2.1: Initial candidate list.

Gene abbrev.	Gene name	Type	Source
Cad74A	Cadherin 74A	Cadherin	Hynes 2000
Cad86C	Cadherin 86C	Cadherin	Hynes 2000
Cad87A	Cadherin 87A	Cadherin	Hynes 2000
Cad88C	Cadherin 88C	Cadherin	Hynes 2000
Cad89D	Cadherin 89D	Cadherin	Hynes 2000
Cad96Ca	Cadherin 96Ca	Cadherin	Hynes 2000
Cad96Cb	Cadherin 96Cb	Cadherin	Hynes 2000
Cad99C	Cadherin 99C	Cadherin	Hynes 2000
CadN	Cadherin-N	Cadherin	Hynes 2000
CadN2	Cadherin-N2	Cadherin	Hynes 2000
Cals	Calsyntenin-1	Cadherin	Hynes 2000
ds	dachsous	Cadherin	Hynes 2000
ft	fat	Cadherin	Hynes 2003
Kug	kugelei	Cadherin	Hynes 2000
Ret	Ret oncogene	Cadherin	Manual curation
shg	shotgun	Cadherin	Hynes 2000
stan	starry night	Cadherin	Hynes 2000
ama	amalgam	IgSF	Hynes 2000, Vogel 2003
babos	babos	IgSF	Hynes 2000, Vogel 2003
bdl	borderless	IgSF	Hynes 2000, Vogel 2003
beat-Ia	beaten path Ia	IgSF	Hynes 2000, Vogel 2003
beat-Ib	beaten path Ib	IgSF	Hynes 2000, Vogel 2003
beat-Ic	beaten path Ic	IgSF	Hynes 2000, Vogel 2003
beat-IIa	beaten path IIa	IgSF	Hynes 2000, Vogel 2003
beat-IIb	beaten path IIb	IgSF	Hynes 2000, Vogel 2003
beat-IIIa	beaten path IIIa	IgSF	Vogel 2003

beat-IIIb	beaten path IIIb	IgSF	Vogel 2003
beat-IIIc	beaten path IIIc	IgSF	Vogel 2003
beat-IV	beaten path IV	IgSF	Vogel 2003
beat-Va	beaten path Va	IgSF	Vogel 2003
beat-Vb	beaten path Vb	IgSF	Vogel 2003
beat-Vc	beaten path Vc	IgSF	Vogel 2003
beat-VI	beaten path VI	IgSF	Vogel 2003
beat-VII	beaten path VII	IgSF	Vogel 2003
boi	brother of ihog	IgSF	Hynes 2000, Vogel 2003
bsg	basigin	IgSF	Vogel 2003
bt	bent	IgSF	Hynes 2000, Vogel 2003
CG13506	CG13506	IgSF	Hynes 2000, Vogel 2003
CG13532	CG13532	IgSF	Hynes 2000, Vogel 2003
CG13992	CG13992	IgSF	Vogel 2003
CG15312	CG15312	IgSF	Hynes 2000, Vogel 2003
CG15744	CG15744	IgSF	Vogel 2003
CG16974	CG16974	IgSF	Hynes 2000, Vogel 2003
CG17839	CG17839	IgSF	Hynes 2000, Vogel 2003
CG31431	CG31431	IgSF	Vogel 2003
CG33543	CG33543	IgSF	Hynes 2000, Vogel 2003
CG34353	CG34353	IgSF	Vogel 2003
CG44153	CG44153	IgSF	Vogel 2003
CG45263	CG45263	IgSF	Hynes 2000, Vogel 2003
CG5597	CG5597	IgSF	Hynes 2000, Vogel 2003
CG6867	CG6867	IgSF	Hynes 2000, Vogel 2003

CG7166	CG7166	IgSF	Hynes 2000, Vogel 2003
CG7607	CG7607	IgSF	Hynes 2000, Vogel 2003
Cont	Contactin	IgSF	Hynes 2000, Vogel 2003
DIP-alpha	Dpr-interacting protein alpha	IgSF	Vogel 2003
DIP-beta	Dpr-interacting protein beta	IgSF	Hynes 2000, Vogel 2003
DIP-delta	Dpr-interacting protein delta	IgSF	Hynes 2000, Vogel 2003
DIP-epsilon	Dpr-interacting protein epsilon	IgSF	Vogel 2003
DIP-eta	Dpr-interacting protein eta	IgSF	Hynes 2000, Vogel 2003
DIP-gamma	Dpr-interacting protein gamma	IgSF	Hynes 2000, Vogel 2003
DIP-iota	Dpr-interacting protein iota	IgSF	Hynes 2000, Vogel 2003
DIP-kappa	Dpr-interacting protein kappa	IgSF	Vogel 2003
DIP-lambda	Dpr-interacting protein lambda	IgSF	Manual curation
DIP-theta	Dpr-interacting protein theta	IgSF	Hynes 2000, Vogel 2003
DIP-zeta	Dpr-interacting protein zeta	IgSF	Hynes 2000, Vogel 2003
dpr1	defective proboscis extension response 01	IgSF	Vogel 2003
dpr10	defective proboscis extension response 10	IgSF	Hynes 2000, Vogel 2003
dpr11	defective proboscis extension response 11	IgSF	Hynes 2000, Vogel 2003
dpr12	defective proboscis extension response 12	IgSF	Hynes 2000, Vogel 2003
dpr13	defective proboscis extension response 13	IgSF	Hynes 2000, Vogel 2003
dpr14	defective proboscis extension response 14	IgSF	Hynes 2000, Vogel 2003
dpr15	defective proboscis extension response 15	IgSF	Hynes 2000, Vogel 2003
dpr16	defective proboscis extension response 16	IgSF	Hynes 2000, Vogel 2003

dpr17	defective proboscis extension response 17	IgSF	Hynes 2000, Vogel 2003
dpr18	defective proboscis extension response 18	IgSF	Hynes 2000, Vogel 2003
dpr19	defective proboscis extension response 19	IgSF	Vogel 2003
dpr2	defective proboscis extension response 02	IgSF	Hynes 2000, Vogel 2003
dpr20	defective proboscis extension response 20	IgSF	Hynes 2000, Vogel 2003
dpr21	defective proboscis extension response 21	IgSF	Manual curation
dpr3	defective proboscis extension response 03	IgSF	Hynes 2000, Vogel 2003
dpr4	defective proboscis extension response 04	IgSF	Hynes 2000, Vogel 2003
dpr5	defective proboscis extension response 05	IgSF	Hynes 2000, Vogel 2003
dpr6	defective proboscis extension response 06	IgSF	Manual curation
dpr7	defective proboscis extension response 07	IgSF	Vogel 2003
dpr8	defective proboscis extension response 08	IgSF	Hynes 2000, Vogel 2003
dpr9	defective proboscis extension response 09	IgSF	Hynes 2000, Vogel 2003
Dscam1	Down syndrome cell adhesion molecule 1	IgSF	Hynes 2000, Vogel 2003
Dscam2	Down syndrome cell adhesion molecule 2	IgSF	Hynes 2000, Vogel 2003
Dscam3	Down syndrome cell adhesion molecule 3	IgSF	Hynes 2000, Vogel 2003
Dscam4	Down syndrome cell adhesion molecule 4	IgSF	Hynes 2000, Vogel 2003
ed	echinoid	IgSF	Hynes 2000, Vogel 2003
Eph	Eph receptor tyrosine kinase	IgSF	Hynes 2000, Vogel 2003
Fas2	Fasciclin 2	IgSF	Hynes 2000, Vogel 2003
Fas3	Fasciclin 3	IgSF	Vogel 2003

fipi	factor of interpulse interval	IgSF	Hynes 2000, Vogel 2003
fra	frazzled	IgSF	Hynes 2000, Vogel 2003
fred	friend of echinoid	IgSF	Hynes 2000, Vogel 2003
hbs	hibris	IgSF	Hynes 2000, Vogel 2003
hig	hikaru genki	IgSF	Hynes 2000, Vogel 2003
ihog	interference hedgehog	IgSF	Hynes 2000, Vogel 2003
Imp-L2	Ecdysone-inducible gene L2	IgSF	Hynes 2000, Vogel 2003
kek1	kekkon-1	IgSF	Hynes 2000, Vogel 2003
kek2	kekkon-2	IgSF	Hynes 2000, Vogel 2004
kek3	kekkon-3	IgSF	Hynes 2000, Vogel 2005
kek4	kekkon4	IgSF	Hynes 2000, Vogel 2006
kek5	kekkon5	IgSF	Hynes 2000, Vogel 2007
kek6	kekkon 6	IgSF	Vogel 2003
kirre	kin of irre	IgSF	Hynes 2000, Vogel 2008
klg	klingon	IgSF	Hynes 2000, Vogel 2009
Lac	Lachesin	IgSF	Hynes 2000, Vogel 2003
Lar	Leukocyte-antigen-related-like	IgSF	Vogel 2003
lbk	lambik	IgSF	Vogel 2003
MnM	myomesin and myosin binding protein	IgSF	Hynes 2000, Vogel 2003
nepl6	Neprilysin-like 6	IgSF	Hynes 2000
nkt	noktochor	IgSF	Hynes 2000, Vogel 2003
nolo	no long nerve cord	IgSF	Hynes 2000, Vogel 2005

Nrg	Neuroglian	IgSF	Hynes 2000, Vogel 2003
nrm	neuromusculin	IgSF	Hynes 2000, Vogel 2004
otk	off-track	IgSF	Hynes 2000, Vogel 2006
otk2	off-track2	IgSF	Hynes 2000, Vogel 2007
plum	plum	IgSF	Hynes 2000, Vogel 2003
ppk12	pickpocket 12	IgSF	Vogel 2003
ppn	papilin	IgSF	Vogel 2003
Ptp69D	Protein tyrosine phosphatase 69D	IgSF	Hynes 2000, Vogel 2003
Pvr	PDGF- and VEGF-receptor related	IgSF	Hynes 2000, Vogel 2003
Pxn	Peroxidasin	IgSF	Hynes 2000, Vogel 2003
robo1	roundabout 1	IgSF	Hynes 2000, Vogel 2003
robo2	roundabout 2	IgSF	Hynes 2000, Vogel 2003
robo3	roundabout 3	IgSF	Hynes 2000, Vogel 2003
rst	roughest	IgSF	Hynes 2000, Vogel 2003
sdk	sidekick	IgSF	Hynes 2000, Vogel 2003
Sema2a	Semaphorin 2a	IgSF	Vogel 2003
side	sidestep	IgSF	Hynes 2000, Vogel 2003
side-II	sidestep II	IgSF	Hynes 2000, Vogel 2003
side-III	sidestep III	IgSF	Hynes 2000, Vogel 2003
side-IV	sidestep IV	IgSF	Hynes 2000, Vogel 2003
side-V	sidestep V	IgSF	Hynes 2000, Vogel 2003
side-VI	sidestep VI	IgSF	Vogel 2003

side-VII	sidestep VII	IgSF	Hynes 2000, Vogel 2003
side-VIII	sidestep VIII	IgSF	Hynes 2000, Vogel 2003
sls	sallismus	IgSF	Hynes 2000, Vogel 2003
sns	sticks and stones	IgSF	Hynes 2000, Vogel 2003
Strn-Mlck	Stretchin-Mlck	IgSF	Hynes 2000, Vogel 2003
tei	teiresias	IgSF	Hynes 2000, Vogel 2003
trol	terribly reduced optic lobes	IgSF	Vogel 2003
tutl	turtle	IgSF	Hynes 2000, Vogel 2003
unc-5	unc-5	IgSF	Hynes 2000, Vogel 2003
Unc-89	Unc-89	IgSF	Hynes 2000, Vogel 2003
vn	vein	IgSF	Hynes 2000, Vogel 2003
wrapper	wrapper	IgSF	Hynes 2000, Vogel 2003
zormin	zormin	IgSF	Hynes 2000, Vogel 2003

Table 2.2: Genes excluded from screen.

Gene abbrev.	Gene name	Criteria for exclusion
ppk12	pickpocket 12	Known to not be adhesion molecule (ENaC subunit); Incorrectly classified as IgSF?
htl	heartless	Known to not be adhesion molecule (RTK)
Ret	Ret oncogene	Known to not be adhesion molecule (RTK)
bt	bent	Known to not be adhesion molecule (sarcomere component)
sls	sallismus	Known to not be adhesion molecule (sarcomere component)
Unc-89	Unc-89	Known to not be adhesion molecule (sarcomere component)
zormin	zormin	Known to not be adhesion molecule (sarcomere component)
Sema2a	Semaphorin 2a	Known to not be adhesion molecule (secreted)
btl	breathless	Known to not be adhesion molecule (RTK)
beat-Ia	beaten path Ia	No expression RNAseq detected in wing disc
beat-Ib	beaten path Ib	No expression RNAseq detected in wing disc
beat-Ic	beaten path Ic	No expression RNAseq detected in wing disc
Cad88C	Cadherin 88C	No expression RNAseq detected in wing disc
Cad89D	Cadherin 89D	No expression RNAseq detected in wing disc
CadN	Cadherin-N	No expression RNAseq detected in wing disc
CadN2	Cadherin-N2	No expression RNAseq detected in wing disc
CG13532	CG13532	No expression RNAseq detected in wing disc
CG17839	CG17839	No expression RNAseq detected in wing disc
CG31431	CG31431	No expression RNAseq detected in wing disc
CG6867	CG6867	No expression RNAseq detected in wing disc
DIP-beta	Dpr-interacting protein beta	No expression RNAseq detected in wing disc
DIP-delta	Dpr-interacting protein delta	No expression RNAseq detected in wing disc
DIP-eta	Dpr-interacting protein eta	No expression RNAseq detected in wing disc
DIP-gamma	Dpr-interacting protein gamma	No expression RNAseq detected in wing disc

DIP-iota	Dpr-interacting protein iota	No expression RNAseq detected in wing disc
DIP-theta	Dpr-interacting protein theta	No expression RNAseq detected in wing disc
DIP-zeta	Dpr-interacting protein zeta	No expression RNAseq detected in wing disc
dpr10	defective proboscis extension response 10	No expression RNAseq detected in wing disc
dpr11	defective proboscis extension response 11	No expression RNAseq detected in wing disc
dpr12	defective proboscis extension response 12	No expression RNAseq detected in wing disc
dpr13	defective proboscis extension response 13	No expression RNAseq detected in wing disc
dpr15	defective proboscis extension response 15	No expression RNAseq detected in wing disc
dpr2	defective proboscis extension response 02	No expression RNAseq detected in wing disc
dpr20	defective proboscis extension response 20	No expression RNAseq detected in wing disc
dpr3	defective proboscis extension response 03	No expression RNAseq detected in wing disc
dpr4	defective proboscis extension response 04	No expression RNAseq detected in wing disc
dpr5	defective proboscis extension response 05	No expression RNAseq detected in wing disc
dpr8	defective proboscis extension response 08	No expression RNAseq detected in wing disc
Dscam2	Down syndrome cell adhesion molecule 2	No expression RNAseq detected in wing disc
Dscam3	Down syndrome cell adhesion molecule 3	No expression RNAseq detected in wing disc
Dscam4	Down syndrome cell adhesion molecule 4	No expression RNAseq detected in wing disc
fipi	factor of interpulse interval	No expression RNAseq detected in wing disc
kek3	kekkon-3	No expression RNAseq detected in wing disc
kek4	kekkon4	No expression RNAseq detected in wing disc
klg	klingon	No expression RNAseq detected in wing disc

nep16	Neprilysin-like 6	No expression RNAseq detected in wing disc; Incorrectly classified as IgSF?
nolo	no long nerve cord	No expression RNAseq detected in wing disc
robo3	roundabout 3	No expression RNAseq detected in wing disc
side-II	sidestep II	No expression RNAseq detected in wing disc
side-III	sidestep III	No expression RNAseq detected in wing disc
side-VI	sidestep VI	No expression RNAseq detected in wing disc
side-VIII	sidestep VIII	No expression RNAseq detected in wing disc

Table 2.3: Results from lines which were screened.

Gene abbrev.	Gene name	Lines	Result (-- = not a hit)	Notes
ama	amalgam	BL 33416	Undergrowth (severe)	Screened with TIE-DYE
babos	babos	BL 36728	--	
bdl	borderless	V 4806	-- see note	Not convincing but some clones on the smaller side
beat-IIIb	beaten path IIIb	BL 57157	--	
beat-IIIa	beaten path IIIa	BL 64526	--	
beat-IIIb	beaten path IIIb	BL 56984 V 36237	-- see note --	Initially thought there could be a slight difference of clone density A/P compartments, but was not replicable
beat-IIIc	beaten path IIIc	BL 50941	--	
beat-IV	beaten path IV	V 52413	--	
beat-Va	beaten path Va	BL 60053	--	
beat-Vb	beaten path Vb	V 17832	--	
beat-Vc	beaten path Vc	BL 60067	Undergrowth (severe)	Few clones survive
beat-VI	beaten path VI	V 6694	--	
beat-VII	beaten path VII	BL 60056	--	
boi	brother of ihog	V 29592	--	
bsg	basigin	BL 52110 V 2789	-- --	
Cad74A	Cadherin 74A	V 36320	--	
Cad86C	Cadherin 86C	BL 53314 BL 61280	-- --	

Cad96Ca	Cadherin 96Ca	BL 55877	--	Screened with TIE-DYE
Cad99C	Cadherin 99C	BL 35037	--	
CG13992	CG13992	V 2642	--	
CG15312	CG15312	V 101286	--	
CG15744	CG15744	BL 42497	--	
CG16974	CG16974	BL 42590	--	
CG33543	CG33543	BL 64879 V 17859	-- --	
CG34353	CG34353	V 22788	--	
CG44153	CG44153	BL 33350	--	Screened with TIE-DYE
CG45263	CG45263	BL 62468 V 18706	-- --	
CG5597	CG5597	V 12875	--	
CG7166	CG7166	V 27116	--	
Cont	Contactin	BL 34867	Undergrowth (Severe)	
DIP- alpha	Dpr- interacting protein alpha	V 17116	--	
DIP- lambda	Dpr- interacting protein lambda	BL 41980	--	
dpr1	defective proboscis extension response 01	V 26879 V 27087	-- see note --	3/6 discs had slightly low clone size/density
dpr14	defective proboscis extension response 14	V 8005	--	
dpr16	defective proboscis extension response 16	V 31986 V 102628	-- --	
dpr18	defective proboscis	V 983	--	

	extension response 18			
dpr6	defective proboscis extension response 06	V 41161	--	
ds	dachsous	BL 32964	Clones in pouch not elongated, round clones	
Dscam1	Down syndrome cell adhesion molecule 1	BL 38945	--	
ed	echinoid	V 938 V 3087 V 104279	Undergrowth (slight), round, smooth Undergrowth (moderate), round, smooth Undergrowth (severe), round, smooth	
Fas2	Fasciclin 2	BL 34084	--	
Fas3	Fasciclin 3	BL 77396	--	Maybe slight undergrowth, not convincing
fra	frazzled	BL 40826	--	
fred	friend of echinoid	BL 42621	--	
ft	fat	BL 34970	Round clones	
hig	hikaru genki	BL 42000	--	
ihog	interference hedgehog	BL 64541	--	
Imp-L2	Ecdysone-inducible gene L2	BL 64936	--	Screened with TIE-DYE
kek2	kekkon-2	V 4745	--	
kek5	kekkon5	BL 40830	--	
kirre	kin of irre	BL 64918	--	
Lar	Leukocyte-antigen-related-like	BL 40938	--	
lbk	lambik	BL 28903	--	

MnM	myomesin and myosin binding protein	BL 65245 V 43603	-- --	
nkt	noktochor	V 43018 V 43017	-- --	
Nrg	Neuroglian	BL 37496	--	
otk	off-track	BL 55869	--	
otk2	off-track2	BL 55892	Clones underrepresented especially in pouch; Rounded, cyst-like clones observed in hinge	Screened with TIE-DYE
plum	plum	BL 60062	--	
ppn	papilin	V 41901 V 16523	-- --	
Pvr	PDGF- and VEGF-receptor related	BL 37520 V 977	-- --	
Pxn	Peroxidasin	V 15276	--	
robo2	roundabout 2	BL 34589	--	Screened with TIE-DYE
sdk	sidekick	BL 33412	--	Screened with TIE-DYE
shg	shotgun	BL 32904	Undergrowth (severe)	
side	sidestep	BL 50642 V 1283	-- --	Screened with TIE-DYE
side-IV	sidestep IV	V 29806 V 16636	-- --	
side-V	sidestep V	V 44997	--	
side-VII	sidestep VII	V 10011	Undergrowth (small clones)	
sns	sticks and stones	BL 64872 V 877	-- see note --	Clones maybe slightly smaller and rounder, but not convincing
stan	starry night	BL 35050	--	
tei	teiresias	V 42236	--	
unc-5	unc-5	V 8137	--	
wrapper	wrapper	BL 29561	--	Screened with TIE-DYE

3 *ed* loss in broad domains leads to organ overgrowth

3.1 Introduction

In Chapter 2 we described how *ed* loss can lead to a growth *disadvantage* due to increased apoptosis which promotes *ed* clone elimination. Multiple groups have reported that *ed* loss or reduction in broad regions (e.g. in entire organs or animals) leads to a growth *advantage* in the context of organ overgrowth (Bai et al., 2001; Yue et al., 2012). We sought to confirm whether *ed* loss can cause organ overgrowth and to better understand the underlying mechanism.

3.2 Results

ed loss in large domains causes overgrowth

To measure the effect of a reduction in *ed* function on entire organs, we examined the wings of *ed^{IF20}/ed^{SIH8}* (null/hypomorph) *trans*-heterozygous and *nub-Gal4, UAS-ed-RNAi* animals where *ed* is depleted in the wing pouch domain. The resulting adult wings were larger than matched controls (Figure 3.1A-I). The *nub-Gal4* chromosome itself had an impact on wing size, so we compared experimental conditions using the *nub-Gal4* driver to controls which also contained *nub-Gal4*. We also generated flies with mostly *ed^{-/-}* eyes using a cell-lethal mitotic recombination assay (Newsome et al., 2000) (Figure 3.1K-L). Constitutive expression of *ey-FLP* causes most cells in the developing eye to undergo mitotic recombination, generating white *ed^{-/-}* clones and red *ed^{+/+}* twin clones that are killed by a recessive cell-lethal construct on the recombinant chromosomal arm (Figure 3.1J). Unlike when the wild-type twin clones are viable, the white *ed^{-/-}* cells survive (Figure 3.1K; compare with Figure 2.4B). These eyes are mostly white (*ed^{-/-}*) and are larger than control eyes (Figure 3.1L) (see also: Yue et al., 2012). These data corroborate the conclusion that loss of *ed* in broad domains can lead to overgrowth.

Overgrowth can occur in two ways that are not mutually exclusive. First, mutant tissue may grow more rapidly than wild-type tissue. Second, mutant tissue may grow at the same rate or a different rate to wild-type tissue but may simply not stop growing when it reaches the appropriate size. To better understand the dynamics of *ed*-driven overgrowth, we examined the wing discs of *hh-Gal4, UAS-ed-RNAi* larvae at different times throughout development. This manipulation reduces *ed* function in the posterior compartment, which allows us to compare the relative growth of the anterior and posterior compartments within a disc. At early time points (96h, 120h after egg lay), posterior compartments depleted of *ed* were smaller than age-matched controls without *ed* depletion, and proportionally undersized relative to the anterior compartment in the same disc (Figure 3.2A-D). However, most *hh-Gal4, UAS-ed-RNAi* larvae experienced a 2–3-day pupariation delay, during which the discs continued to grow (Figure 3.2E-F). In an extreme case, a larva with pupariation delay of >4 days was observed, and discs taken from this larva were more than double the size of a fully grown L3 wing disc (Figure 3.2G). In this disc, we observed that the anterior compartment was also overgrown indicating that overgrowth of one compartment can result in the overgrowth of the other.

This may be the result “accommodation,” in which a growth perturbation in one territory of an organ exerts a non-autonomous effect on adjacent unaffected regions (Díaz-Benjumea et al., 1989; Milán et al., 1997). From this experiment, we conclude that tissues with reduced *ed* function grow more slowly than wild-type tissue, but fail to terminate growth when an appropriate final size is reached.

Ed contains an extracellular N-terminal domain which participates in adhesion, a transmembrane domain, and an intracellular C-terminal domain which can bind to intracellular binding partners. To determine which domain(s) of Ed are required for regulation of organ size, we generated *ed^{IF20}/ed^{SIH8}* *trans*-heterozygous mutant wings that also expressed *nub-Gal4*-driven rescue constructs in the wing pouch domain. Expression of full-length Ed or Ed^{ΔC} (which lacks the intracellular domain) reduced the size *ed*-depleted wings (Figure 3.2B-E). The reduction of growth caused by expression of Ed^{ΔC} was greater than that caused by Ed^{Full}, although we do not know whether this is biologically meaningful or whether it reflects differences in expression strength of the two rescue constructs. Additionally, we examined the effects of these rescue constructs on the shape of *ed*-depleted wings, which are rounder than controls (Figure 3.3E) (Chan et al., 2021). Both constructs reduced the roundness of *ed*-depleted wings, although the effect was greater with Ed^{Full}. Although not conclusive, these experiments suggest that the extracellular domain of Ed is primarily involved in the organ size-control function of Ed, and that the C-terminal intracellular has a significant role in promoting proper proximo-distal elongation of the wing.

3.3 Discussion

Whereas loss of *ed* in clones leads to elimination of the mutant cells, loss in entire compartments, organs, or whole organisms leads to organ overgrowth. Here we show that *ed*-depleted organs grow slowly but are capable of reaching significantly larger final sizes than their wild-type counterparts. The slower growth of *ed*-depleted tissues could be caused by increased cell death (see Figure 2.5C-D), a reduced rate of cell proliferation, or both.

ed-depleted wings are large, short, and broad. The shape has been attributed to a defect in the geometrical reorganization of cells during the pupal wing elongation (Chan et al., 2021), and this constellation of phenotypes is reminiscent of those associated with *ft/ds* manipulations (Bryant et al., 1988; Clark et al., 1995). Expression of Ed with or without its C-terminal domain counteracts the overgrowth phenotype. Since the extracellular domain is known to participate in cell adhesion, it is possible that the adhesive function of Ed is responsible for its role in growth termination, although we cannot rule out an alternative model where Ed participates in signaling or regulation via its extracellular domain independently of cell adhesion.

Although the C-terminal domain is largely dispensable for the growth termination function of Ed, it is required for wing elongation. Why, then, do *ed^{IF20}/ed^{SIH8}* *trans*-heterozygotes have broad wings when *ed^{IF20}/+* wings elongate properly? The *ed^{SIH8}* hypomorphic allele contains a missense mutation in a conserved serine that disrupts a disulfide bond in an extracellular Ig-loop, which is thought to weaken interactions

involving Ed's extracellular domain (Escudero et al., 2003), but Ed^{SIH8} should still have a functional C-terminal domain. The observation that different phenotypes are caused by *nub*-driven expression of Ed^{Full} and Ed^{ΔC} in an *ed^{IF20}/ed^{SIH8}* background suggests that the function of the C-terminal domain in regulating wing morphology is at least partially dependent on the function of the extracellular domain. One model which could explain this is if the Ed C-terminal domain must be properly localized to the cell surface to enable its function. Ed-Ed *trans*-homodimerization is necessary for stabilization at the cell surface, as evidenced by the observation that Ed is lost from the interface of Ed-expressing and -nonexpressing cells (Laplante & Nilson, 2006, 2011; Rawlins, Lovegrove, et al., 2003; Wei et al., 2005). Since Ed^{SIH8} adhesive interactions are compromised, these molecules may not be efficiently stabilized at the cell surface, thereby limiting opportunities for the intact C-terminal domain to function.

Why don't Ed-depleted organs stop growing when they reach an appropriate final size? The prevailing view is that *ed* loss leads to organ overgrowth via reduced Hippo pathway signaling. In the next chapter, we will revisit this model in the light of our own data which partially contradict the current model for Ed's interactions with the Hippo pathway.

3.4 Figures

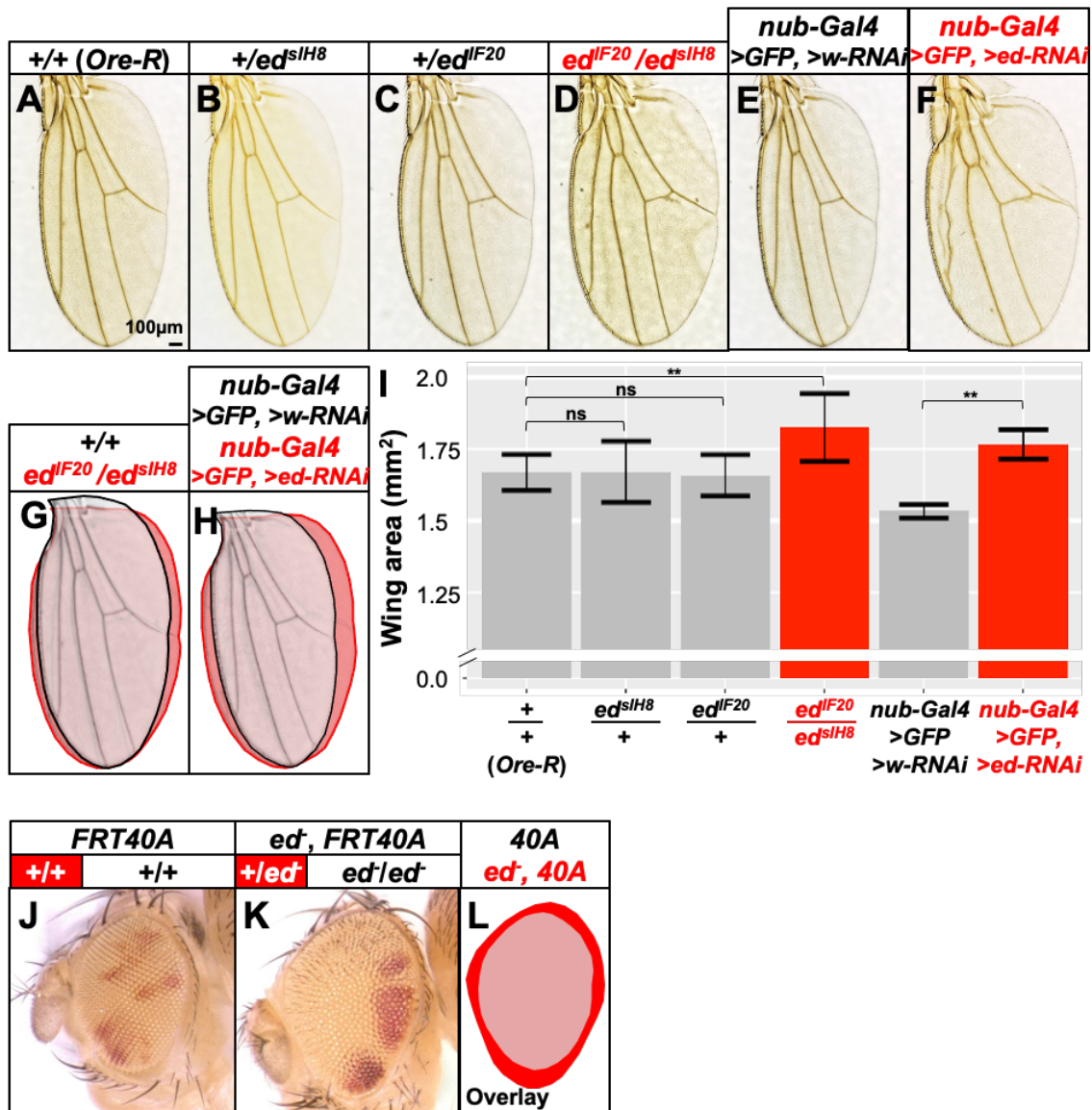


Figure 3.1: Loss of *ed* in large domains causes overgrowth.

A-F) Adult wings from flies of the following genotypes: *+/+* (*Ore-R*) (A), *+/*ed*^{IF20}* (B), *+/*ed*^{SIH8}* (C), *ed*^{IF20}/*ed*^{SIH8} (D), *nub-Gal4*, *UAS-GFP*, *UAS-w-RNAi* (E), *nub-Gal4*, *UAS-GFP*, *UAS-ed-RNAi* (E). G) Overlay of the wings shown in A and D. H) Overlay of the wings shown in E and F. I) Quantification of wing areas is shown in (I). n=10 wings (*+/+* [*Oregon-R*]; *ed*^{SIH8}/*+*; *ed*^{IF20}/*+*; *ed*^{SIH8}/*ed*^{IF20}; *nub-Gal4*, >*GFP*, >*w-RNAi*), 9 wings (*nub-Gal4*, >*GFP*, >*ed-RNAi*). “ns” indicates p > .05, ** indicates p < .01, calculated using ANOVA with post-hoc Tukey’s HSD test. Error bars indicate standard deviation. J-L) White twin-spot clones were induced by mitotic recombination in a heterozygous background using *eyeless-FLP*; red twin-spot clones were killed using a recessive lethal construct. Mostly white eye tissues are recovered in the FRT40A control condition (J). When the white tissue is *ed*^{-/-} and the eye is rough and overgrown (K). Overlay traces of the eyes in J and K are shown in (L). Scale bars: 100µm.

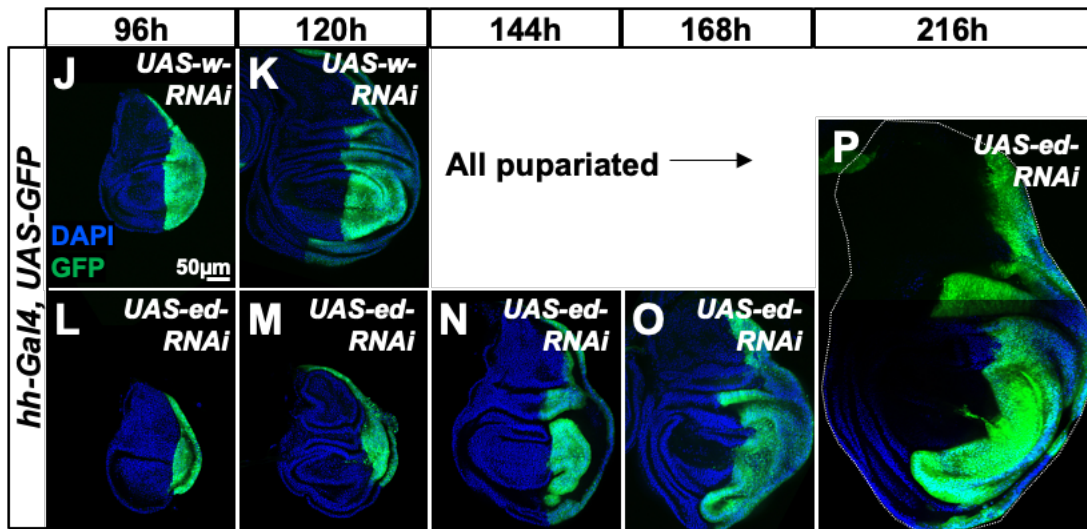


Figure 3.2: *hh-Gal4, UAS-ed-RNAi* wing discs grow slowly, but eventually exceed appropriate final size.

Wing imaginal discs taken with *hh-Gal4* driving expression of *UAS-GFP* and *UAS-w-RNAi* (A-B) or *UAS-ed-RNAi* (C-G) dissected at different timepoints after egg lay. At 144h, all *UAS-w-RNAi* larvae have pupariated. Scale bars: 50µm.

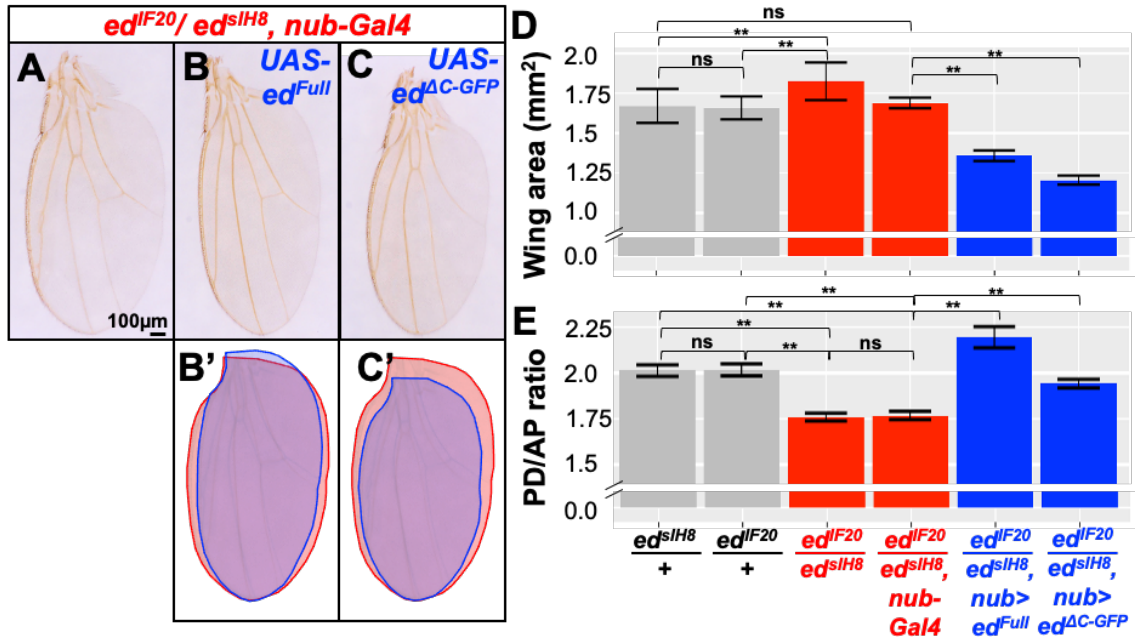


Figure 3.3: The C-terminal intracellular domain of Ed is not required to regulate wing size but is required for elongation of the wing.

(A-E) Effect of expressing full length *ed* (*ed^{Full}*) and a version where the cytoplasmic domain has been replaced by GFP (*ed^{AC-GFP}*) on wing size and wing shape. (A) Wings of a heteroallelic combination of *ed* alleles that generate viable adults together with *nub-Gal4*. Inclusion of *UAS-ed^{Full}* (B) and *UAS-ed^{AC-GFP}* (C) reduces wing size and brings the aspect ratio closer to wild-type. (B') and (C') show overlays of (B) and (C) over (A) respectively. For (D), n=10 wings (*ed^{siH8}/+*; *ed^{IF20}/+*; *ed^{siH8}/ed^{IF20}*; same as shown in Fig 3.1I), 4 wings (*ed^{siH8}/ed^{IF20}, nub-Gal4*; *ed^{siH8}/ed^{IF20}, nub-Gal4, UAS-ed^{Full}*), 6 wings (*ed^{siH8}/ed^{IF20}, nub-Gal4, UAS-ed^{AC-GFP}*). For (E), n=10 wings (*ed^{siH8}/+*; *ed^{IF20}/+*), 9 wings (*ed^{siH8}/ed^{IF20}, ed^{siH8}/ed^{IF20}, nub-Gal4, UAS-ed^{AC-GFP}*), 4 wings (*ed^{siH8}/ed^{IF20}, nub-Gal4; ed^{siH8}/ed^{IF20}, nub-Gal4, UAS-ed^{Full}*). The same wings were used in (D) and (E); n's differ if damage or mounting artifacts prevented measurement of both wing area and aspect ratio. "ns" indicates $p > .05$, ** indicates $p < .01$, calculated using ANOVA with post-hoc Tukey's HSD test. Error bars indicate standard deviation. Scale bars: 100 μ m.

4 Downstream effects of *ed* perturbations

4.1 Introduction

Yue et al. (2012) proposed that the overgrowth that occurs in tissues with reduced *ed* function is because Ed is a negative regulator of growth through the Hippo pathway. In their model, loss of *ed* function leads to a reduction in Hippo pathway activity, causing an increase in nuclear Yorkie which drives the expression of pro-growth and anti-apoptotic genes including *Diap1*, *bantam* (*ban*), *four-jointed* (*ff*) and *expanded* (*ex*). This should cause cells to behave as super-competitors, since Hippo pathway mutant cells have a growth advantage over, and can even induce apoptosis in, neighboring wild-type cells (Tyler et al., 2007; Ziosi et al., 2010). However, our findings that *ed*-depleted clones have a growth and survival disadvantage, increased apoptosis, decreased Hippo-dependent *Diap1* transcription, and lower Diap1 protein levels are inconsistent with the published model of how Ed interacts with the Hippo pathway. Here, we independently assess how *ed* affects the Hippo pathway and demonstrate a more complex relationship than previously appreciated.

4.2 Results

Ed regulates expression of Yorkie target genes autonomously and non-autonomously

The activity of the Hippo pathway is often inferred from the level of transcription of Yorkie target genes, or the abundance of proteins encoded by these genes. We examined some readouts of Hippo signaling—Diap1 protein levels and *lacZ* reporters for *ban* and *ff*—in *ed-RNAi* clones. If Ed promotes Hippo signaling as previously described, then *ed-RNAi* should reduce Hippo signaling, resulting in increased expression of the three Yorkie targets within the clones. However, we did not observe an increase of Diap1, *ban-lacZ*, or *ff-lacZ* expression levels in the clones (Figure 4.1). In the case of Diap1, as already described in Chapter 2, protein levels are considerably *lower* within the clones than in unaffected regions (Figure 4.1A, see also Figure 2.7). These results do not support the prevailing view that *ed* negatively regulates growth via the activity of the Hippo pathway.

When examining the Yorkie targets in *ed-RNAi* clones, we also observed lower apparent Hippo pathway activity (*i.e.*, increased expression of Yorkie targets) in the wild-type neighbors of *ed-RNAi* cells (Figure 4.1). This phenotype was incompletely penetrant—we did not observe a border effect around every *ed-RNAi* clone, and when we did observe a border effect, it did not always appear along the entire perimeter of the clone. The boundary effects observed lead us to conclude that loss of *ed* can reduce activity of the Hippo pathway non-autonomously.

Loss of *ed* has been reported to increase the nuclear localization of Yki based on antibody staining (Yue et al., 2012). In our hands, antibody staining of Yki is not reliable in wing

imaginal discs (data not shown). Instead, we examined the localization of GFP-tagged Yki (Fletcher et al., 2018) in mosaic discs containing *UAS-ed-RNAi* clones (Figure 4.2). We did not observe any obvious difference in the localization of Yki:GFP in *ed-RNAi* clones or in wild-type cells next to the clones. This could indicate that the effects of *ed* loss on Hippo pathway target genes are Yki-independent, or that the changes to Yki localization are too subtle to be detected with this reagent.

Because the overall effect of *ed* loss on growth is context-dependent (e.g., *ed* loss in clones leads to a growth disadvantage whereas *ed* loss in broader domains leads to overgrowth), we examined the effects on *ed-RNAi* on Hippo pathway activity in non-clonal contexts. We used the *hh-Gal4* driver to express *UAS-ed-RNAi* in the posterior compartment. Similar to what we observed in clones, this manipulation led to an autonomous decrease in Diap1 protein levels (Figure 4.3A). We observed an autonomous increase in *ex-lacZ* in the posterior compartment (Figure 4.3B), which is consistent with what others have shown (Yue et al., 2012). We conclude that not all Yorkie target genes respond to *ed* reduction in the same way.

Comparing knockdown conditions to wild type gives insight into how a gene normally functions—if the absence of a gene product disrupts the physiology of a cell in some way, we can infer that it is required for that aspect of physiology in the wild type. Overexpression (OE) of a gene product can also yield insight into its function, although the interpretation of these experiments is less straightforward. OE is the most informative in cases when the abundance of a gene product scales proportionately with its level of function—in these cases, the OE phenotype will typically be the opposite of the knockdown phenotype. In other cases, the absence or presence of a gene product may matter while levels of expression beyond a threshold do not, so the OE phenotype may not differ from wild type. In yet other cases, OE may disrupt the physiology of a cell in a way that is not necessarily informative to understanding the gene's normal function (e.g., forming aggregates, inducing translational stress, triggering the unfolded protein response).

With the above caveats in mind, we examined the impact of *ed* overexpression on the Hippo pathway. *ed-OE* had no appreciable effect on Diap1 levels in clones, but it did reduce Diap1 levels autonomous when the entire posterior compartment was affected (some domains of the Diap1 expression pattern were less obviously affected, such as the stripe at the D-V boundary) (Figure 4.4A, B). We examined *ban-lacZ* levels in *ed-OE* clones and observed a strong autonomous increase within the overexpression clones (Figure 4.4C). Finally, we examined the *ex-lacZ* reporter when overexpressing *ed* in the posterior compartment. There was a slight, autonomous increase of *ex-lacZ* which is most visible in the notum. In the pouch where the *ex-lacZ* reporter expression was overall low, the *ed-OE* cells at the interface with wild-type cells had noticeably elevated *ex-lacZ* expression (Figure 4.4D).

The atypical cadherins Fat (Ft) and Dachshous (Ds) are binding partners which regulate the Hippo pathway in both autonomous and non-autonomous fashions (Baena-Lopez et al., 2008; Bennett & Harvey, 2006; Gou et al., 2018). Non-uniform Hippo pathway

boundary effects have been observed in *ds* loss-of-function clones (Willecke et al., 2008), clones of cells overexpressing the Ft (Matakatsu & Blair, 2012), clones with activated Tkv which increases Ft signaling (Rogulja et al., 2008), and in cells overexpressing *fbxl7* which in turn leads to an upregulation of Ft (Bosch et al., 2014). We examined Ft expression within *ed-RNAi* clones and observed increased Ft staining within the clones (Figure 4.5). Ft is therefore responsive to the expression of *ed* and could potentially mediate some of the border effects described earlier.

Ed has been reported to interact with multiple signaling pathways that regulate growth, including Hippo and EGFR. To better understand how *ed* interacts with EGFR in the wing disc, we examined the levels of Cic protein inside and outside of *ed-RNAi* clones. Cic levels are inversely proportional to EGFR signaling. We observed an extremely slight decrease in Cic in *ed-RNAi* cells as compared to wild-type neighbors (Figure 4.6). Our findings support the generally accepted model that Ed antagonizes EGFR activity.

4.3 Discussion

Ed was initially thought to be a straightforward negative regulator of growth via the Hippo pathway. However, here we show that the relationship between Ed and the Hippo pathway is more complicated than previously described. We observed non-uniform, context-dependent effects of *ed* perturbations on Yorkie target genes. Although the expression of these genes is often assumed to reflect Hippo pathway activity, some Yorkie target genes responded differently from others to identical manipulations (e.g. increased *ex-lacZ* and decreased Diap1 in the posterior compartment of *hh-Gal4*, *UAS-ed-RNAi* discs).

Ed is known to interact with multiple signaling pathways, and the expression of a gene is often regulated by multiple inputs. It is possible that Ed may regulate some or all the Yorkie target genes examined in this study through signaling pathways other than Hippo. One candidate is the EGFR pathway, which Ed is known to antagonize in some contexts. We examined Cic levels and observed very slight Cic reduction in wing disc *ed-RNAi* clones, indicating greater EGFR activity. This trend is consistent with previous work on *ed* and the EGFR pathway. Whether EGFR signaling is at all responsible for the apparent discrepancy in how Hippo-responsive genes respond to *ed* perturbations remains to be tested.

We observed many instances where the expression of Yorkie target genes was uniquely regulated at the border of wild-type cells and *ed-RNAi* or *ed-OE*, indicating that *ed* can non-autonomously regulate these transcriptional targets of the Hippo pathway. Diap1, *ex-lacZ*, and *ban-lacZ* were elevated in wild-type cells abutting *ed-RNAi* clones. We also saw elevated *ex-lacZ* in the Ed-overexpressing cells at the boundary with wild-type cells when overexpression was driven by the *hh-Gal4* driver. Given the similarity to border-effects seen with *fi/ds* manipulations, and the increase in Ft levels within *ed-RNAi* it is plausible that these border effects are the consequence of Ed's effect on Ft.

In all cases where we observed a boundary effect, it occurred in the cells with more Ed at an interface between cells with different Ed levels. This is reminiscent of a different

boundary effect associated with discontinuities of Ed expression: the formation of an actomyosin cable in Ed-expressing cells at the interface with Ed-non-expressing cells (Chang et al., 2011; Laplante & Nilson, 2006, 2011; Wei et al., 2005). Whether these two boundary effects—increased expression of Yorkie target genes and actomyosin cable induction—share a common mechanism remains to be determined.

In Chapter 2, we described how *ed* loss can cause an undergrowth phenotype in clones, and in Chapter 3, we described how *ed* loss can lead to an overgrowth phenotype in entire organs. Phenomena like cell competition can underlie phenotypic differences between clonal and non-clonal perturbations of the same gene. The apparent induction of Yorkie target genes in cells abutting *ed* clones could create a competitive interface, with the wild-type neighbors adopting a “super-competitor” status due to decreased Hippo pathway activity. This would have a negative effect on the survival of cells within the *ed* clone, specifically at the competitive interface. The overall impact of this competitive interaction would be greatest when the percentage of *ed* cells in direct contact with wild-type neighbors is highest—such as when *ed* clones are scattered throughout the tissue at low density. The impact would be lower when the competitive interface is minimized—such as when Ed is depleted in a contiguous region like a compartment. The impact would be lowest when there is no competitive interface at all. Although Hippo-based competition could contribute to the elimination of *ed*-depleted clones in mosaics, we also observed elevated apoptosis in *ed* tissue that is not near wild type neighbors. Therefore, even if Hippo pathway-mediated competition occurs at the interface of *ed* clones, competition-independent apoptosis likely contributes substantially to clonal elimination.

4.4 Figures

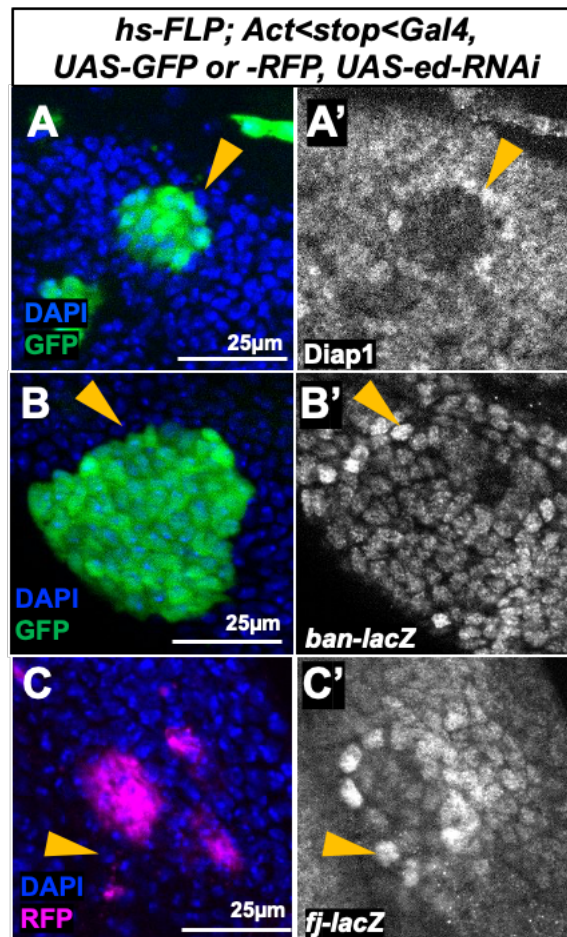


Figure 4.1: *ed-RNAi* non-autonomously increases the expression of Yorkie target genes outside of clones.

ed-RNAi clones express low levels of Diap1 (A) *ban-lacZ* (B), and *fj-lacZ* (C), however, expression is elevated in neighboring WT cells (yellow arrowheads). Scale bars: 25µm.

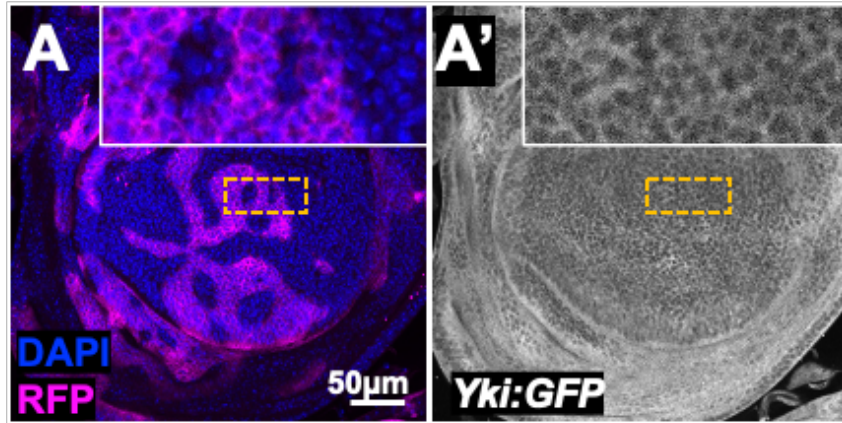


Figure 4.2 Localization of Yki:GFP is not obviously changed in or around *ed-RNAi* clones.

RFP-labeled clones expressing *UAS-ed-RNAi* show no obvious alteration in the localization of a GFP-tagged Yki. The region of the disc enclosed by the dashed line is shown at higher magnification in the insets.

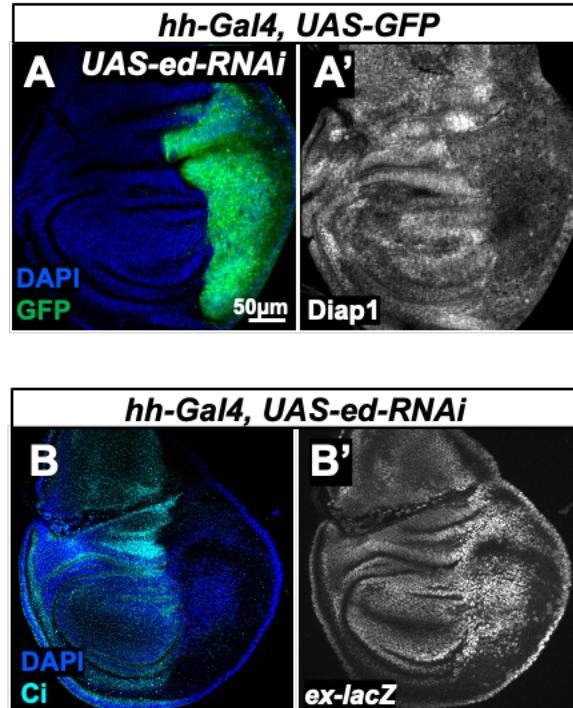


Figure 4.3: *ed-RNAi* in the posterior compartment has different effects on different Yorkie target genes.

ed-RNAi in the posterior compartment autonomously decreases levels of Diap1 (A) and increases expression of *ex-lacZ* (B). Scale bars: 50 μm.

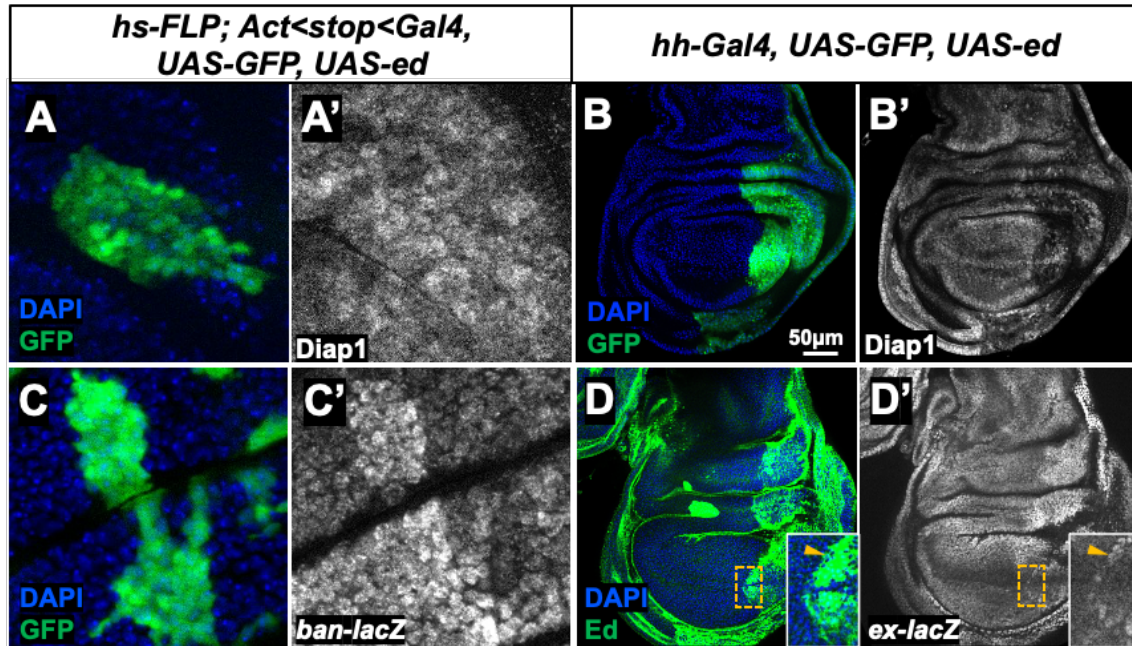


Figure 4.4: *ed* overexpression has diverse effects on Yorkie target genes.

Overexpression of *ed* in clones (A, C) or in the posterior compartment (B, D). A-B) *ed-OE* does not effect the levels of Diap1 protein in clones (A), but OE in the entire posterior compartment leads to an autonomous reduction of Diap1 (B). C) *ed-OE* leads to an increase in *ban-lacZ* activity in clones. D) *ed-OE* in the posterior compartment leads to an autonomous increase in *ex-lacZ* in the hinge and notum. In the pouch, elevated *ex-lacZ* is visible in the *ed*-overexpressing cells bordering wild-type neighbors (arrowheads, insets). In (D), the posterior compartment is labeled by high levels of Ed. (Note: endogenous Ed is also present in the anterior compartment, but is only clearly visible in regions where the adherens junctions are in the focal plane, such as in folds and in margin cells toward the lateral edge of the disc. Scale bars: 25µm (A,C), 50µm (B, D).

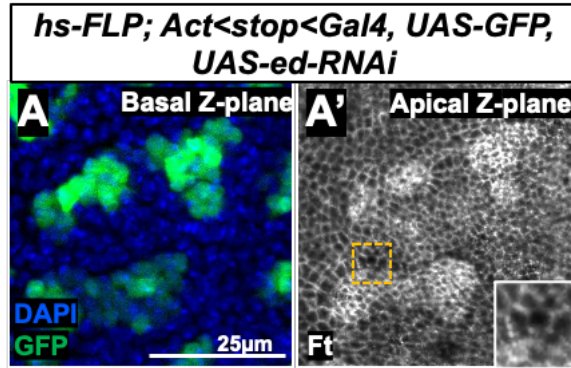


Figure 4.5: *ed-RNAi* clones have high levels of Fat.

(A) is shown at a Z plane which clearly shows GFP expression labeling clones; (A') is shown at a more apical Z plane where Ft is localized. Since *ed-RNAi* clones apically constrict and form smooth borders with wild type neighbors at the level of the adherens junctions, the clones appear slightly smaller, rounder, and offset in the X-Y plane when viewed in the apical Z plane as compared to the Z basal plane. Scale bars: 25µm.

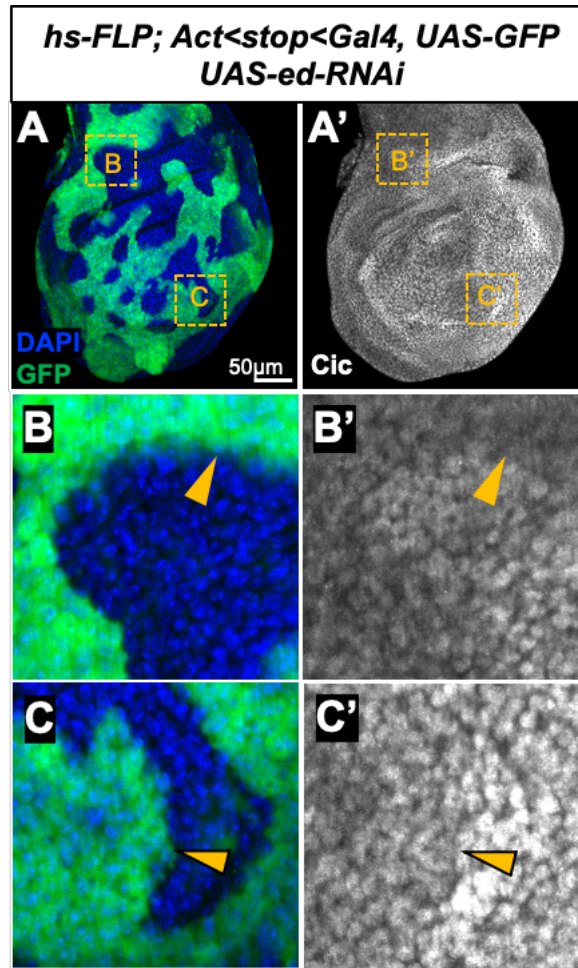


Figure 4.6: *ed-RNAi* clones have lowered levels of Cic.

ed-RNAi clones (GFP+) were generated at high density with a long heat shock. Cic protein is slightly higher in wild-type cells (absence of GFP) than in *ed-RNAi* cells. Indicated regions (boxes) are shown at higher magnification in (B-C). Clone borders where disparities in Cic levels are easily seen are marked with yellow arrowheads. Scale bars: 50µm.

5 Genetic modifiers of *ed*-mediated overgrowth

5.1 Introduction

Loss-of-function mutations often produce obvious mutant phenotypes when homozygous, but not when heterozygous. This is because a single dose of functional gene product is usually sufficient for wild-type function, however, this may not be the case under sensitized conditions. Dominant modifier screens take advantage of this conditional haploinsufficiency to identify genes involved in a common pathway. By screening for heterozygous loss-of-function mutations which cause a phenotype only when a particular pathway is sensitized, new members of that pathway can be identified. The use of heterozygous mutants simplifies the genetics and allows for the inclusion of recessive-lethal mutations in the candidate pool. Dominant modifier screens in genetically-amenable model organisms have been successful at uncovering key players in many signaling pathways (Jorgensen & Mango, 2002; Simon et al., 1991; St Johnston, 2002).

Drosophila wings depleted of *ed* are larger and broader than wild-type wings. Yue et al. (2012) have proposed that this overgrowth occurs because *ed* is a negative regulator of growth through the Hippo pathway; loss of *ed* leads to increased transcription of Yorkie-target genes which promote cell survival and proliferation. In the light of our inability to replicate some of the findings from Yue et al. (2012) (see Chapter 4), we sought to independently investigate the mechanism underlying overgrowth driven by the loss of *ed*. We designed a dominant modifier screen aimed to uncover mutations that enhance or suppress *ed-RNAi*-driven overgrowth in the wing, with the goal of identifying which signaling pathway(s) mediate *ed*'s effect on organ size.

5.2 Results

Flies of the genotype *w; nub-Gal4, UAS-ed-RNAi*/*CyO.Tb*> were crossed to stocks carrying mutations in candidates of interest (Figure 5.1). Adult wings were collected from ~10 female progeny which inherited one copy of the *nub-Gal4, UAS-ed-RNAi* and one copy of the mutation of interest.

We screened loss-of-function alleles (null alleles, when possible) of all known genetic or physical interactors with *ed* for which reagents were easily available from the Bloomington *Drosophila* Stock Center. We additionally included a few members of every major growth-control pathway, regardless of whether an interaction with *ed* had been previously reported. We also included a small number *UAS*- driven knockdown or overexpression lines, with the caveat that these are not heterozygous loss-of-function mutations and must be analyzed using appropriate controls outside of the “dominant modifier” framework.

We set up crosses with approximately the same number of parental flies and limited the egg-laying period to ~24h to prevent overcrowding of vials, since overcrowding can

reduce adult body size. Our methodology does not fully control for larval density, so batch effects may still be present. We therefore focused on identifying strong modifiers or patterns of multiple members of the same pathway causing modifications.

A total of 62 loss-of-function lines and 7 *UAS*-knockdown or overexpression lines were included in this screen. 28 loss-of-function lines dominantly modified wing size in some fashion (4/7 of the *UAS*- driven knockdown or overexpression lines also modified wing size). Of the loss-of-function lines, 13 were scored as causing a “moderate” to “strong” modification. The results are reported in Table 5.1. Notable hits are described below.

Hippo Pathway

nub-Gal4, UAS-ed-RNAi in combination with various mutations affecting the Hippo pathway (*wts³⁻¹⁷, Mer³, Diap1¹ + crb^{1A22}*) led to enhanced overgrowth (Figure 5.3). The most dramatic overgrowth is seen with the *Mer³*, however, this allele also produces overgrowth when heterozygous in the absence of *nub-Gal4, UAS-ed-RNAi* (not shown), so the phenotype may be additive rather than a dominant enhancement.

Notch Pathway

nub-Gal4, UAS-ed-RNAi in combination with *Notch^{55E11} (N^{55E11})* yielded flies with notched wings of varying severity. *N^{55E11}* heterozygotes without *nub-Gal4, UAS-ed-RNAi* usually have a small notch at the distal tip of the wing blade (Figure 5.3A). The notching phenotype in *N^{55E11}* heterozygotes with *nub-Gal4, UAS-ed-RNAi* was incompletely penetrant and variable in strength, with the most severe notching much more extensive than typically seen with *N^{55E11}* heterozygosity alone (Figure 5.3B). *N^{55E11}/+; nub-Gal4, UAS-ed-RNAi* wings without severe notching were somewhat larger than wings with *nub-Gal4, UAS-ed-RNAi* alone (compare Figure 5.3B’ and C). *nub-Gal4, UAS-ed-RNAi* in combination with *Delta^X* leads to wings with reduced size, widened veins, and terminal deltas (Figure 5.3D), phenotypes which are frequently observed with enhancement of *Delta* loss-of-function alleles (Klein & Campos-Ortega, 1992). These results do not indicate that reduction of Notch signaling consistently enhances or suppresses *nub-Gal4, UAS-ed-RNAi* wing overgrowth but are consistent with previously published work indicating that Ed synergizes with Notch signaling during the organ patterning and cell-fate specification (Ahmed et al., 2003; Escudero et al., 2003; Rawlins, Lovegrove, et al., 2003).

Canoe

We did not have a loss-of-function allele of *canoe (cno)*, so we instead examined the effects of co-depletion of *ed* and *cno* by RNAi. Whereas *nub-Gal4, UAS-ed-RNAi* produces a large, broad wing (Figure 5.4A), *nub-Gal4, UAS-cno-RNAi* alone generates a wing that is small and narrow (Figure 5.4B). *nub-Gal4, UAS-ed-RNAi, UAS-cno-RNAi* in combination yielded extremely reduced wing rudiment (Figure 5.4C). The enhancement of the *UAS-cno-RNAi* wing reduction phenotype by *ed-RNAi* suggests either a) depletion of Cno by *nub-Gal4, UAS-cno-RNAi* is incomplete, so these animals retain sufficient function of the Ed-Cno complex to partially support wing morphogenesis, or b) that Ed has Cno-independent function which is required for cell survival and/or wing morphogenesis in the absence of Cno.

upd2Δ

nub-Gal4, UAS-ed-RNAi in combination with *upd2Δ* (BL#55727) (Osman et al., 2012) produced a dramatic modification of the wing phenotype. When the female parent provided the *nub-Gal4, UAS-ed-RNAi* chromosome and the male provided the *upd2Δ* chromosome, most female progeny failed to eclose from their pupal cases and had leg segments that were shorter and less straight than wild-type (*upd2* is on the X chromosome, so male progeny did not inherit the *upd2* deletion). The few that did eclose had wings that were reduced in size with large blisters in the proximal region near the wing-hinge junction (Figure 5.5B). None of these aberrant phenotypes are seen in *upd2Δ* homozygotes or hemizygotes in the absence of *nub-Gal4, UAS-ed-RNAi*. (Figure 5.5C). This blistering phenotype is occasionally seen with *nub-Gal4, UAS-ed-RNAi* alone, but with much lower penetrance. The leg and wing defects may underlie the high rate of eclosion failure—flies who did eclose typically had less severe leg defects than those who didn't (compare Figure 5.5E and E'), and many flies who partially eclosed appeared to have ruptured blisters which caused their wings to stick to the wall of the pupal case. Similar phenotypes were observed with the double mutant *upd2Δ, upd3Δ* stock (BL#55729; data not shown).

Because loss of *ed* is associated with increased apoptosis in clones (see Chapter 3), we assessed apoptosis levels in *upd2Δ/+; nub-Gal4, UAS-ed-RNAi* L3 wing imaginal discs by Dcp-1 staining. We performed the experiment in such a way that female progeny would be *upd2Δ/+; nub-Gal4, UAS-ed-RNAi*, and male progeny would be *+/Y; nub-Gal4, UAS-ed-RNAi*, so only ~half of the progeny (the females) should have modifier activity. We observed a bimodal distribution of phenotypes: some discs had moderate apoptosis levels, which are presumed to be discs taken from male offspring (Figure 5.6A). The rest of the discs had extremely elevated levels of apoptosis, which are presumed to be discs taken from female offspring that have the genetic modifier (Figure 5.6B). The apoptosis occurs primarily in proximal portions of the wing pouch, which is consistent with elevated apoptosis being the cause of the proximal wing blisters observed in adults. This result suggests that the genetic modifier behaves as an enhancer of apoptosis. The change in overall wing size may reflect increased apoptosis which reduces the total number of cells contributing to the adult wing, rather than reflecting a genetic interaction between *ed* and another member of the pathway directly responsible for *ed*-mediated overgrowth.

Upd2 is a ligand in the Jak-STAT pathway. If reduced Jak-STAT signaling is responsible for the genetic interaction between *upd2Δ* and *nub-Gal4, UAS-ed-RNAi*, we would expect that mutations in other Jak-STAT pathway members would also modify the *nub-Gal4, UAS-ed-RNAi* phenotype in a similar fashion. However, we did not observe a comparable genetic interaction between *ed* and any other member of the Jak-STAT pathway (Figure 5.7). From this, we conclude that reduced dosage of Jak-STAT signaling is unlikely to be the causative mechanism for the genetic interaction between *ed* and the *upd2Δ* chromosome.

To further test whether deletion of *upd2* is responsible for the modification associated with the *upd2Δ* chromosome, we tested an independently-generated *upd2* null allele, *upd2Δ³⁻⁶²* (Hombria et al., 2005), for modifier activity when in combination with *nub-Gal4*, *UAS-ed-RNAi*. We did not observe any modification when using the *upd2Δ³⁻⁶²* allele (Figure 5.8B). We also did not observe any modification in *nub-Gal4*, *UAS-ed-RNAi*, *UAS-upd2-RNAi* (BL#33988) double-knockdown wings (Figure 5.8C). These experiments suggest that reduction of *upd2* does not account for the genetic interaction between the *upd2Δ* chromosome and *nub-Gal4*, *UAS-ed-RNAi*.

It is possible that a second-site mutation or transgene on the *upd2Δ* chromosome is responsible for the genetic modification we observed. If this were the case, the modifier could be located anywhere on the X chromosome. We performed recombination mapping to determine the location of the causative genetic modifier on the *upd2Δ* X chromosome (Figure 5.9). Modifier activity was closely linked to the *Bar* locus (recombination frequency 2.2%, $N=318$). This result is consistent with *upd2Δ* being the causative genetic lesion, since the distance between the *upd2* and *Bar* loci is about 3 map units, although it does not rule out the possibility that the modifier is something other than the *upd2Δ* allele that is also closely linked to *Bar*.

The *upd2Δ* allele was generated by FLP-FRT recombination between a P{XP} element and a PBac{WH} element which were inserted into regions flanking the *upd2* gene (Osman et al., 2012). The recombination event removed the entire *upd2* gene, which we confirmed by whole-genome sequencing. However, the P+PBac{XP5.WH5} hybrid element generated by the recombination event retains a *UAS* site capable of driving Gal4-mediated misexpression. We hypothesize that *UAS*-misexpression of a nearby downstream gene is responsible for the genetic modification associated with the *upd2Δ* allele. Consistent with a model where the modifier activity of the *upd2Δ* chromosome relies on Gal4 activity, not just a reduction in *ed*, we did not observe a strong genetic interaction between *ed^{IF20}* (null) and *upd2Δ*. Some double heterozygotes appeared to have a slightly reduced wing size compared to *upd2Δ/+* alone and *ed^{IF20} (Null)/+* alone, but this was not consistent. We did not observe any other abnormal phenotypes observed associated with *upd2Δ/+*; *nub-Gal4*, *UAS-ed-RNAi* (e.g. eclosion failure, blisters) (Figure 5.10).

Also consistent with the hypothesis of *UAS*-misexpression is that *upd2Δ* heterozygotes that also express *nub-Gal4*, without any perturbations to *ed*, have small wings with proximal blisters (Figure 5.11). We conclude that the “modifier” phenotypes associated with the *upd2Δ* represent the phenotypes caused by *UAS*-misexpression from the *upd2Δ* rather than a bona fide genetic interaction with *ed*.

5.3 Discussion

***ed* genetically interacts with multiple signaling pathways during wing development**

Our dominant modifier screen identified a number of genetic interactions with *nub-Gal4*, *UAS-ed-RNAi*. Given the curated list of candidates, it is unsurprising that we saw genetic interactions with several genes known to interact with *ed* in other contexts, including members of the Notch pathway, Hippo pathway, and *cno*.

The Hippo pathway has previously been implicated as the responsible pathway for *ed* loss-driven overgrowth; our results from this screen are in line with that model, although additional exploration would be prudent in light of the conflicting data presented in Chapter 4.

We report the phenotypes with *Notch* and *cno* as they may be of interest to others, although the data do not point to these being likely candidates for mediating the overgrowth.

The *upd2Δ* allele modifies *nub-Gal4*, *UAS-ed-RNAi* phenotypes via a *UAS*-misexpression element

The strongest dominant modifier in our screen was the *upd2Δ* allele. Heterozygosity or hemizygoty for *upd2Δ* in combination with *nub-Gal4*, *UAS-ed-RNAi* led to eclosion defects, leg malformations, and wings with reduced size and prominent blisters, which are likely the result of highly elevated apoptosis in the wing discs. However, we think it is unlikely that the deletion of *upd2* is responsible for these phenotypes, since they were not observed with a second *upd2* null allele nor with *nub-Gal4*, *UAS-ed-RNAi*, *UAS-upd2-RNAi*. The presence of a *UAS*-misexpression element in the *upd2Δ* allele, and the observation many of the “modifier” phenotypes are elicited by crossing *upd2Δ* to *nub-Gal4* even without *UAS-ed-RNAi*, leads us to believe that *UAS*-driven expression of a nearby gene is the most likely cause of the genetic modification caused by the *upd2Δ* allele.

Additional experiments are necessary to determine what gene is misexpressed in *upd2Δ* animals when Gal4 is present. The closest genes downstream of the *upd2Δ* *UAS*-misexpression construct—likely candidates to be misexpressed—are the long noncoding RNA lncRNA:CR45622 and the unnamed gene CG33639, a putative neuropeptide/protein hormone GPCR (Alliance of Genome Resources, n.d.).

Many deletion alleles have been made in a similar manner to the *upd2Δ* allele and harbor *UAS*-misexpression constructs. We caution other researchers who use these reagents as deletion alleles to be aware of potential confounding effects caused by *UAS*-driven misexpression.

Relationship between *ed* and Jak-STAT signaling

Our data do not support that there is a genetic interaction between *ed* and the Jak-STAT pathway, at least in the context of wing growth and morphogenesis. Another study has shown that heterozygosity of *ed* does not modify the Jak-STAT-dependent tumorigenic phenotype of *hopTum-1/+* flies (Anderson et al., 2017). Ed has been implicated as a positive regulator of STAT92E phosphorylation by a single study (Baeg et al., 2005). However, this claim is entirely based on an interference RNA screen in S2-NP cells (a line of S2 cells). It is puzzling that dsRNAi targeting *ed* would have any effect in S2-derived cells, since S2 cells do not endogenously express cell adhesion molecules, including Ed (Hortsch & Bieber, 1991; Islam et al., 2003). As such, we suspect the

interaction between Ed and STAT92E reported by Baeg et al. (2005) is likely to be a false positive.

5.4 Figures and tables

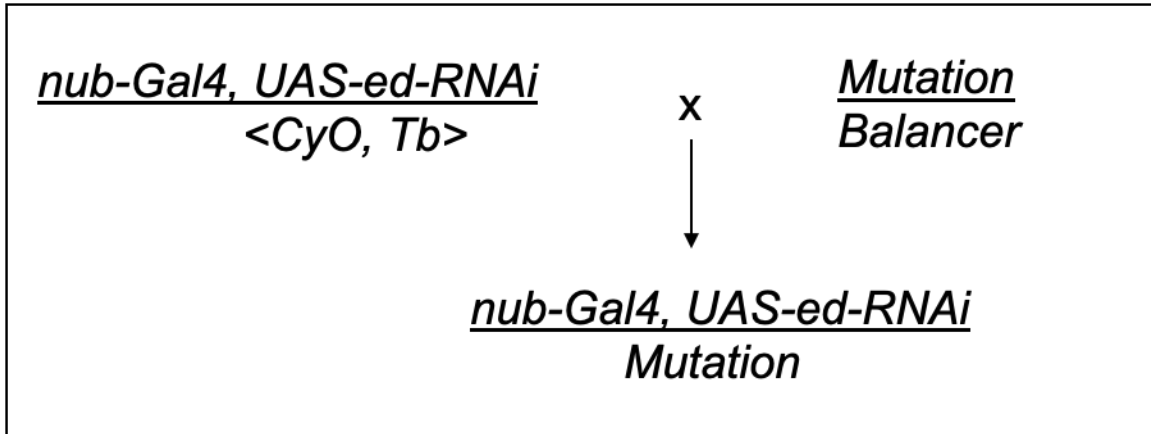


Figure 5.1: Genetic scheme used for the dominant modifier screen.

Only chromosome 2 is shown. The same overall scheme is also used for mutations on chromosome X or 3. Crosses were conducted using *nub-Gal4, UAS-ed-RNAi*/*<CyO, Tb>* as the female parent, except when screening balanced mutations on the X chromosome.

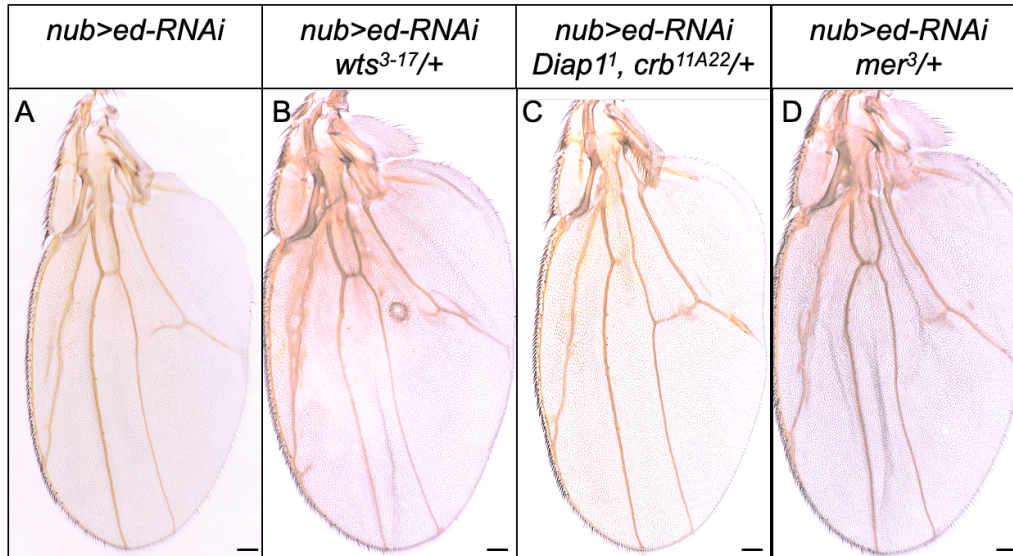


Figure 5.2: *ed* genetically interacts with the Hippo pathway.

A) *nub-Gal4, UAS-ed-RNAi* wings are large and broad. B-D) RNAi targeting various Hippo pathway genes dominantly enhances the overgrowth seen with *nub-Gal4, UAS-ed-RNAi*. Scale bars: 100 μ m

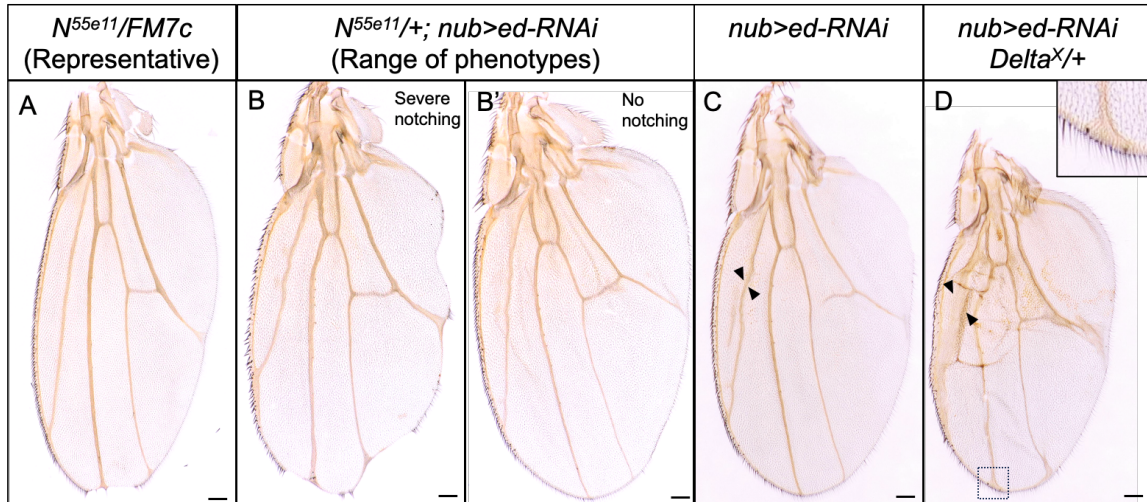


Figure 5.3: *ed* genetically interacts with the Notch pathway.

A) *N^{55e11}* heterozygotes present with subtle notching at the distal tip of the wing blade. B) *N^{55e11}* heterozygotes that also express *nub-Gal4*, *UAS-ed-RNAi* present with notching phenotypes ranging from severe notching (left) to no notching (right). Wings that are not notched (B, right) show enhanced overgrowth as compared to *nub-Gal4*, *UAS-ed-RNAi* alone (C). D) *nub-Gal4*, *UAS-ed-RNAi*; *Delta^X/+* wings are reduced in size with widened veins (arrowheads) and terminal deltas (inset). Scale bars: 100µm

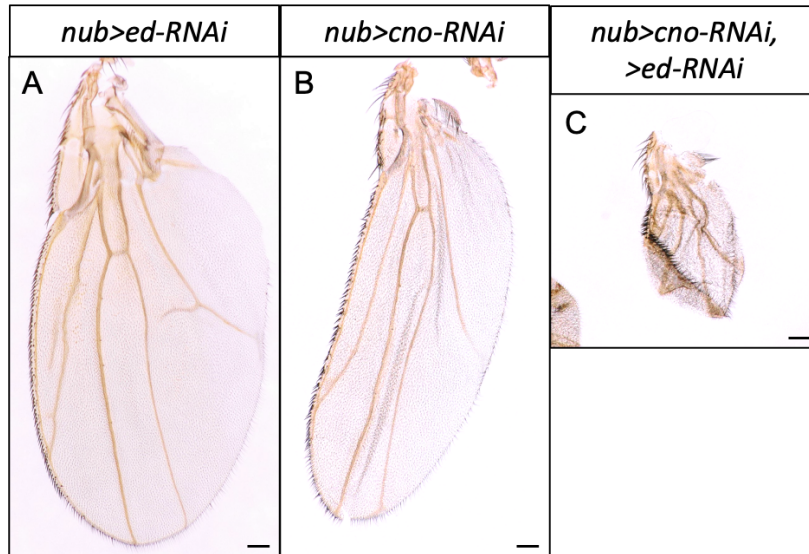


Figure 5.4: Co-depletion of *ed* and *cno* has a synergistic negative effect on growth.

A) *nub-Gal4, UAS-ed-RNAi* wings are large and broad. B) *nub-Gal4, UAS-cno-RNAi* wings are small and narrow. C) *nub-Gal4, UAS-cno-RNAi, UAS-ed-RNAi* wings are rudimentary. Scale bars: 100 μ m

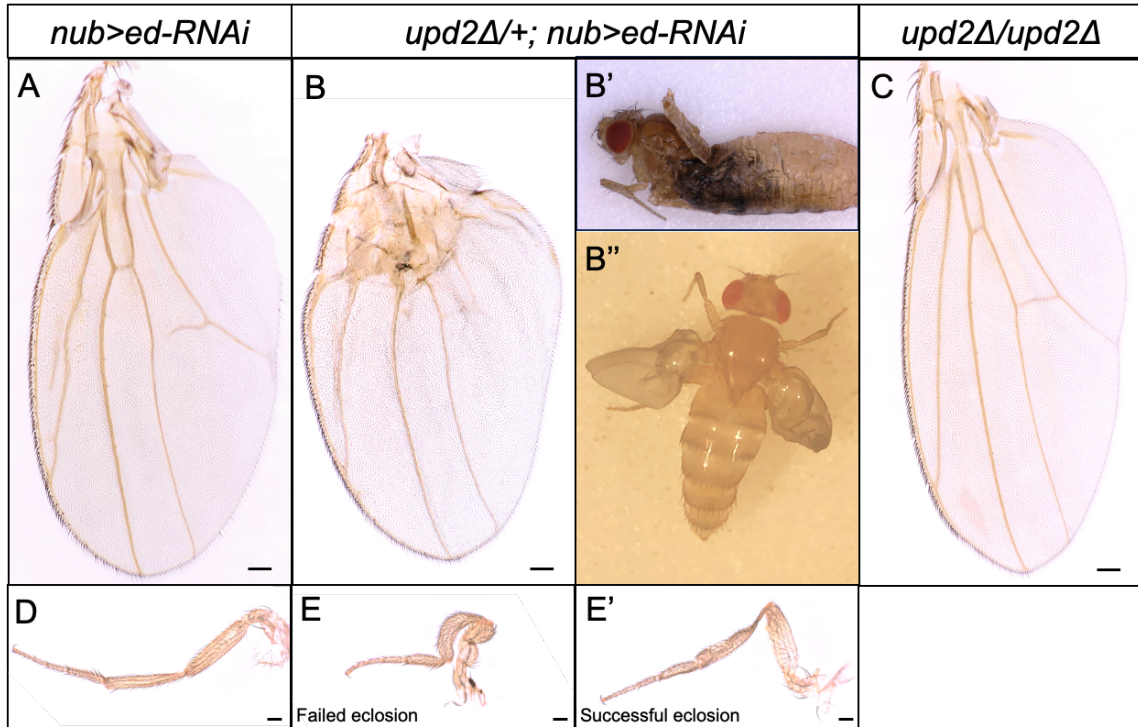


Figure 5.5: The *upd2Δ* allele dominantly modifies the *nub-Gal4*, *UAS-ed-RNAi* wing phenotype.

A) *nub-Gal4*, *UAS-ed-RNAi* wings are large and broad. B) *upd2Δ/+; nub-Gal4*, *UAS-ed-RNAi* flies have reduced wings with proximal blisters or blister scars. Many fail to fully eclose (B'). Prominent blisters are visibly on the wings of flies that do manage to eclose (B''). C) Homozygosity for *upd2Δ* does not cause of the phenotypes seen when a single copy of *upd2Δ* is in combination with *nub-Gal4*, *UAS-ed-RNAi*. D) legs from *nub-Gal4*, *UAS-ed-RNAi* flies have straight leg segments. E) *upd2Δ/+; nub-Gal4*, *UAS-ed-RNAi* flies have shortened, convoluted legs. The phenotype is less severe in the flies which successfully eclose (E'). Scale bars: 100μm

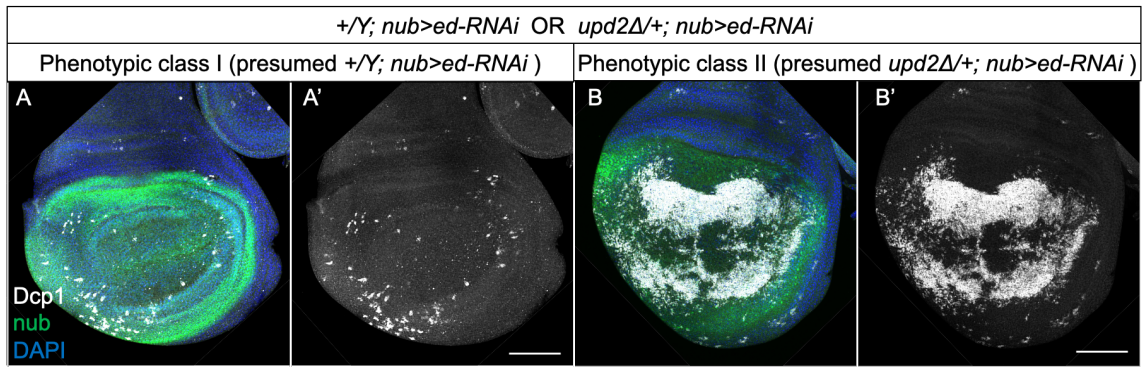


Figure 5.6: High levels of apoptosis in *upd2Δ/+; nub-Gal4, UAS-ed-RNAi* wing imaginal discs.

(A) Phenotypic class I discs show an apoptosis pattern typical of *nub-Gal4, UAS-ed-RNAi* alone and are presumed to be *+Y; nub-Gal4, UAS-ed-RNAi*. B) Phenotypic class II discs show a much higher level of apoptosis pattern than is typical of *nub-Gal4, UAS-ed-RNAi* alone and are presumed to be *upd2Δ/+; nub-Gal4, UAS-ed-RNAi*. Scale bars: 100μm.

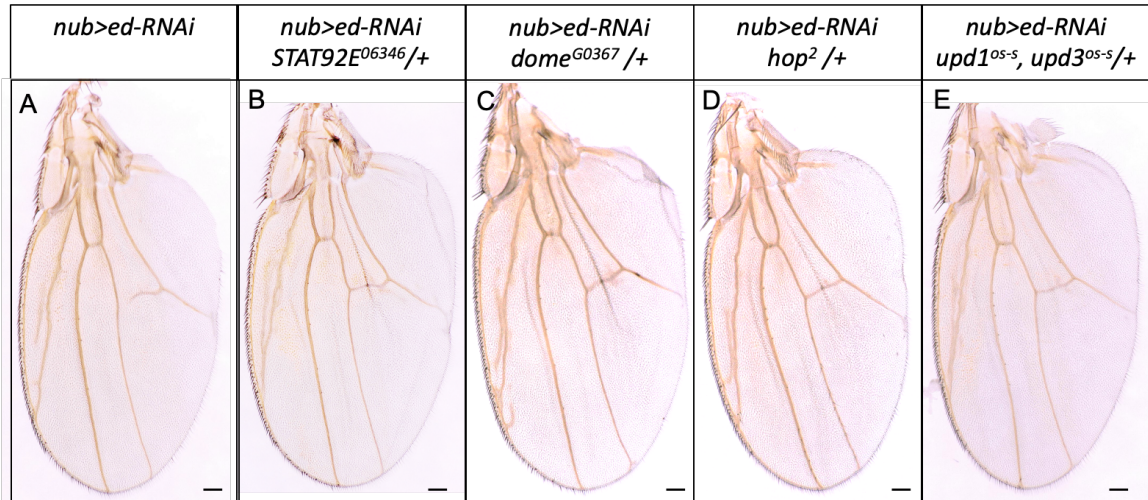


Figure 5.7: Various members of the Jak-STAT pathway do not modify the *nub-Gal4*, *UAS-ed-RNAi* phenotype in the same manner as *upd2A*.

A) *nub-Gal4*, *UAS-ed-RNAi* wings are large and broad. Heterozygosity for loss-of-function mutations in B) *STAT92E*, C) *dome*, D) *hop*, or E) *upd1* and *upd3* does not reduce size of *nub-Gal4*, *UAS-ed-RNAi* wings or cause blisters. Scale bars: 100 μ m

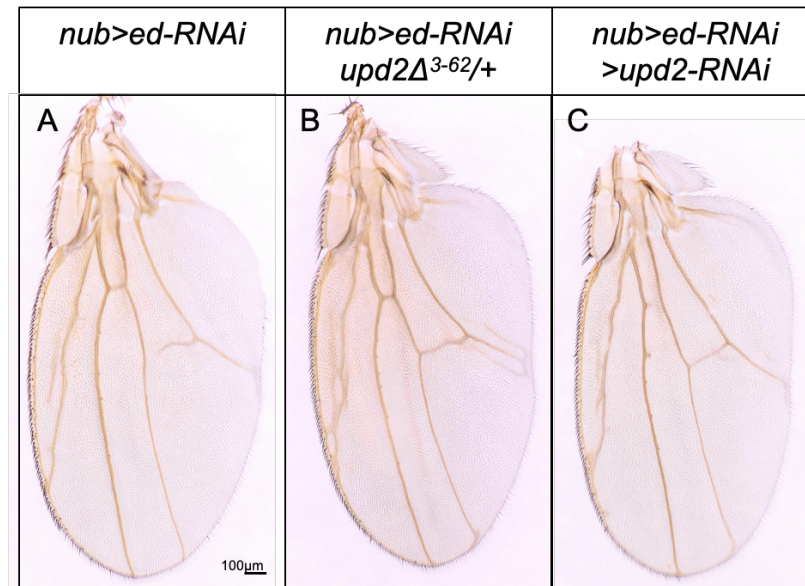


Figure 5.8: Depletion of *upd2* using reagents other than the *upd2Δ* allele does not modify the *nub-Gal4*, *UAS-ed-RNAi* phenotype.

A) *nub-Gal4*, *UAS-ed-RNAi* wings are large and broad. B) heterozygosity for the *upd2Δ³⁻⁶²* null allele or C) co-expression of *UAS-ed-RNAi* and *UAS-upd2-RNAi* by *nub-Gal4* does not result in reduced wing size or blisters. Scale bars: 100µm

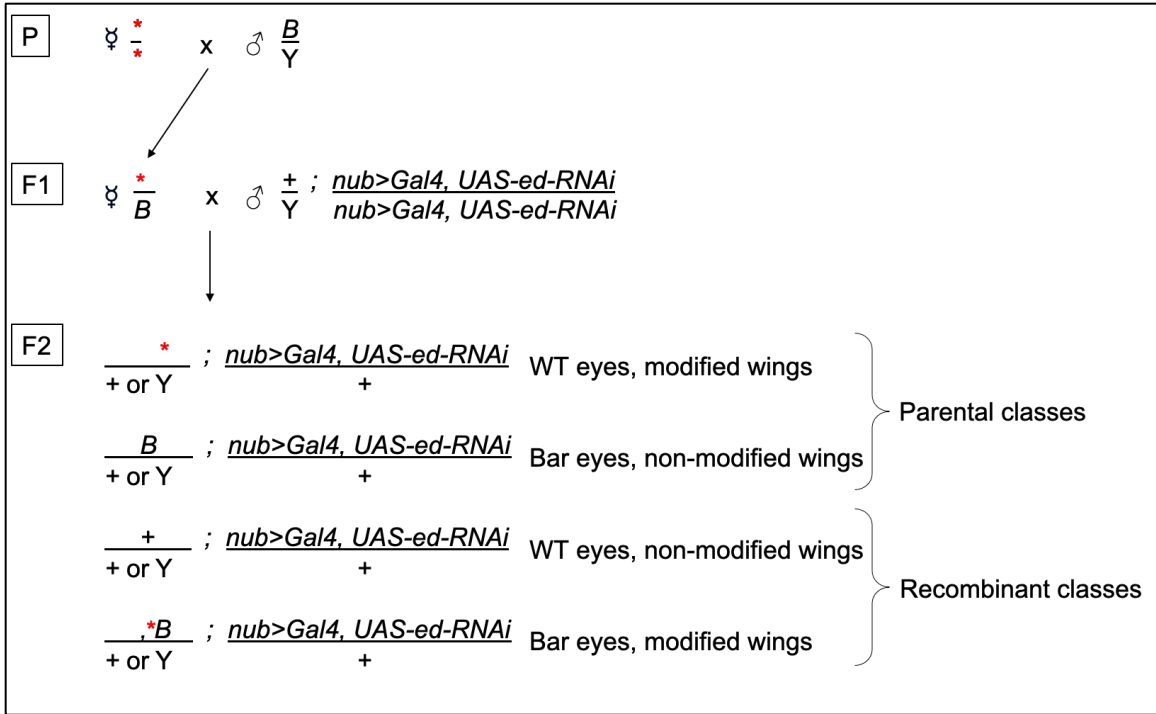


Figure 5.9: Genetic scheme used for recombination mapping.

Only relevant genetic features are shown. The genetic modifier associated with the *upd2A* chromosome is represented as a red asterisk.

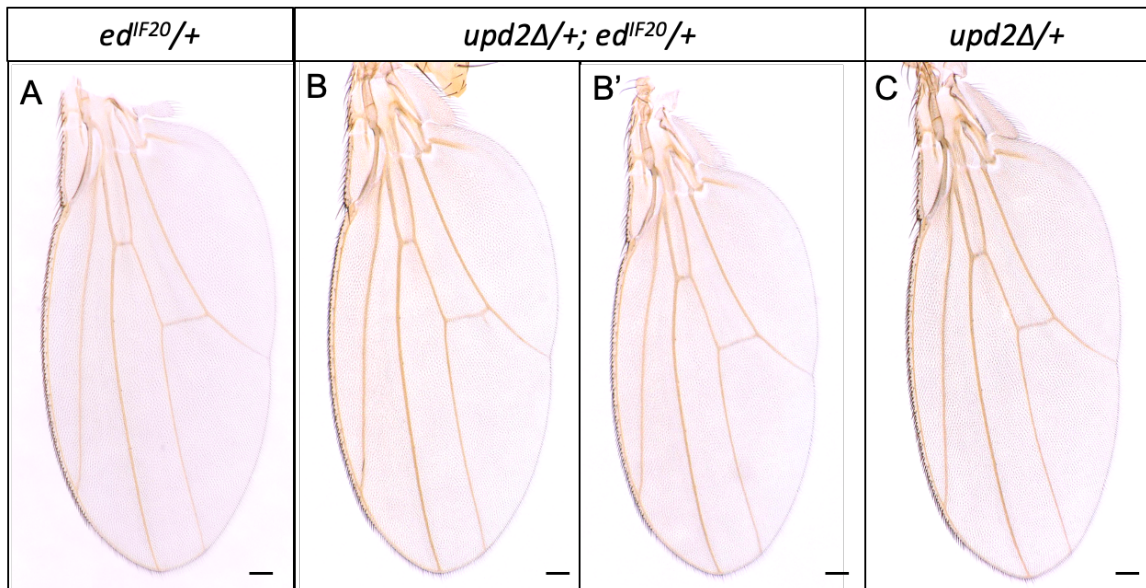


Figure 5.10: *upd2Δ* does not strongly genetically interact with the null *ed^{IF20}* allele.

A) *ed^{IF20}/+* heterozygote. B) Range of wing sizes seen in *upd2Δ/+; ed^{IF20}/+* double heterozygotes. Scale bars: 100μm

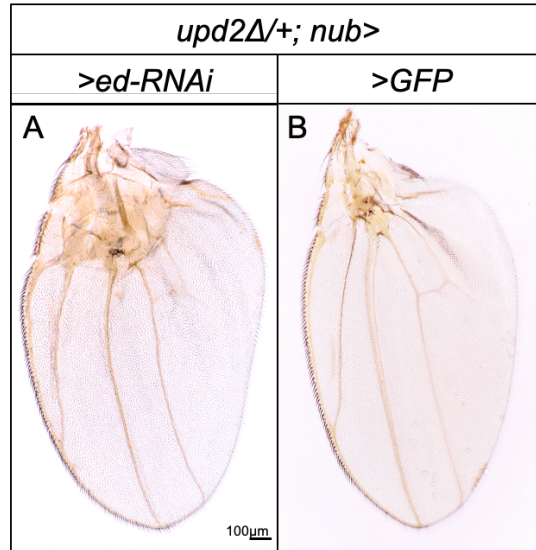


Figure 5.11: *upd2Δ*, which contains a *UAS* misexpression site, genetically interacts with *nub-Gal4*.

A) Wings of the genotype *upd2Δ/+; nub-Gal4, UAS-ed-RNAi* are small and have proximal blister scars. B) Wings of the genotype *upd2Δ/+; nub-Gal4, UAS-GFP* are also small and have proximal blister scars. Scale bars: Scale bars: 100μm.

Table 5.1: Results from dominant modifier screen.

Crosses with loss-of-function alleles					
Allele	Pathway/Processes	BDSC #	Full Genotype	Interaction	Notes on observation
eff[mer4]	[diap1 regulator]	BL6401	w[1118];; eff[mer4]/TM3, Sb[1]	None	
Grip[M10366]	[known interaction w/ ed]	BL55472	y,w;MiMlc.Grip[M10366]	Growth enhancement (slight)	a few outliers show very small enlargement of wing length
Smurf[M107104]	[known interaction w/ ed]	BL44700	y[1] w[*]; Mi {y[+mDint2]=MIC} Smurf[M107104]	None	
tutl[M108144]	[known interaction w/ ed]	BL44758	y[1] w[*]; Mi {y[+mDint2]=MIC} tutl[M108144] /<SM6a>	None	
jar[2095]	Actomyosin contractility	BL7246	w[*];; P {w[+tAR] ry[+t7.2AR]=wA[R]} jar[2095]/TM3, Sb[1] Ser[1]	None	
Sqh[Ax3]	Actomyosin contractility	BL25712	w[*] sqh[AX3] P {ry[+t7.2]=neoFRT} 19A/FM7c	None	Close call, maybe very slight enhancement?
zip[1]	Actomyosin contractility	BL4199	; sn[1],bw[1],speck[1],zip[1]/CyO	Growth suppression (moderate)	medium range of suppression, both wing length and weight
hid[1]	Apoptosis	BL631	;; hid[1]	Growth suppression (slight)	very small shrinkage of wing width

morgue[EP1184]	Apoptosis	BL16996	w[1118]; P{w[+mC]=EP}morgue[EP1184]/CyO	Growth enhancement (moderate)	consistent yet small enlargement of wings (both length and width)
Df(3L)H99	Apoptosis	BL1576	:: Df(3L)H99, kni[ri-1] p[p]/TM3, Sb[1]	None	
arm[4]	Cell junctions	BL68161	y[1] arm[4] P{ry[+t7.2]=neoFRT}19A/FM0	Growth enhancement (slight)	very small enlargement of wing length
baz[4]	Cell junctions	BL3295	y[1] baz[4]/FM7a	Growth enhancement (slight)	very small trend towards enhancement of wing length
fred[MI02235]	Cell junctions	BL34300	y[1] w[*]; Mi{y[+mDint2]=MIC}fred[MI02235]/SM6a	None	
fred[MI03208]	Cell junctions	BL36263	y[1] w[*]; Mi{y[+mDint2]=MIC}fred[MI03208]/SM6a	None	
Nrg[14]	Cell junctions	BL5708	Nrg[14]/FM7c	Growth enhancement (moderate)	noticeable enlargement of wing length and width
Nrg[17]	Cell junctions	BL5595	Nrg[17]/FM7c, sn[+]	None	Close call, maybe very slight enhancement?
aos[Δ7]	EGFR/Ras	BL1004	:: aos[Delta7]/TM3, Sb[1]	None	
Egfr[f2]	EGFR/Ras	BL2768	; cn[1] Egfr[f2] bw[1] speck[1]/CyO	None	
Raf[7]	EGFR/Ras	BL7338	Raf[7]/FM7a	Growth enhancement (slight)	very very small enlargement of wing

Ras85D[e2F], sev[14]	EGFR/Ras	BL5690	sev[14];; Ras85D[e2F]/TM3, Sb[1]	None	
rl[1]	EGFR/Ras	BL386	rl[1]	None	
S[1]	EGFR/Ras	BL8616	; S[1]/SM1; Sb[1]/TM6	None	
Sos[34Ea-6]	EGFR/Ras	BL2240	; b[1] Sos[34Ea-6] Adh[n4]/CyO	None	
spi[1]	EGFR/Ras	BL1859	; spi[1] cn[1] bw[1] speck[1]/CyO	None	
sty[Δ5]	EGFR/Ras	BL6382	w[*];; sty[Delta5]/TM3, Sb[1] P{w[+mC]=35UZ}2	None	
Sty[226]	EGFR/Ras	BL6383	w[*];; sty[226] hry[1] e[*] ca[1]/TM6B, Tb[1]	Growth enhancement (moderate)	small trend towards enlargement of wing length in particular
Ap2μ[G4842]	Endocytic trafficking	BL30102	w[1118]; P{w[+mC]=EP}AP-2mu[G4842]/TM6C, Sb[1]	None	
Rab11[93Bi]	Endocytic trafficking	BL4158	; Rab11[93Bi] e[LE1] cd[1]/TM3, Sb[1] Ser[1]	Growth enhancement (slight)	very very small enlargement of wing length
Rab11[EP3017]	Endocytic trafficking	BL42708	w[*];; P{w[+mC]=EP}Rab11[EP3017]/TM6B, Tb[1]	None*	some of wings had noticeable suppression of both wing length and height, rest were normal
RASSF8[MI10112]	Endocytic trafficking	BL53462	y[1] w[*];; Mi{y[+mDint2]=MIC}RASSF8[MI10112]	None	
RASSF8[G15974]	Endocytic trafficking	BL31807	w[1118];; P{w[+mC]=EP}RASSF8[G15974]	Growth suppression (slight, variable)	

ex[1]	Hippo	BL295	ex[1]	Growth enhancement (slight)	very small enhancement of wing length
kibra[MI01487]	Hippo	BL40175	y[1] w[*];; Mi{y[+mDint2]=MIC}kibra[MI01487]/TM3, Sb[1] Ser[1]	Growth enhancement (slight)	consistent yet small enlargement of wing length
Mer[MI02931]	Hippo	BL36167	y[1] w[*] Mi{y[+mDint2]=MIC}Mer[MI02931]	None	
Mer[3]	Hippo	BL9103	w[*] Mer[3] P{ry[+t7.2]=neoFRT}19A/FM7c	Growth enhancement* (strong)	very noticeable enlargement of wing length and width. *NOTE: Mer[3] heterozygotes have enlarged wings, phenotypes may be additive
sd[1]	Hippo	BL1027	sd[1]	None	
wts[3-17]	Hippo	BL7052	;; st[1] in[1] kni[ri-1] p[p] wts[3-17]/TM3, Sb[1]	Growth enhancement (moderate)	noticeable enhancement of wing height
Diap1[th-1], cno	Hippo, Apoptosis, Cell junctions	BL3107	;; ru[1] hry[1] Diap1[th-1] st[1] cno[2] cu[1] sr[1] e[s] ca[1]/TM3, Sb[1] Ser[1]	None	
Diap1[th-1], crb[11A22]	Hippo, Apoptosis, Cell junctions	BL3448	;; ru[1] hry[1] Diap1[th-1] st[1] cu[1] sr[1] e[s] crb[11A22] ca[1]/TM3, Sb[1] Ser[1]	Growth enhancement (moderate)	consistent yet small enlargement of wings (seems like both length and height)
ex[1], ds[1], S[X]	Hippo, EGFR/Ras, PCP	BL296	; ex[1], ds[1], S[X], ast[X]/SM1	Growth suppression	medium range of variation, yet several are noticeably

				(slight, variable)	shrunk in height but especially length
ds[W]	Hippo, PCP	BL287	; ds[W]/CyO	None	
ft[1]	Hippo, PCP	BL304	; ft[1];	Growth enhancement (slight)	
ft[G-rv]	Hippo, PCP	BL1894	; ft[G-rv]/SM5	Growth enhancement (slight)	consistent yet small enlargement of wing length
?	included by accident?	BL6698	Df(1)hl-a, w[1] cv[1] Bar[1]/C(1)DX, y[1] f[1]; Dp(1;2)sn[+]72d/Dp(?;2)bw[D], bw[D]	Growth enhancement (slight)	very small trend towards wing length enlargement
dome[G0367]	Jak-STAT	BL11986	w[67c23] P{w[+mC]=lacW}dome[G0367]/F M7c	Growth enhancement (moderate)	very small enlargement of wing height
hop[2]	Jak-STAT	BL6032	hop[2]/FM7a	None	
Stat92E[F]	Jak-STAT	BL24757	w[*];; e[1] Stat92E[F]/TM6C, cu[1] Sb[1]	None	
Stat92E[06346]	Jak-STAT	BL11681	; ry[506] P{ry[+t7.2]=PZ} Stat92E[06346]/T M3, ry[RK] Sb[1] Ser[1]	None	
upd1[os-s], upd3[os-s]	Jak-STAT	BL79	Ab(1)os[s], upd1[os-s] upd3[os-s]	None	
upd2Δ	Jak-STAT	BL55727	w, upd2Δ	Growth suppression (strong),	very noticeable shrinkage of wing length and width;

				blistering, eclosion failure	many wings damaged, unfolded as well
upd2Δ, upd3Δ	Jak-STAT	BL55729	w,upd2[Δ],upd3[Δ];;	Growth suppression (strong), blistering, eclosion failure	very noticeable shrinkage of wing length and width; many wings damaged, unfolded as well
Delta[X]	Notch	BL60336	; Delta[X]/TM3.Sb	Growth suppression (moderate, variable)	wide range of suppression
N[55e11]	Notch	BL34814	N[55e11] P{ry[+7.2]=neoFRT}19A/FM7c	Growth enhancement (moderate, in wings w/o notching), enhancement of notching	high rate of wing notching/scalloping. noticeable enlargement of wing length & height in wings that aren't notched
Su(H)[1]	Notch	BL417	; Su(H)[1]/In(2L)Cy, In(2R)Cy, Duox[Cy] pr[1]	None	
Akt[04226]	Pi3K/Insulin	BL11627	; ry[506] P{ry[+7.2]=PZ}Akt[04226]/TM3, ry[RK] Sb[1] Ser[1]	Growth enhancement (slight)	very very small enlargement of wing height
chico[1]	Pi3K/Insulin	BL10738	; cn[1] P{ry[+7.2]=ry11}chico[1]/CyO; ry[506]	Growth enhancement (moderate)	noticeable enhancement of wing length

foxo[21]	Pi3K/Insulin	BL80943	y[1] w[*];; foxo[21]/TM6B, Tb[1]	None	
Pi3K92E[KO]	Pi3K/Insulin	BL93737	w[*];; Pi3K92E[KO]/TM3, Sb[1]	None	no sig. change
Pten[117]	Pi3K/Insulin	BL80967	y[1] w[*]; Pten[117]/CyO	None	
gig[109]	Tor	BL4739	; mwh[1] jv[1] gig[109] red[1] ro[1]/TM3, Ser[1]	None	
mTor[R97C]	Tor	BL80931	y[1] w[*]; mTor[R97C]/T(2;3)SM6a-TM6B, Tb[1]	None	
Tsc1[Q600X]	Tor	BL82163	y[1] w[*]; P{ry[+t7.2]=neoFRT}82B Tsc1[Q600X]/TM6B, Tb[1]	Growth enhancement (slight)	consistent yet small enlargment of length (maybe also width to smaller degree)
Crosses with UAS-RNAi or UAS-OE (Need control cross to nub-Gal4 alone to interpret phenotype)					
Allele	Pathway/Processes	BDSC #	Full Genotype	Interaction	Notes on observation
UAS.eff.HA	[diap1 regulator]	BL26691	w[*];; P{w[+mC]=UAS-eff.HA}1.4	None	
UAS-kibra-RNAi	Hippo	BL51499	y[1] sc[*] v[1] sev[21]; P{y[+t7.7] v[+t1.8]=TRiP.HMC03256}attP2	Growth enhancement (moderate)	wide range yet trending towards enhancement of both wing length and width
UAS-cno-RNAi	[known interaction w/ ed]	BL33367	y[1] sc[*] v[1] sev[21]; P{y[+t7.7] v[+t1.8]=TRiP.HMS00239}attP2	Growth suppression (extreme) [enhancement of nub>cno- RNAi alone phenotype]	all so small and cup-shaped, none measurable

UAS-raptor-RNAi	mTor	BL34814	y[1] sc[*] v[1] sev[21]; P{y[+t7.7] v[+t1.8]=TRiP.HMS00124}attP2	Growth suppression (extreme) [Not a hit; nub>raptor-RNAi alone gave similar phenotype]	wide range of shrinkage, yet very immense shrinkage, many wings still folded.
UAS-Grip-RNAi	[known interaction w/ ed]	BL41978	y[1] sc[*] v[1] sev[21]; P{y[+t7.7] v[+t1.8]=TRiP.HMS02376}attP2	None	
UAS-Smurf-RNAi	[known interaction w/ ed]	BL40905	y[1] sc[*] v[1] sev[21]; P{y[+t7.7] v[+t1.8]=TRiP.HMS02153}attP40/<CyO>	Growth enhancement (slight)	consistent yet small percent of wing length
UAS-tutl-RNAi	[known interaction w/ ed]	BL54850	y[1] v[1]; P{y[+t7.7] v[+t1.8]=TRiP.HMJ21587}attP40/<CyO>	None	

Conclusion

To identify genes that regulate growth in mosaic contexts, we conducted an RNAi screen of genes encoding cell adhesion molecules. We recovered a handful of hits which alter the growth, survival, or morphology of knockdown clones and we focused on characterizing the phenotypes associated with reduction of one hit, *echinoid* (*ed*). Like others (Chang et al., 2011; Escudero et al., 2003; Wei et al., 2005), we observed that *ed* clones have a growth and survival disadvantage in mosaic discs. Our work expands on this observation to provide some mechanistic insight into why: *ed* clones have autonomously decreased levels of Diap1 protein and are consequently more prone to apoptosis. Whether cell competition plays a role in the elimination of *ed* clones—and if so, to what extent—is unknown. However, it is plausible that the fitness disadvantage of *ed* clones may be exacerbated by the fact that wild-type cells bordering *ed* clones often express increased levels of Hippo pathway target genes, which could cause these them to behave like supercompetitors which contribute to the elimination of “loser” *ed* cells.

Although *ed* cells are often eliminated from mosaic tissues, they are viable in some non-mosaic contexts such as when comprising entire compartments or organs, which overgrow. The overgrowth does not require faster growth—when *ed* was knocked down in only posterior cells, the affected compartments grew at a slower rate—rather, *ed* tissue continues growing beyond the size at which growth would normally terminate. Expression of full-length Ed or Ed lacking the C-terminal domain can rescue the overgrowth of Ed-depleted wings, indicating that Ed regulates organ size via its extracellular and/or transmembrane domain(s). Although dispensable for size control, the C-terminal domain is required for proper elongation of the wing.

Prior to this work, the generally accepted view of *ed*'s role in the Hippo pathway was that Ed autonomously promotes Hippo pathway activation to restrict growth, which would explain why *ed*-depleted organs overgrow. However, our experiments revealed that the relationship between *ed* and the Hippo pathway is more complex and less straightforward than previously thought. While some of our experiments faithfully replicated findings upon which the “textbook” view is based, (e.g., knockdown of Ed in the posterior compartment leads to autonomously increased activity of *ex-lacZ*), in other cases, we failed to replicate earlier findings (e.g., knockdown of *ed* in clones did not lead to a clone-autonomous increase in Diap1 proteins in our hands). We also showed that Ed perturbations can non-autonomously increase the expression of Yorkie target genes in neighboring cells.

While the discrepancies between our findings and previously published work seem difficult to reconcile, another one of our key findings may provide a clue as to why: *ed*'s effects on downstream targets of the Hippos pathway are context specific. It was already known that some phenotypes associated with *ed* loss are tissue-specific (for example, Ed clones do not have an apparent survival disadvantage in the follicle [Laplante & Nilson, 2006]), and we showed that *ed* reduction reduces growth in some contexts (clonal

elimination) yet promotes growth in other contexts (overgrowth of *ed* organs). We found that the impact of a particular *ed* manipulation on Hippo pathway target genes vary depending on whether clones or broader regions are affected (e.g., *ed-OE* does not affect Diap1 levels in clones but decreases Diap1 levels when entire compartments are affected).

The expression of Yorkie target genes is often used as an indirect measure of Hippo pathway activity. However, not all genes with Yorkie-dependent transcription responded to *ed* manipulations in the same way (as would be expected if their levels were reflective of Hippo pathway activity and nothing else). This means that one or more of these genes must have additional regulatory inputs beyond the Hippo pathway which are operating in the context of *ed* manipulation. Crosstalk between Hippo and other pathways which Ed can regulate (e.g., EGFR, Notch) could account for this variation in response.

Lastly, in an attempt to identify dominant modifiers of the overgrowth phenotype caused by loss of *ed* in the wing, we discovered a genetic interaction between the *upd2Δ* allele and *nub-Gal4*, *UAS-ed-RNAi*. We ultimately determined that this was an *ed*-independent artifact of *UAS*-misexpression from a *UAS* sequence present at the *upd2Δ* deletion site. Many other deletion alleles have been generated in a similar manner to the *upd2Δ* allele and contain *UAS*-misexpression sites. We present our experience as a cautionary tale and urge other researchers to confirm the nature of the lesion when using any deletion lines, and to be aware of misexpression artifacts when using *UAS*-containing deletion alleles in experiments involving Gal4.

In sum, this work advances our understanding of the role of *ed* in growth regulation in a few major ways. First, I show that *ed*-depleted clones are eliminated by apoptosis, which is the result of decreased Diap1 expression and may be exacerbated by competition from neighbors. Second, I confirm that *ed*-depleted tissue can overgrow due to a failure of the mechanism that arrests growth when an organ reaches its final size. Third, I have provided a more complex picture of how *ed* interacts with the Hippo pathway, which indicates that prevailing view cannot account for many of the phenotypes associated with *ed*.

Materials and Methods

Fly Stocks & Husbandry

Unless otherwise noted, all experimental crosses were raised at 25°C on food prepared according to the recipe from the Bloomington Stock Center.

Stocks used in this study include or were derived from the following:

Oregon-R (“Ore-R,” used as wild type), *y w hs-FLP; act<[y+]<Gal4 UAS-GFP/SM5-TM6B, hs-FLP;*; *act<stop<Gal4 UAS-RFP/SM5-TM6B, TIE-DYE* (Worley et al., 2013), *FRT40A* and *FRT40A, white+ ubi-GFP* (T. Xu & Rubin, 1993), *FRT40A MARCM* (Lee & Luo, 1999), *eyFLP; FRT40A CL white+/CyO* (BL5622), *UAS-ed* (Bai et al., 2001), *ed^{IF20} FRT40A, ed^{IX5} FRT40A, and ed^{SIH8} FRT40A* (Bai et al., 2001), *UAS-ed^{Full}* and *UAS-ed^{AC}-GFP* (Laplante & Nilson, 2011), *nub-Gal4 (AC-62, BL25754), hh-Gal4* (BL45169), *UAS-w-RNAi* (BL33644), *UAS-ama-RNAi* (BL33416), *UAS-beat-Vc-RNAi* (BL60067), *UAS-Cont-RNAi* (BL34867), *UAS-shg-RNAi* (BL32904), *UAS-side-VII-RNAi* (V10011), *UAS-ft-RNAi* (BL34970), *UAS-ds-RNAi* (BL32964), *UAS-ed-RNAi* (V104279, V3087, V938, BL38423 [“*ed-RNAi*” refers to V104279 unless otherwise indicated]), *UAS-otk2-RNAi* (BL), *UAS-p35* (BL5073), *UAS-cno-RNAi* (BL3367), *UAS-upd2-RNAi* (BL33949), *Mer³* (BL9103), *wts³⁻¹⁷* (BL7052), *Diap^{th-1} crb^{11A22}* (BL3448), *N^{55e11}* (BL34814), *Delta^X* (BL60336), *upd2Δ* and *upd2Δ, upd3Δ* (BL55727, BL55729, (Osman et al., 2012), *upd2Δ³⁻⁶²* (Hombria et al., 2005), *Stat92E⁰⁶³⁴⁶* (11682), *dome^{G0367}* (BL11986), *hop²* (BL6032), *upd1^{os-s}, upd3^{os-s}* (BL79), and *Bar¹* (BL2969). “BL#” or “V#” indicates stocks obtained from the Bloomington Stock Center (Bloomington, IN, USA) or Vienna Drosophila Resource Center (Vienna, Austria), respectively.

Additional stocks which were included in genetic screens but are not mentioned in the main text are listed Table 2.3 (clonal screen) and Table 5.1 (dominant modifier screen) with BDSC or VDRC numbers indicated.

Mosaic tissue generation

Clones induced by heat shock were generated in a 37°C water bath 48 h before dissection, unless otherwise noted. FLP-out Gal4 clones were made using heat shocks of 12 minutes (to generate clones at low density), 15 minutes (for medium density), or 30 minutes (for high density). MARCM clones and mitotic recombination clones were generated using a 1-hr heat shock.

Mitotic recombination clones made in the eye were induced by expression of the *eyFLP* driver.

Clonal screen

~10 *UAS-RNAi* males were crossed to ~20 *y, w, hs-FLP; act<[y+]<Gal4, UAS-GFP/SM5-TM6B* or *TIE-DYE (Act<stop<lacZnls, Ubi <stop<GFPnls; Act<stop<GAL4,*

UAS-his2A::RFP/SM5-TM6B) virgin females. Crosses were kept on Bloomington food supplemented with yeast and flipped once daily. Clones were induced by heat shock on day 3. Early rounds of screening used a 15-minute heat shock, although we later switched to a 12-minute heat shock for the majority of the screen since the low clone density made identifying deviations in either direction easier. Wing imaginal discs from ~6 wandering L3 larvae per line were dissected ~48h after heat shock, stained with DAPI, and imaged.

Immunohistochemistry and fluorescence microscopy

Imaginal discs were dissected in PBS, fixed in 4% paraformaldehyde in PBS, and permeabilized in 0.1% Triton in PBS. Primary antibody incubations were done overnight at 4°C. Secondary antibody incubations were done for 2-3h at room temperature, or overnight at 4°C. Discs were mounted in SlowFade Diamond Antifade Mountant (S36963, Invitrogen).

Primary antibodies used are: rabbit anti-Ed (1:500, J-C. Hsu, [Wei et al., 2005]) rabbit anti-cleaved Dcp-1 (1:250; Asp216, Cell Signaling Technology), mouse anti-Diap1 (1:200, B. Hay), mouse anti- β -Galactosidase (1:500, WH0051083M1 Sigma-Aldrich), mouse anti- β -Galactosidase (1:500, SAB4200805, Sigma-Aldrich), rat anti-Ci (1:500, #2A1; Developmental Studies Hybridoma Bank, DSHB), rat anti-Fat (1:400, K. Irvine, [Feng & Irvine, 2009]), and guinea pig anti-Cic (1:300, [Tseng et al., 2007]).

Secondary Alexa-Fluor antibodies from Invitrogen were used at 1:500. Nuclei were stained with DAPI (1:1,000, Cell Signaling).

Fluorescence images were taken on a Zeiss Axio Imager M2 equipped with a 20 \times objective (Plan-Apochromat, 20 \times /0.8, Zeiss), LED light source (Excelitas Technologies), AxioCam 506 mono camera (Zeiss), and ApoTome.2 slider for optical sectioning. Images and image stacks were acquired and optically sectioned in ZEN 2.3 software (Zeiss). Images were processed using FIJI software (Schindelin et al., 2012). Unless otherwise noted, images show a single Z-plane.

Adult wing imaging and quantification

Adult wings were dissected from female flies. One wing per fly was mounted in Gary's Magic Mountant (Lawrence et al., 1986). Wings were imaged using a Keyence VHX-5000 digital microscope, using the 20-200 \times lens at 150 \times . Brightness, contrast, and color tone of wing images have been adjusted on some images for improved visibility of features relevant to this study (wing shape and size).

For qualitative comparisons of wing sizes, wing images or traced silhouettes were overlaid in Powerpoint or GoogleSlides. For quantitative comparisons of wing sizes, wings were traced and surface area was quantified in Fiji. Charts were generated using the ggplot2 package in RStudio (Wickham, 2016).

Wing aspect ratios were calculated by dividing the length of proximodistal (PD) axis (measured from the posterior junction of the wing and hinge to the tip of the L3 vein) by

the length of the anteroposterior (AP) axis (measured as the shortest distance from the tip of the L5 vein to the L1 margin).

Statistical analysis

P values were obtained by one-way ANOVA with Tukey's HSD test using Astatsa freeware (Vasavada, 2016). P value significance <0.01: **; 0.01 to 0.05: *; >0.05: not significant. All error bars show standard deviation.

Hybridization Chain Reaction

In situ hybridization chain reaction (HCR) was performed on wing discs based on HCR v3.0 protocol (Bruce et al., 2021; Choi et al., 2018) excluding methanol dehydration. Larvae were dissected, fixed in 4% paraformaldehyde in PBS, permeabilized, and incubated overnight with RNA probes at 37°C. Samples were then washed and incubated overnight with fluorescently-tagged RNA hairpins and DAPI at room temperature. Probe sequences were designed in an open-source probe design program (ÖzpolatLab-HCR, 2021) and synthesized by Integrated DNA Technologies. Hairpins and buffers were from Molecular Instruments.

Dominant modifier screen

~10 males with loss-of-function mutations were crossed to ~20 *w; nub-Gal4, UAS-ed-RNAi*/*<CyO, Tb>* virgin females (for mutations balanced over FM7, the male and female parents were swapped to enable X-linked inheritance from the female parent). Egg lays were done on Bloomington food and limited to 1 day as a minimal density control measure. Adult wings from ~10 females (one wing per animal) were dissected, mounted, and imaged. Wing outlines were manually traced in GoogleSlides. All outlines from a particular genotype were overlaid to visualize the distribution of wings sizes for that genotype. These were then compared to the combined traces from the no-modification control (*w; nub-Gal4, UAS-ed-RNAi*/*<CyO, Tb>* x *OreR*).

Recombination mapping

Crosses were conducted as outlined in Figure 5.9. Recombination frequency was calculated using the following formula: (# of recombinant offspring / total # of offspring) x 100

All progeny were scored, including offspring which failed to eclose from their pupal cases.

Whole genome sequencing

Genomic DNA was prepared as described by (Huang et al., 2009), with the following modifications: addition of a 1hr incubation with RNAse after Step 2, addition of Proteinase K immediately before Step 3, and addition of a 5 minute incubation at 95C to denature Proteinase K after Step 3. Library prep, Next Generation short-read whole genome sequencing, read calling, and genome alignment was performed by Azenta/Genewiz.

References

- Ahmed, A., Chandra, S., Magarinos, M., & Vaessin, H. (2003). Echinoid mutants exhibit neurogenic phenotypes and show synergistic interactions with the Notch signaling pathway. *Development*, *130*(25), 6295–6304. <https://doi.org/10.1242/dev.00796>
- Akieda, Y., Ogamino, S., Furuie, H., Ishitani, S., Akiyoshi, R., Nogami, J., Masuda, T., Shimizu, N., Ohkawa, Y., & Ishitani, T. (2019). Cell competition corrects noisy Wnt morphogen gradients to achieve robust patterning in the zebrafish embryo. *Nature Communications*, *10*(1), 4710. <https://doi.org/10.1038/s41467-019-12609-4>
- Alliance of Genome Resources. (n.d.). *CG33639*. Retrieved July 23, 2023, from <https://www.alliancegenome.org/gene/FB:FBgn0053639>
- Amoyel, M., & Bach, E. A. (2014). Cell competition: How to eliminate your neighbours. *Development*, *141*(5), 988–1000. <https://doi.org/10.1242/dev.079129>
- Anderson, A. M., Bailetti, A. A., Rodkin, E., De, A., & Bach, E. A. (2017). A Genetic Screen Reveals an Unexpected Role for Yorkie Signaling in JAK/STAT-Dependent Hematopoietic Malignancies in *Drosophila melanogaster*. *G3 Genes|Genomes|Genetics*, *7*(8), 2427–2438. <https://doi.org/10.1534/g3.117.044172>
- Baeg, G.-H., Zhou, R., & Perrimon, N. (2005). Genome-wide RNAi analysis of JAK/STAT signaling components in *Drosophila*. *Genes & Development*, *19*(16), 1861–1870. <https://doi.org/10.1101/gad.1320705>
- Baena-López, L. A., Baonza, A., & García-Bellido, A. (2005). The Orientation of Cell Divisions Determines the Shape of *Drosophila* Organs. *Current Biology*, *15*(18), 1640–1644. <https://doi.org/10.1016/j.cub.2005.07.062>
- Baena-Lopez, L. A., Rodríguez, I., & Baonza, A. (2008). The tumor suppressor genes *dachsous* and *fat* modulate different signalling pathways by regulating *dally* and *dally-like*. *Proceedings of the National Academy of Sciences*, *105*(28), 9645–9650. <https://doi.org/10.1073/pnas.0803747105>
- Bai, J.-M., Chiu, W.-H., Wang, J.-C., Tzeng, T.-H., Perrimon, N., & Hsu, J.-C. (2001). The cell adhesion molecule Echinoid defines a new pathway that antagonizes the *Drosophila* EGF receptor signaling pathway. *Development*, *128*, 591–601.
- Baker, N. E. (2011). Cell competition. *Current Biology*, *21*(1), R11–R15. <https://doi.org/10.1016/j.cub.2010.11.030>

- Bennett, F. C., & Harvey, K. F. (2006). Fat Cadherin Modulates Organ Size in *Drosophila* via the Salvador/Warts/Hippo Signaling Pathway. *Current Biology*, 16(21), 2101–2110. <https://doi.org/10.1016/j.cub.2006.09.045>
- Bielmeier, C., Alt, S., Weichselberger, V., La Fortezza, M., Harz, H., Jülicher, F., Salbreux, G., & Classen, A.-K. (2016). Interface Contractility between Differently Fated Cells Drives Cell Elimination and Cyst Formation. *Current Biology*, 26(5), 563–574. <https://doi.org/10.1016/j.cub.2015.12.063>
- Bilder, D., Li, M., & Perrimon, N. (2000). Cooperative Regulation of Cell Polarity and Growth by *Drosophila* Tumor Suppressors. *Science*, 289(5476), 113–116. <https://doi.org/10.1126/science.289.5476.113>
- Blackburn, T. M., & Gaston, K. J. (1994). Animal body size distributions: Patterns, mechanisms and implications. *Trends in Ecology & Evolution*, 9(12), 471–474. [https://doi.org/10.1016/0169-5347\(94\)90311-5](https://doi.org/10.1016/0169-5347(94)90311-5)
- Blair, S. S. (2003). Genetic mosaic techniques for studying *Drosophila* development. *Development*, 130(21), 5065–5072. <https://doi.org/10.1242/dev.00774>
- Bosch, J. A., Sumabat, T. M., Hafezi, Y., Pellock, B. J., Gandhi, K. D., & Hariharan, I. K. (2014). The *Drosophila* F-box protein Fbx17 binds to the protocadherin Fat and regulates Dachs localization and Hippo signaling. *ELife*, 3, e03383. <https://doi.org/10.7554/eLife.03383>
- Brankatschk, B., Wichert, S. P., Johnson, S. D., Schaad, O., Rossner, M. J., & Gruenberg, J. (2012). Regulation of the EGF Transcriptional Response by Endocytic Sorting. *Science Signaling*, 5(215). <https://doi.org/10.1126/scisignal.2002351>
- Brodland, G. W. (2002). The Differential Interfacial Tension Hypothesis (DITH): A Comprehensive Theory for the Self-Rearrangement of Embryonic Cells and Tissues. *Journal of Biomechanical Engineering*, 124(2), 188. <https://doi.org/10.1115/1.1449491>
- Bruce, H. S., Jerz, G., Kelly, S. R., McCarthy, J., Pomerantz, A., Senevirathne, G., Sherrard, A., Sun, D. A., Wolff, C., & Patel, N. H. (2021). *Hybridization Chain Reaction (HCR) In Situ Protocol v1* [Preprint]. <https://doi.org/10.17504/protocols.io.bunznvf6>
- Brumby, A. M., & Richardson, H. E. (2003). Scribble mutants cooperate with oncogenic Ras or Notch to cause neoplastic overgrowth in *Drosophila*. *The EMBO Journal*, 22(21), 5769–5779. <https://doi.org/10.1093/emboj/cdg548>
- Bryant, P. J., Huettner, B., Held, L. I., Ryerse, J., & Szidonya, J. (1988). Mutations at the fat locus interfere with cell proliferation control and epithelial morphogenesis in *Drosophila*. *Developmental Biology*, 129(2), 541–554. [https://doi.org/10.1016/0012-1606\(88\)90399-5](https://doi.org/10.1016/0012-1606(88)90399-5)

- Bryant, P. J., & Levinson, P. (1985). Intrinsic growth control in the imaginal primordia of *Drosophila*, and the autonomous action of a lethal mutation causing overgrowth. *Developmental Biology*, *107*(2), 355–363. [https://doi.org/10.1016/0012-1606\(85\)90317-3](https://doi.org/10.1016/0012-1606(85)90317-3)
- Buchon, N., Broderick, N. A., Kuraishi, T., & Lemaitre, B. (2010). *Drosophila* EGFR pathway coordinates stem cell proliferation and gut remodeling following infection. *BMC Biology*, *8*(1), 152. <https://doi.org/10.1186/1741-7007-8-152>
- Burke, R., & Basler, K. (1996). Dpp receptors are autonomously required for cell proliferation in the entire developing *Drosophila* wing. *Development*, *122*(7), 2261–2269. <https://doi.org/10.1242/dev.122.7.2261>
- Chan, E. H. Y., Zhou, Y., Aerne, B. L., Holder, M. V., Weston, A., Barry, D. J., Collinson, L., & Tapon, N. (2021). RASSF8-mediated transport of Echinoid via the exocyst promotes *Drosophila* wing elongation and epithelial ordering. *Development*, *148*(20), dev199731. <https://doi.org/10.1242/dev.199731>
- Chandra, S., Ahmed, A., & Vaessin, H. (2003). The *Drosophila* IgC2 domain protein friend-of-echinoid, a paralogue of echinoid, limits the number of sensory organ precursors in the wing disc and interacts with the Notch signaling pathway. *Developmental Biology*, *256*(2), 302–316. [https://doi.org/10.1016/S0012-1606\(03\)00038-1](https://doi.org/10.1016/S0012-1606(03)00038-1)
- Chang, L.-H., Chen, P., Lien, M.-T., Ho, Y.-H., Lin, C.-M., Pan, Y.-T., Wei, S.-Y., & Hsu, J.-C. (2011). Differential adhesion and actomyosin cable collaborate to drive Echinoid-mediated cell sorting. *Development*, *138*(17), 3803–3812. <https://doi.org/10.1242/dev.062257>
- Chell, J. M., & Brand, A. H. (2010). Nutrition-Responsive Glia Control Exit of Neural Stem Cells from Quiescence. *Cell*, *143*(7), 1161–1173. <https://doi.org/10.1016/j.cell.2010.12.007>
- Chen, C.-L., Gajewski, K. M., Hamaratoglu, F., Bossuyt, W., Sansores-Garcia, L., Tao, C., & Halder, G. (2010). The apical-basal cell polarity determinant Crumbs regulates Hippo signaling in *Drosophila*. *Proceedings of the National Academy of Sciences*, *107*(36), 15810–15815. <https://doi.org/10.1073/pnas.1004060107>
- Choi, H. M. T., Schwarzkopf, M., Fornace, M. E., Acharya, A., Artavanis, G., Stegmaier, J., Cunha, A., & Pierce, N. A. (2018). Third-generation *in situ* hybridization chain reaction: Multiplexed, quantitative, sensitive, versatile, robust. *Development*, *145*(12), dev165753. <https://doi.org/10.1242/dev.165753>
- Clark, H. F., Brentrup, D., Schneitz, K., Bieber, A., Goodman, C., & Noll, M. (1995). Dachous encodes a member of the cadherin superfamily that controls imaginal disc morphogenesis in *Drosophila*. *Genes & Development*, *9*(12), 1530–1542. <https://doi.org/10.1101/gad.9.12.1530>

- Clavería, C., Giovinazzo, G., Sierra, R., & Torres, M. (2013). Myc-driven endogenous cell competition in the early mammalian embryo. *Nature*, *500*(7460), 39–44. <https://doi.org/10.1038/nature12389>
- Conklin, E. G. (1905). *The organization and cell-lineage of the ascidian egg*. Academy of Natural Sciences. <https://doi.org/10.5962/bhl.title.4801>
- Day, S. J., & Lawrence, P. A. (2000). Measuring dimensions: The regulation of size and shape. *Development*, *127*(14), 2977–2987. <https://doi.org/10.1242/dev.127.14.2977>
- de la Cova, C., Abril, M., Bellosta, P., Gallant, P., & Johnston, L. A. (2004). Drosophila Myc Regulates Organ Size by Inducing Cell Competition. *Cell*, *117*(1), 107–116. [https://doi.org/10.1016/S0092-8674\(04\)00214-4](https://doi.org/10.1016/S0092-8674(04)00214-4)
- del Valle Rodríguez, A., Didiano, D., & Desplan, C. (2012). Power tools for gene expression and clonal analysis in *Drosophila*. *Nature Methods*, *9*(1), 47–55. <https://doi.org/10.1038/nmeth.1800>
- Díaz-Benjumea, J., Gaitán, M. A. F. G., & García-Bellido, A. (1989). Developmental genetics of the wing vein pattern of *Drosophila*. *Genome*, *31*(2), 612–619. <https://doi.org/10.1139/g89-114>
- Ding, J., Yannam, G. R., Roy-Chowdhury, N., Hidvegi, T., Basma, H., Rennard, S. I., Wong, R. J., Avsar, Y., Guha, C., Perlmutter, D. H., Fox, I. J., & Roy-Chowdhury, J. (2011). Spontaneous hepatic repopulation in transgenic mice expressing mutant human α 1-antitrypsin by wild-type donor hepatocytes. *Journal of Clinical Investigation*, *121*(5), 1930–1934. <https://doi.org/10.1172/JCI45260>
- Ding, R., Weynans, K., Bossing, T., Barros, C. S., & Berger, C. (2016). The Hippo signalling pathway maintains quiescence in *Drosophila* neural stem cells. *Nature Communications*, *7*(1), 10510. <https://doi.org/10.1038/ncomms10510>
- Dupont, S., Morsut, L., Aragona, M., Enzo, E., Giulitti, S., Cordenonsi, M., Zanconato, F., Le Digabel, J., Forcato, M., Bicciato, S., Elvassore, N., & Piccolo, S. (2011). Role of YAP/TAZ in mechanotransduction. *Nature*, *474*(7350), 179–183. <https://doi.org/10.1038/nature10137>
- Duraivelan, K., & Samanta, D. (2020). Tracing the evolution of nectin and nectin-like cell adhesion molecules. *Scientific Reports*, *10*(1), 9434. <https://doi.org/10.1038/s41598-020-66461-4>
- Eigenmann, J. E., Patterson, D. F., & Froesch, E. R. (1984). Body size parallels insulin-like growth factor I levels but not growth hormone secretory capacity. *Acta Endocrinol (Copenh)*, *106*(4), 448–453. <https://doi.org/10.1530/acta.0.1060448>

- Ellis, S. J., Gomez, N. C., Levorse, J., Mertz, A. F., Ge, Y., & Fuchs, E. (2019). Distinct modes of cell competition shape mammalian tissue morphogenesis. *Nature*, *569*(7757), 497–502. <https://doi.org/10.1038/s41586-019-1199-y>
- Enomoto, M., Vaughen, J., & Igaki, T. (2015). Non-autonomous overgrowth by oncogenic niche cells: Cellular cooperation and competition in tumorigenesis. *Cancer Science*, *106*(12), 1651–1658. <https://doi.org/10.1111/cas.12816>
- Escudero, L. M., Wei, S.-Y., Chiu, W.-H., Modolell, J., & Hsu, J.-C. (2003). Echinoid synergizes with the Notch signaling pathway in *Drosophila* mesothorax bristle patterning. *Development*, *130*(25), 6305–6316. <https://doi.org/10.1242/dev.00869>
- Everetts, N. J., Worley, M. I., Yasutomi, R., Yosef, N., & Hariharan, I. K. (2021). Single-cell transcriptomics of the *Drosophila* wing disc reveals instructive epithelium-to-myoblast interactions. *ELife*, *10*, e61276. <https://doi.org/10.7554/eLife.61276>
- Fagotto, F., & Gumbiner, B. M. (1996). Cell Contact-Dependent Signaling. *Developmental Biology*, *180*(2), 445–454. <https://doi.org/10.1006/dbio.1996.0318>
- Feng, Y., & Irvine, K. D. (2009). Processing and phosphorylation of the Fat receptor. *Proceedings of the National Academy of Sciences*, *106*(29), 11989–11994. <https://doi.org/10.1073/pnas.0811540106>
- Finegan, T. M., & Bergstrahl, D. T. (2020). Neuronal immunoglobulin superfamily cell adhesion molecules in epithelial morphogenesis: Insights from *Drosophila*. *Philosophical Transactions of the Royal Society B: Biological Sciences*, *375*(1809), 20190553. <https://doi.org/10.1098/rstb.2019.0553>
- Fletcher, G. C., Diaz-de-la-Loza, M.-C., Borreguero-Muñoz, N., Holder, M., Aguilar-Aragon, M., & Thompson, B. J. (2018). Mechanical strain regulates the Hippo pathway in *Drosophila*. *Development*, *145*(5), dev159467. <https://doi.org/10.1242/dev.159467>
- García-Bellido, A. (1965). Larvalentwicklung transplantierte Organe von *Drosophila melanogaster* im Adultmilieu. *Journal of Insect Physiology*, *11*(8), 1071–1078. [https://doi.org/10.1016/0022-1910\(65\)90179-4](https://doi.org/10.1016/0022-1910(65)90179-4)
- García-Bellido, A. C., & García-Bellido, A. (1998). Cell proliferation in the attainment of constant sizes and shapes: The Entelechia model. *Int. J. Dev. Biol.*, *42*, 353–362.
- García-Bellido, A., & Merriam, J. R. (1971). Parameters of the wing imaginal disc development of *Drosophila melanogaster*. *Developmental Biology*, *24*(1), 61–87. [https://doi.org/10.1016/0012-1606\(71\)90047-9](https://doi.org/10.1016/0012-1606(71)90047-9)
- García-Bellido, A., Ripoll, P., & Morata, G. (1973). Developmental Compartmentalisation of the Wing Disk of *Drosophila*. *Nature New Biology*, *245*(147), 251–253.

- Gou, J., Lin, L., & Othmer, H. G. (2018). A Model for the Hippo Pathway in the *Drosophila* Wing Disc. *Biophysical Journal*, *115*(4), 737–747. <https://doi.org/10.1016/j.bpj.2018.07.002>
- Grzeschik, N. A., Parsons, L. M., Allott, M. L., Harvey, K. F., & Richardson, H. E. (2010). Lgl, aPKC, and Crumbs Regulate the Salvador/Warts/Hippo Pathway through Two Distinct Mechanisms. *Current Biology*, *20*(7), 573–581. <https://doi.org/10.1016/j.cub.2010.01.055>
- Hafen, E., & Stocker, H. (2003). How Are the Sizes of Cells, Organs, and Bodies Controlled? *PLoS Biology*, *1*(3), e86. <https://doi.org/10.1371/journal.pbio.0000086>
- Hall, E. T., Hoising, E., Sinkovics, E., & Verheyen, E. M. (2019). Actomyosin contractility modulates Wnt signaling through adherens junction stability. *Molecular Biology of the Cell*, *30*(3), 411–426. <https://doi.org/10.1091/mbc.E18-06-0345>
- Hariharan, I. K. (2015). Organ Size Control: Lessons from *Drosophila*. *Developmental Cell*, *34*(3), 255–265. <https://doi.org/10.1016/j.devcel.2015.07.012>
- Hashimoto, M., & Sasaki, H. (2019). Epiblast Formation by TEAD-YAP-Dependent Expression of Pluripotency Factors and Competitive Elimination of Unspecified Cells. *Developmental Cell*, *50*(2), 139–154.e5. <https://doi.org/10.1016/j.devcel.2019.05.024>
- Ho, Y.-H., Lien, M.-T., Lin, C.-M., Wei, S.-Y., Chang, L.-H., & Hsu, J.-C. (2010). Echinoid regulates Flamingo endocytosis to control ommatidial rotation in the *Drosophila* eye. *Development*, *137*(5), 745–754. <https://doi.org/10.1242/dev.040238>
- Hogan, C., Dupré-Crochet, S., Norman, M., Kajita, M., Zimmermann, C., Pelling, A. E., Piddini, E., Baena-López, L. A., Vincent, J.-P., Itoh, Y., Hosoya, H., Pichaud, F., & Fujita, Y. (2009). Characterization of the interface between normal and transformed epithelial cells. *Nature Cell Biology*, *11*(4), 460–467. <https://doi.org/10.1038/ncb1853>
- Holley, C. L., Olson, M. R., Colón-Ramos, D. A., & Kornbluth, S. (2002). Reaper eliminates IAP proteins through stimulated IAP degradation and generalized translational inhibition. *Nature Cell Biology*, *4*(6), 439–444. <https://doi.org/10.1038/ncb798>
- Hombria, J. C.-G., Brown, S., Häder, S., & Zeidler, M. P. (2005). Characterisation of Upd2, a *Drosophila* JAK/STAT pathway ligand. *Developmental Biology*, *288*(2), 420–433. <https://doi.org/10.1016/j.ydbio.2005.09.040>

- Hortsch, M. (1996). The L1 Family of Neural Cell Adhesion Molecules: Old Proteins Performing New Tricks. *Neuron*, *17*(4), 587–593. [https://doi.org/10.1016/S0896-6273\(00\)80192-0](https://doi.org/10.1016/S0896-6273(00)80192-0)
- Hortsch, M. (2003). Drosophila Echinoid is an antagonist of Egfr signalling, but is not a member of the L1-type family of cell adhesion molecules. *Development*, *130*(22), 5295–5295. <https://doi.org/10.1242/dev.00852>
- Hortsch, M., & Bieber, A. J. (1991). Sticky molecules in not-so-sticky cells. *Trends in Biochemical Sciences*, *16*, 283–287. [https://doi.org/10.1016/0968-0004\(91\)90116-D](https://doi.org/10.1016/0968-0004(91)90116-D)
- Huang, A. M., Rehm, E. J., & Rubin, G. M. (2009). Quick Preparation of Genomic DNA from *Drosophila*. *Cold Spring Harbor Protocols*, *2009*(4), pdb.prot5198. <https://doi.org/10.1101/pdb.prot5198>
- Hynes, R. O., & Zhao, Q. (2000). The Evolution of Cell Adhesion. *The Journal of Cell Biology*, *150*(2), F89–F96. <https://doi.org/10.1083/jcb.150.2.F89>
- Islam, R., Wei, S.-Y., Chiu, W.-H., Hortsch, M., & Hsu, J.-C. (2003). Neuroglian activates Echinoid to antagonize the Drosophila EGF receptor signaling pathway. *Development*, *130*(10), 2051–2059. <https://doi.org/10.1242/dev.00415>
- Jiang, H., Grenley, M. O., Bravo, M.-J., Blumhagen, R. Z., & Edgar, B. A. (2011). EGFR/Ras/MAPK Signaling Mediates Adult Midgut Epithelial Homeostasis and Regeneration in *Drosophila*. *Cell Stem Cell*, *8*(1), 84–95. <https://doi.org/10.1016/j.stem.2010.11.026>
- Jorgensen, E. M., & Mango, S. E. (2002). The art and design of genetic screens: *Caenorhabditis elegans*. *Nature Reviews Genetics*, *3*(5), 356–369. <https://doi.org/10.1038/nrg794>
- Kai, H., Muraishi, A., Sugiu, Y., Nishi, H., Seki, Y., Kuwahara, F., Kimura, A., Kato, H., & Imaizumi, T. (1998). Expression of Proto-oncogenes and Gene Mutation of Sarcomeric Proteins in Patients With Hypertrophic Cardiomyopathy. *Circulation Research*, *83*(6), 594–601. <https://doi.org/10.1161/01.RES.83.6.594>
- Kajita, M., Hogan, C., Harris, A. R., Dupre-Crochet, S., Itasaki, N., Kawakami, K., Charras, G., Tada, M., & Fujita, Y. (2010). Interaction with surrounding normal epithelial cells influences signalling pathways and behaviour of Src-transformed cells. *Journal of Cell Science*, *123*(2), 171–180. <https://doi.org/10.1242/jcs.057976>
- Kanda, H., & Igaki, T. (2020). Mechanism of tumor-suppressive cell competition in flies. *Cancer Science*, *111*(10), 3409–3415. <https://doi.org/10.1111/cas.14575>

- Klein, T., & Campos-Ortega, J. A. (1992). Second-site modifiers of the Delta wing phenotype in *Drosophila melanogaster*. *Roux's Archives of Developmental Biology*, 202(1), 49–60. <https://doi.org/10.1007/BF00364596>
- Lahvic, J. L., & Hariharan, I. K. (2019). Harnessing epithelial homeostatic mechanisms to fight cancer. *Molecular Biology of the Cell*, 30(14), 1641–1644. <https://doi.org/10.1091/mbc.E19-03-0177>
- Laplante, C., & Nilson, L. A. (2006). Differential expression of the adhesion molecule Echinoid drives epithelial morphogenesis in *Drosophila*. *Development*, 133(16), 3255–3264. <https://doi.org/10.1242/dev.02492>
- Laplante, C., & Nilson, L. A. (2011). Asymmetric distribution of Echinoid defines the epidermal leading edge during *Drosophila* dorsal closure. *The Journal of Cell Biology*, 192(2), 335–348. <https://doi.org/10.1083/jcb.201009022>
- Lawrence, P., Johnston, P., & Morata, G. (1986). Methods of marking cells. In Roberts (Ed.), *Drosophila: A Practical Approach* (pp. 229–242). IRL Press.
- Lee, T., & Luo, L. (1999). Mosaic Analysis with a Repressible Cell Marker for Studies of Gene Function in Neuronal Morphogenesis. *Neuron*, 22(3), 451–461. [https://doi.org/10.1016/S0896-6273\(00\)80701-1](https://doi.org/10.1016/S0896-6273(00)80701-1)
- Leung, C. T., & Brugge, J. S. (2012). Outgrowth of single oncogene-expressing cells from suppressive epithelial environments. *Nature*, 482(7385), 410–413. <https://doi.org/10.1038/nature10826>
- Levayer, R., & Moreno, E. (2013). Mechanisms of cell competition: Themes and variations. *Journal of Cell Biology*, 200(6), 689–698. <https://doi.org/10.1083/jcb.201301051>
- Li, Z., Liu, S., & Cai, Y. (2015). EGFR/MAPK Signaling Regulates the Proliferation of *Drosophila* Renal and Nephric Stem Cells. *Journal of Genetics and Genomics*, 42(1), 9–20. <https://doi.org/10.1016/j.jgg.2014.11.007>
- Ling, C., Zheng, Y., Yin, F., Yu, J., Huang, J., Hong, Y., Wu, S., & Pan, D. (2010). The apical transmembrane protein Crumbs functions as a tumor suppressor that regulates Hippo signaling by binding to Expanded. *Proceedings of the National Academy of Sciences*, 107(23), 10532–10537. <https://doi.org/10.1073/pnas.1004279107>
- Liu, N., Matsumura, H., Kato, T., Ichinose, S., Takada, A., Namiki, T., Asakawa, K., Morinaga, H., Mohri, Y., De Arcangelis, A., Geroges-Labouesse, E., Nanba, D., & Nishimura, E. K. (2019). Stem cell competition orchestrates skin homeostasis and ageing. *Nature*, 568(7752), 344–350. <https://doi.org/10.1038/s41586-019-1085-7>

- Madhavan, M. M., & Schneiderman, H. A. (1977). Histological analysis of the dynamics of growth of imaginal discs and histoblast nests during the larval development of *Drosophila melanogaster*. *Wilhelm Roux's Archives of Developmental Biology*, 183(4), 269–305. <https://doi.org/10.1007/BF00848459>
- Mamada, H., Sato, T., Ota, M., & Sasaki, H. (2015). Cell competition in mouse NIH3T3 embryonic fibroblasts controlled by Tead activity and Myc. *Journal of Cell Science*, jcs.163675. <https://doi.org/10.1242/jcs.163675>
- Mandai, K., Rikitake, Y., Shimono, Y., & Takai, Y. (2013). Afadin/AF-6 and Canoe. In *Progress in Molecular Biology and Translational Science* (Vol. 116, pp. 433–454). Elsevier. <https://doi.org/10.1016/B978-0-12-394311-8.00019-4>
- Mao, Y., Tournier, A. L., Bates, P. A., Gale, J. E., Tapon, N., & Thompson, B. J. (2011). Planar polarization of the atypical myosin Dachs orients cell divisions in *Drosophila*. *Genes & Development*, 25(2), 131–136. <https://doi.org/10.1101/gad.610511>
- Martín, F. A., Herrera, S. C., & Morata, G. (2009). Cell competition, growth and size control in the *Drosophila* wing imaginal disc. *Development*, 136(22), 3747–3756. <https://doi.org/10.1242/dev.038406>
- Martín, F. A., & Morata, G. (2006). Compartments and the control of growth in the *Drosophila* wing imaginal disc. *Development*, 133(22), 4421–4426. <https://doi.org/10.1242/dev.02618>
- Martincorena, I., & Campbell, P. J. (2015). Somatic mutation in cancer and normal cells. *Science*, 349(6255), 1483–1489. <https://doi.org/10.1126/science.aab4082>
- Martins, V. C., Busch, K., Juraeva, D., Blum, C., Ludwig, C., Rasche, V., Lasitschka, F., Mastitsky, S. E., Brors, B., Hielscher, T., Fehling, H. J., & Rodewald, H.-R. (2014). Cell competition is a tumour suppressor mechanism in the thymus. *Nature*, 509(7501), 465–470. <https://doi.org/10.1038/nature13317>
- Matakatsu, H., & Blair, S. S. (2012). Separating planar cell polarity and Hippo pathway activities of the protocadherins Fat and Dachsous. *Development*, 139(8), 1498–1508. <https://doi.org/10.1242/dev.070367>
- Milán, M., Campuzano, S., & García-Bellido, A. (1997). Developmental parameters of cell death in the wing disc of *Drosophila*. *Proceedings of the National Academy of Sciences*, 94(11), 5691–5696. <https://doi.org/10.1073/pnas.94.11.5691>
- Morata, G., & Ripoll, P. (1975). Minutes: Mutants of *Drosophila* autonomously affecting cell division rate. *Developmental Biology*, 42(2), 211–221.
- Moreno, E., Basler, K., & Morata, G. (2002). Cells compete for Decapentaplegic survival factor to prevent apoptosis in *Drosophila* wing development. *Nature*, 416(6882), 755–759. <https://doi.org/10.1038/416755a>

- Nellen, D., Burke, R., Struhl, G., & Basler, K. (1996). Direct and Long-Range Action of a DPP Morphogen Gradient. *Cell*, *85*(3), 357–368. [https://doi.org/10.1016/S0092-8674\(00\)81114-9](https://doi.org/10.1016/S0092-8674(00)81114-9)
- Newsome, T. P., Åsling, B., & Dickson, B. J. (2000). Analysis of *Drosophila* photoreceptor axon guidance in eye-specific mosaics. *Development*, *127*(4), 851–860. <https://doi.org/10.1242/dev.127.4.851>
- Norman, M., Wisniewska, K. A., Lawrenson, K., Garcia-Miranda, P., Tada, M., Kajita, M., Mano, H., Ishikawa, S., Ikegawa, M., Shimada, T., & Fujita, Y. (2012). Loss of Scribble causes cell competition in mammalian cells. *Journal of Cell Science*, *125*(1), 59–66. <https://doi.org/10.1242/jcs.085803>
- Oertel, M., Menthen, A., Dabeva, M. D., & Shafritz, D. A. (2006). Cell Competition Leads to a High Level of Normal Liver Reconstitution by Transplanted Fetal Liver Stem/Progenitor Cells. *Gastroenterology*, *130*(2), 507–520. <https://doi.org/10.1053/j.gastro.2005.10.049>
- Oliver, E. R., Saunders, T. L., Tarlé, S. A., & Glaser, T. (2004). Ribosomal protein L24 defect in Belly spot and tail (*Bst*), a mouse *Minute*. *Development*, *131*(16), 3907–3920. <https://doi.org/10.1242/dev.01268>
- Osman, D., Buchon, N., Chakrabarti, S., Huang, Y.-T., Su, W.-C., Poidevin, M., Tsai, Y.-C., & Lemaitre, B. (2012). Autocrine and paracrine unpaired signaling regulate intestinal stem cell maintenance and division. *Journal of Cell Science*, *125*(24), 5944–5949. <https://doi.org/10.1242/jcs.113100>
- ÖzpolatLab-HCR. (2021). *Özpolat Lab HCR probe generator*. [Computer software]. https://github.com/rwnull/insitu_probe_generator
- Parks, A. L., Klueg, K. M., Stout, J. R., & Muskavitch, M. A. T. (2000). Ligand endocytosis drives receptor dissociation and activation in the Notch pathway. *Development*, *127*(7), 1373–1385. <https://doi.org/10.1242/dev.127.7.1373>
- Penzo-Méndez, A. I., Chen, Y.-J., Li, J., Witze, E. S., & Stanger, B. Z. (2015). Spontaneous Cell Competition in Immortalized Mammalian Cell Lines. *PLOS ONE*, *10*(7), e0132437. <https://doi.org/10.1371/journal.pone.0132437>
- Poon, C. L. C., Mitchell, K. A., Kondo, S., Cheng, L. Y., & Harvey, K. F. (2016). The Hippo Pathway Regulates Neuroblasts and Brain Size in *Drosophila melanogaster*. *Current Biology*, *26*(8), 1034–1042. <https://doi.org/10.1016/j.cub.2016.02.009>
- Rathjen, F. G., & Schachner, M. (1984). Immunocytological and biochemical characterization of a new neuronal cell surface component (L1 antigen) which is involved in cell adhesion. *The EMBO Journal*, *3*(1), 1–10. <https://doi.org/10.1002/j.1460-2075.1984.tb01753.x>

- Rawlins, E. L., Lovegrove, B., & Jarman, A. P. (2003). Echinoid facilitates Notch pathway signalling during Drosophila neurogenesis through functional interaction with Delta. *Development*, *130*(26), 6475–6484. <https://doi.org/10.1242/dev.00882>
- Rawlins, E. L., White, N. M., & Jarman, A. P. (2003). Echinoid limits R8 photoreceptor specification by inhibiting inappropriate EGF receptor signalling within R8 equivalence groups. *Development*, *130*(16), 3715–3724. <https://doi.org/10.1242/dev.00602>
- Restrepo, S., Zartman, J. J., & Basler, K. (2014). Coordination of Patterning and Growth by the Morphogen DPP. *Current Biology*, *24*(6), R245–R255. <https://doi.org/10.1016/j.cub.2014.01.055>
- Robinson, B. S., Huang, J., Hong, Y., & Moberg, K. H. (2010). Crumbs Regulates Salvador/Warts/Hippo Signaling in Drosophila via the FERM-Domain Protein Expanded. *Current Biology*, *20*(7), 582–590. <https://doi.org/10.1016/j.cub.2010.03.019>
- Rogulja, D., Rauskolb, C., & Irvine, K. D. (2008). Morphogen Control of Wing Growth through the Fat Signaling Pathway. *Developmental Cell*, *15*(2), 309–321. <https://doi.org/10.1016/j.devcel.2008.06.003>
- Ruoslahti, E., & Öbrink, B. (1996). Common Principles in Cell Adhesion. *Experimental Cell Research*, *227*(1), 1–11. <https://doi.org/10.1006/excr.1996.0243>
- Sancho, M., Di-Gregorio, A., George, N., Pozzi, S., Sánchez, J. M., Pernaute, B., & Rodríguez, T. A. (2013). Competitive Interactions Eliminate Unfit Embryonic Stem Cells at the Onset of Differentiation. *Developmental Cell*, *26*(1), 19–30. <https://doi.org/10.1016/j.devcel.2013.06.012>
- Schindelin, J., Arganda-Carreras, I., Frise, E., Kaynig, V., Longair, M., Pietzsch, T., Preibisch, S., Rueden, C., Saalfeld, S., Schmid, B., Tinevez, J.-Y., White, D. J., Hartenstein, V., Eliceiri, K., Tomancak, P., & Cardona, A. (2012). Fiji: An open-source platform for biological-image analysis. *Nature Methods*, *9*(7), 676–682. <https://doi.org/10.1038/nmeth.2019>
- Shimono, Y., Rikitake, Y., Mandai, K., Mori, M., & Takai, Y. (2012). Immunoglobulin Superfamily Receptors and Adherens Junctions. In T. Harris (Ed.), *Adherens Junctions: From Molecular Mechanisms to Tissue Development and Disease* (Vol. 60, pp. 137–170). Springer Netherlands. https://doi.org/10.1007/978-94-007-4186-7_7
- Simon, A., Bowtell, D. D. L., Steven, G., Laverty, T. R., Rubin, G. M., & Medical, H. H. (1991). Ras1 and a Putative Guanine Nucleotide Exchange Factor Perform Crucial Steps in Signaling by the Sevenless Protein Tyrosine Kinase. *Cell*, *67*, 701–716.

- Simpson, P. (1979). Parameters of cell competition in the compartments of the wing disc of *Drosophila*. *Developmental Biology*, 69(1), 182–193. [https://doi.org/10.1016/0012-1606\(79\)90284-7](https://doi.org/10.1016/0012-1606(79)90284-7)
- Simpson, P., & Morata, G. (1981). Differential mitotic rates and patterns of growth in compartments in the *Drosophila* wing. *Developmental Biology*, 85(2), 299–308. [https://doi.org/10.1016/0012-1606\(81\)90261-X](https://doi.org/10.1016/0012-1606(81)90261-X)
- Sood, C., Justis, V. T., Doyle, S. E., & Siegrist, S. E. (2022). Notch signaling regulates neural stem cell quiescence entry and exit in *Drosophila*. *Development*, 149(4), dev200275. <https://doi.org/10.1242/dev.200275>
- Sousa-Nunes, R., Yee, L. L., & Gould, A. P. (2011). Fat cells reactivate quiescent neuroblasts via TOR and glial insulin relays in *Drosophila*. *Nature*, 471(7339), 508–512. <https://doi.org/10.1038/nature09867>
- Spencer, S. A., & Cagan, R. L. (2003). Echinoid is essential for regulation of Egfr signaling and R8 formation during *Drosophila* eye development. *Development*, 130(16), 3725–3733. <https://doi.org/10.1242/dev.00605>
- St Johnston, D. (2002). The art and design of genetic screens: *Drosophila melanogaster*. *Nature Reviews Genetics*, 3(3), 176–188. <https://doi.org/10.1038/nrg751>
- Steinberg, M. S. (1963). Reconstruction of Tissues by Dissociated Cells. *Science*, 141(3579), 401–408. <https://doi.org/10.1126/science.141.3579.401>
- Sutter, N. B., Bustamante, C. D., Chase, K., Gray, M. M., Zhao, K., Zhu, L., Padhukasahasram, B., Karlins, E., Davis, S., Jones, P. G., Quignon, P., Johnson, G. S., Parker, H. G., Fretwell, N., Mosher, D. S., Lawler, D. F., Satyaraj, E., Nordborg, M., Lark, K. G., ... Ostrander, E. A. (2007). A Single IGF1 Allele Is a Major Determinant of Small Size in Dogs. *Science*, 316(5821), 112–115. <https://doi.org/10.1126/science.1137045>
- Takahashi, K., Nakanishi, H., Miyahara, M., Mandai, K., Satoh, K., Satoh, A., Nishioka, H., Aoki, J., Nomoto, A., Mizoguchi, A., & others. (1999). Nectin/PRR: An immunoglobulin-like cell adhesion molecule recruited to cadherin-based adherens junctions through interaction with afadin, a PDZ domain-containing protein. *The Journal of Cell Biology*, 145(3), 539–549.
- Takai, Y., Irie, K., Shimizu, K., Sakisaka, T., & Ikeda, W. (2003). Nectins and nectin-like molecules: Roles in cell adhesion, migration, and polarization. *Cancer Science*, 94(8), 655–667. <https://doi.org/10.1111/j.1349-7006.2003.tb01499.x>
- Takai, Y., Miyoshi, J., Ikeda, W., & Ogita, H. (2008). Nectins and nectin-like molecules: Roles in contact inhibition of cell movement and proliferation. *Nature Reviews Molecular Cell Biology*, 9(8), 603–615. <https://doi.org/10.1038/nrm2457>

- Tamori, Y., Bialucha, C. U., Tian, A.-G., Kajita, M., Huang, Y.-C., Norman, M., Harrison, N., Poulton, J., Ivanovitch, K., Disch, L., Liu, T., Deng, W.-M., & Fujita, Y. (2010). Involvement of Lgl and Mahjong/VprBP in Cell Competition. *PLoS Biology*, *8*(7), e1000422. <https://doi.org/10.1371/journal.pbio.1000422>
- Teleman, A. A., & Cohen, S. M. (2000). Dpp Gradient Formation in the Drosophila Wing Imaginal Disc. *Cell*, *103*(6), 971–980. [https://doi.org/10.1016/S0092-8674\(00\)00199-9](https://doi.org/10.1016/S0092-8674(00)00199-9)
- Tepass, U., & Harris, K. P. (2007). Adherens junctions in Drosophila retinal morphogenesis. *Trends in Cell Biology*, *17*(1), 26–35. <https://doi.org/10.1016/j.tcb.2006.11.006>
- Togashi, H. (2016). Differential and Cooperative Cell Adhesion Regulates Cellular Pattern in Sensory Epithelia. *Frontiers in Cell and Developmental Biology*, *4*. <https://doi.org/10.3389/fcell.2016.00104>
- Tomas, A., Futter, C. E., & Eden, E. R. (2014). EGF receptor trafficking: Consequences for signaling and cancer. *Trends in Cell Biology*, *24*(1), 26–34. <https://doi.org/10.1016/j.tcb.2013.11.002>
- Tseng, A.-S. K., Tapon, N., Kanda, H., Cigizoglu, S., Edelmann, L., Pellock, B., White, K., & Hariharan, I. K. (2007). Capicua Regulates Cell Proliferation Downstream of the Receptor Tyrosine Kinase/Ras Signaling Pathway. *Current Biology*, *17*(8), 728–733. <https://doi.org/10.1016/j.cub.2007.03.023>
- Tyler, D. M., Li, W., Zhuo, N., Pellock, B., & Baker, N. E. (2007). Genes Affecting Cell Competition in Drosophila. *Genetics*, *175*(2), 643–657. <https://doi.org/10.1534/genetics.106.061929>
- Vasavada, N. (2016). *Astatsa*. <https://astatsa.com/> [Computer software]. <https://astatsa.com/>
- Vieira, A. V., Lamaze, C., & Schmid, S. L. (1996). Control of EGF Receptor Signaling by Clathrin-Mediated Endocytosis. *Science*, *274*(5295), 2086–2089. <https://doi.org/10.1126/science.274.5295.2086>
- Vogel, C., Teichmann, S. A., & Chothia, C. (2003). The immunoglobulin superfamily in *Drosophila melanogaster* and *Caenorhabditis elegans* and the evolution of complexity. *Development*, *130*(25), 6317–6328. <https://doi.org/10.1242/dev.00848>
- Vogel, G. (2013). How Do Organs Know When They Have Reached the Right Size? *Science*, *340*(6137), 1156–1157. <https://doi.org/10.1126/science.340.6137.1156-b>
- Wada, Y., Ohsawa, S., & Igaki, T. (2021). Yorkie ensures robust tissue growth in Drosophila ribosomal protein mutants. *Development*, *148*(14), dev198705. <https://doi.org/10.1242/dev.198705>

- Wartlick, O., Mumcu, P., Kicheva, A., Bittig, T., Seum, C., Jülicher, F., & González-Gaitán, M. (2011). Dynamics of Dpp Signaling and Proliferation Control. *Science*, *331*(6021), 1154–1159. <https://doi.org/10.1126/science.1200037>
- Wei, S.-Y., Escudero, L. M., Yu, F., Chang, L.-H., Chen, L.-Y., Ho, Y.-H., Lin, C.-M., Chou, C.-S., Chia, W., Modolell, J., & Hsu, J.-C. (2005). Echinoid Is a Component of Adherens Junctions That Cooperates with DE-Cadherin to Mediate Cell Adhesion. *Developmental Cell*, *8*(4), 493–504. <https://doi.org/10.1016/j.devcel.2005.03.015>
- Wickham, H. (2016). Programming with ggplot2. In *Ggplot2*. Springer International Publishing. <https://doi.org/10.1007/978-3-319-24277-4>
- Willecke, M., Hamaratoglu, F., Sansores-Garcia, L., Tao, C., & Halder, G. (2008). Boundaries of Dachsous Cadherin activity modulate the Hippo signaling pathway to induce cell proliferation. *Proceedings of the National Academy of Sciences*, *105*(39), 14897–14902. <https://doi.org/10.1073/pnas.0805201105>
- Wolpert, L. (1989). Positional information revisited. *Development*, *107*(Supplement), 3–12. <https://doi.org/10.1242/dev.107.Supplement.3>
- Worley, M. I., Setiawan, L., & Hariharan, I. K. (2013). TIE-DYE: A combinatorial marking system to visualize and genetically manipulate clones during development in *Drosophila melanogaster*. *Development*, *140*(15), 3275–3284. <https://doi.org/10.1242/dev.096057>
- Wu, S., Liu, Y., Zheng, Y., Dong, J., & Pan, D. (2008). The TEAD/TEF Family Protein Scalloped Mediates Transcriptional Output of the Hippo Growth-Regulatory Pathway. *Developmental Cell*, *14*(3), 388–398. <https://doi.org/10.1016/j.devcel.2008.01.007>
- Xu, N., Wang, S. Q., Tan, D., Gao, Y., Lin, G., & Xi, R. (2011). EGFR, Wingless and JAK/STAT signaling cooperatively maintain *Drosophila* intestinal stem cells. *Developmental Biology*, *354*(1), 31–43. <https://doi.org/10.1016/j.ydbio.2011.03.018>
- Xu, T., & Rubin, G. M. (1993). Analysis of genetic mosaics in developing and adult *Drosophila* tissues. *Development*, *117*(4), 1223–1237. <https://doi.org/10.1242/dev.117.4.1223>
- Yang, X., & Xu, T. (2011). Molecular mechanism of size control in development and human diseases. *Cell Research*, *21*(5), 715–729. <https://doi.org/10.1038/cr.2011.63>
- Yue, T. (2011). *Studies of the Hippo Signaling Pathway*. The University of Texas Southwestern Medical Center at Dallas.

- Yue, T., Tian, A., & Jiang, J. (2012). The Cell Adhesion Molecule Echinoid Functions as a Tumor Suppressor and Upstream Regulator of the Hippo Signaling Pathway. *Developmental Cell*, 22(2), 255–267. <https://doi.org/10.1016/j.devcel.2011.12.011>
- Zhan, L., Rosenberg, A., Bergami, K. C., Yu, M., Xuan, Z., Jaffe, A. B., Allred, C., & Muthuswamy, S. K. (2008). Deregulation of Scribble Promotes Mammary Tumorigenesis and Reveals a Role for Cell Polarity in Carcinoma. *Cell*, 135(5), 865–878. <https://doi.org/10.1016/j.cell.2008.09.045>
- Zhao, B., Wei, X., Li, W., Udan, R. S., Yang, Q., Kim, J., Xie, J., Ikenoue, T., Yu, J., Li, L., Zheng, P., Ye, K., Chinnaiyan, A., Halder, G., Lai, Z.-C., & Guan, K.-L. (2007). Inactivation of YAP oncoprotein by the Hippo pathway is involved in cell contact inhibition and tissue growth control. *Genes & Development*, 21(21), 2747–2761. <https://doi.org/10.1101/gad.1602907>
- Ziosi, M., Garoia, F., Trotta, V., Bellosta, P., Cavicchi, S., & Pession, A. (2010). DMyc Functions Downstream of Yorkie to Promote the Supercompetitive Behavior of Hippo Pathway Mutant Cells. *PLoS Genetics*, 6(9), 11.